MONTHLY NOTICES

OF THE

ROYAL ASTRONOMICAL SOCIETY

Vol. 99 No. 2

MEETING OF 1938 DECEMBER 9

Dr. H. Spencer Jones, President, in the Chair.

The following candidates were proposed for election as Fellows of the Society, the name of the proposer from personal knowledge being appended :—

William Charles Aubrey-Rees, 63 Cannon Lane, Pinner, Middlesex (proposed by W. Denne) ;

Edward Barker-Jones, B.Sc., 4 St. George's Avenue, Grays, Essex (proposed by G. H. Gilbert) ;

Samuel Morris Green, 22 Church Street, Prescot, Lancs (proposed by Robert Barker) ;

B. Gopala Narayan, B.Sc., Solar Physics Observatory, Kodaikanal, S. India (proposed by A. K. Das) ;

Robert Albert Newing, University College of North Wales, Bangor (proposed by S. Chapman) ;

Albert Thomas Price, Imperial College of Science and Technology, South Kensington, London, S.W. 7 (proposed by S. Chapman) ; and

John Wadsworth, late Director of the Apia Observatory, 16 Wavertree Court, Streatham Hill, London, S.W. 2 (proposed by D. Brunt).

Sixty-seven presents were announced as having been received since the last meeting, including :—

H. Spencer Jones, The Measurement of Time (two copies).

Mr. W. E. Candler and Mr. F. J. Sellers were appointed auditors of the Treasurer's accounts for 1938.

UNIVERSITY LIBRARY LEEDS.

The President announced that in consequence of the joint meeting with the Physical Society, which is to be held on January 27, the Geophysical Discussion on *The Night Sky and Aurora* arranged for that date is postponed to 1939 May 19. The Discussion arranged for 1939 May 26 is cancelled, and in its place a Discussion on *Recent Geophysical Investigations at Sea* (opener, Dr. E. C. Bullard) has been provisionally arranged for 1939 March 24.

DETERMINATION OF THE CONSTANTS OF THE VELOCITY ELLIPSOID FROM RADIAL SPEEDS.

W. M. Smart.

1. In a recent paper Dr. S. Chandrasekhar and the writer developed a method for deriving the constants of the velocity ellipsoid from the radial speeds of the stars.* It was suggested that the application of the procedure outlined in the paper would prove comparatively simple in practice, and this anticipation appears to be fully realised in the statistical investigation to be described.

The radial velocities were taken directly from Schlesinger's *Catalogue of Bright Stars* (1930). The same material had already been used by the author in two papers, which we shall refer to as A and B ; the first † showed that the distribution of the radial velocities satisfied the requirements of the two-drifts theory with the stars equally divided between the two drifts, and the second paper ‡ (written in collaboration with Mr. H. E. Green) contained an investigation on the solar motion and on the galactic rotation as shown by the B-type stars. The first paper, A, alluded to and the present one are complementary ; the former, however, was essentially a verification, while the latter, as will be seen, deals with the positive problem of the determination of the constants of the velocity ellipsoid, namely, the values of the semi-axes with their ratio and the direction of the vertex.

2. The division of the sky into large areas according to galactic latitude, as in papers A and B, has been followed. There are 8 galactic equatorial areas H, I, J and K with their antipodal regions h, i, j and k, 12 areas centred in galactic latitude $\pm 20°$ designated E, F, G, L, M and N with their antipodal areas e, f, g, l, m and n, and 12 areas centred in $\pm 45°$ denoted by B, C, D, P, Q and R with antipodal areas b, c, d, p, q and r. We ignore the two large polar areas A and a used in papers A and B. The galactic co-ordinates of the centres of the regions designated by capital letters are to be found in paper A, p. 168. In the sequel the data relating to a pair of antipodal areas are combined together.

The statistics were arranged according to spectral type. A correction κ (in km./sec.) was applied in bulk to the stars of a given spectral type in each region. For the stars of types A to M, κ is equivalent to $C_z - K$ where C_z is the correction, tabulated in paper B, p. 475, arising from the large extent of the areas, and K is the value of the K-term derived from the solutions for the solar motion according to spectral class and tabulated in paper B, p. 476. The value of κ for the B-type stars includes the correction for galactic rotation derived from the data in paper B, p. 479. Some care has to be taken in applying the total correction for the B-type stars ; as

* *M.N.*, **98**, 658, 1938. † *M.N.*, **96**, 165, 1936. ‡ *M.N.*, **96**, 471, 1936.

we are to be concerned with radial speeds only the correction κ (which happens to be negative for all the regions) can be applied in bulk to (i) all positive radial velocities greater than $|\kappa|$, (ii) to positive radial velocities between 0 and $|\kappa|$, and (iii) to all the negative radial velocities. We denote the radial speeds, in km./sec., so obtained by R_0. The values of κ in km./sec. are shown in Table I.

TABLE I

Values of κ

Region	B	A	F	G	K	M
h	−0·56	−0·10	+0·52	+1·00	+0·23	+0·13
i	−5·47	−0·39	+0·22	+0·66	−0·17	−0·29
j	−9·82	−0·47	+0·14	+0·49	−0·36	−0·56
k	−5·19	−0·29	+0·31	+0·61	−0·23	−0·52
e	−4·91	−0·20	+0·43	+0·94	+0·15	+0·13
f	−7·82	−0·66	−0·02	+0·32	−0·55	−0·63
g	−3·81	−0·49	+0·15	+0·39	−0·47	−0·77
l	−4·99	−0·26	+0·40	+0·90	+0·11	+0·05
m	−7·90	−0·72	−0·09	+0·26	−0·62	−0·71
n	−3·89	−0·56	+0·08	+0·32	−0·55	−0·84
b	−4·49	+0·07	+0·73	+1·05	+0·32	+0·23
c	−4·90	−0·16	+0·49	+0·75	−0·02	−0·17
d	−4·90	−0·06	+0·57	+0·79	+0·02	−0·25
p	−4·87	−0·33	+0·28	+0·82	−0·02	−0·15
q	−5·28	−0·56	+0·03	+0·52	−0·36	−0·56
r	−5·28	−0·46	+0·12	+0·56	−0·32	−0·63
H	−0·64	+0·04	+0·66	+0·94	+0·15	−0·21
I	−4·73	+0·33	+0·96	+1·28	+0·55	+0·21
J	−8·62	+0·41	+1·04	+1·45	+0·74	+0·48
K	−4·25	+0·23	+0·87	+1·33	+0·61	+0·44
E	−4·99	+0·14	+0·75	+1·00	+0·23	−0·21
F	−6·30	+0·60	+1·20	+1·62	+0·93	+0·55
G	−2·29	+0·43	+1·03	+1·55	+0·85	+0·69
L	−4·91	+0·20	+0·78	+1·04	+0·27	−0·13
M	−6·22	+0·66	+1·27	+1·68	+1·00	+0·63
N	−2·21	+0·50	+1·10	+1·62	+0·93	+0·76
B	−4·87	−0·13	+0·45	+0·89	+0·06	−0·31
C	−4·46	+0·10	+0·69	+1·19	+0·40	+0·09
D	−4·46	0·00	+0·61	+1·15	+0·36	+0·17
P	−4·49	+0·27	+0·90	+1·12	+0·40	+0·07
Q	−4·08	+0·50	+1·15	+1·42	+0·74	+0·48
R	−4·08	+0·40	+1·06	+1·38	+0·70	+0·55

Table II contains for each of the combined regions the values of $\bar{R}_0$, the mean corrected radial speed, for each spectral type B to K and for all spectral types A to M and B to M (the number of stars of type M is too small for independent analysis, but the data are incorporated in the last two columns of Table II; a similar remark applies to the B-type stars in

the high galactic zones, $\pm 45°$). The number of stars corresponding to each tabulated value of $\bar{R}_0$ is given in parentheses.

TABLE II

Values of $\bar{R}_0$

Region	B	A	F	G	K	A to M	B to M
h, H	11·14	11·68	16·84	18·80	15·24	15·14	13·92
	(64)	(38)	(32)	(16)	(53)	(145)	(209)
i, I	15·27	19·17	20·75	20·00	22·89	21·60	19·80
	(51)	(35)	(20)	(14)	(50)	(128)	(179)
j, J	18·87	19·72	23·53	18·37	21·35	21·11	20·47
	(71)	(40)	(38)	(27)	(64)	(177)	(248)
k, K	18·23	16·15	15·33	14·90	15·54	15·65	16·58
	(95)	(39)	(30)	(19)	(71)	(169)	(264)
e, E	10·40	10·16	16·71	17·21	19·67	16·76	16·04
	(20)	(37)	(21)	(24)	(63)	(157)	(177)
f, F	19·74	15·29	18·81	20·91	21·30	19·54	19·56
	(19)	(35)	(27)	(33)	(62)	(167)	(186)
g, G	14·16	11·97	15·84	16·41	20·67	17·04	16·53
	(31)	(36)	(31)	(17)	(54)	(145)	(176)
l, L	8·65	11·30	14·38	16·35	20·11	16·27	13·99
	(70)	(43)	(24)	(23)	(63)	(162)	(232)
m, M	20·21	19·19	22·00	21·44	22·35	21·32	20·95
	(77)	(57)	(21)	(16)	(52)	(155)	(232)
n, N	21·14	16·83	17·10	18·36	21·40	19·30	19·59
	(36)	(46)	(39)	(25)	(72)	(195)	(231)
b, B	...	8·44	16·52	16·22	20·00	15·73	15·42
		(43)	(33)	(36)	(71)	(196)	(206)
c, C	...	13·66	14·41	22·65	20·62	18·25	17·89
		(44)	(27)	(31)	(71)	(190)	(207)
d, D	...	10·11	11·04	14·29	14·72	12·89	12·18
		(27)	(27)	(24)	(61)	(160)	(178)
p, P	...	9·41	14·16	16·70	18·86	16·65	16·21
		(37)	(37)	(30)	(70)	(187)	(207)
q, Q	...	15·48	18·42	25·00	22·20	20·89	20·24
		(42)	(19)	(28)	(65)	(169)	(189)
r, R	...	11·48	14·12	21·08	22·78	17·84	17·54
		(44)	(32)	(24)	(50)	(166)	(177)

3. The method involves, for each combined region, the solution of the equation in ξ:

$$t = \frac{1}{\xi} F(\xi), \tag{1}$$

where

$$F(\xi) = \tilde{e}^{\xi^2} + 2\xi \int_0^{\xi} \tilde{e}^{x^2} dx \tag{2}$$

and

$$t = \frac{\pi^{1/2} \bar{R}_0}{S \cos \lambda}, \tag{3}$$

in which S is the appropriate solar motion and λ is the angular distance of the centre of the region from the solar apex, or antapex, whichever is less than 90°. The values of $S \cos \lambda$ are computed from the data in paper B, Table IV, p. 476, and they are shown in Tables IV–VII.

The values of the function $F(\xi)$ are tabulated in paper A, p. 167. The following table (Table III) gives the values of the function $\frac{1}{\xi}F(\xi)$, which are of great use in deriving the values of ξ for given values of t. A necessary condition for the solution of (1) is evident from Table III; it is that $t > 1{\cdot}772$ (or $\pi^{1/2}$); from (3) this leads to the condition that $\bar{R}_0 > S \cos \lambda$.

TABLE III

Values of $t \equiv \frac{1}{\xi}F(\xi)$

ξ	t	ξ	t	ξ	t	ξ	t
0·0	∞	0·13	7·823	0·65	2·147	1·30	1·795
0·01	100·01	0·14	7·282	0·70	2·076	1·35	1·791
0·02	50·02	0·15	6·816	0·75	2·020	1·40	1·788
0·03	33·36	0·16	6·409	0·80	1·974	1·45	1·785
0·04	25·04	0·20	5·200	0·85	1·936	1·50	1·782
0·05	20·05	0·25	4·248	0·90	1·907	1·55	1·780
0·06	16·73	0·30	3·630	0·95	1·881	1·60	1·778
0·07	14·36	0·35	3·200	1·00	1·861	1·65	1·777
0·08	12·58	0·40	2·890	1·05	1·844	1·70	1·776
0·09	11·20	0·45	2·658	1·10	1·831	1·75	1·775
0·10	10·10	0·50	2·480	1·15	1·820	1·80	1·774
0·11	9·20	0·55	2·341	1·20	1·811	1·85	1·774
0·12	8·45	0·60	2·233	1·25	1·803	1·90	1·774
0·13	7·82	0·65	2·147	1·30	1·795	1·95	1·773

It is to be noted that for small values of ξ (corresponding to large values of t) we have, with sufficient accuracy,

$$t = \frac{1}{\xi}(1 - \xi^2) + 2\xi$$

$$= \frac{1}{\xi} + \xi. \qquad (4)$$

For a given large value of t we obtain from Table III, at a glance, an approximate value of ξ, correct to two places of decimals; denoting this approximate value of ξ by ξ_0 we obtain from (4), and as a sufficiently accurate solution of (1),

$$\xi = \frac{1}{t - \xi_0}.$$

For example, if $t = 12$, we take ξ_0 to be 0·08 from Table III, and the corresponding value of ξ is then given by

$$\xi = \frac{1}{12 - 0{\cdot}08} = \frac{1}{11{\cdot}92} = 0{\cdot}0839.$$

This approximate method of solving equation (1) is sufficiently accurate for values of $t > 5$.

For values of t less than 5, recourse was had to a graphical method of solution, based on curves derived from the entries in Table III. This proved simple and rapid in application.

The values of ξ satisfying (1) are shown in Tables IV–VII.

4. We assume that the velocity ellipsoid is given by the equation

$$K^2U^2 + H^2(V^2 + W^2) = 1, \quad (K < H)$$

from which $1/K$ is the semi-major axis and $1/H$ the semi-minor axis. We write *

$$\frac{1}{H^2} = p\,; \qquad \frac{1}{K^2} - \frac{1}{H^2} = q. \tag{5}$$

The vertex, or the direction of the major axis of the velocity ellipsoid, is assumed to lie in the galactic plane ; its longitude is denoted by G_0.

The equation of condition for a region whose centre, in galactic co-ordinates, is (G, g) is

$$P + Q\cos 2G + R\sin 2G = C, \tag{6}$$

where

$$P = p + \tfrac{1}{2}q\cos^2 g, \tag{7}$$

$$Q = \tfrac{1}{2}q\cos^2 g\cos 2G_0, \tag{8}$$

$$R = \tfrac{1}{2}q\cos^2 g\sin 2G_0 \tag{9}$$

and

$$C = \left(\frac{S\cos\lambda}{\xi}\right)^2. \tag{10}$$

We have seen how ξ can be determined for a given region, and with $S\cos\lambda$ known we obtain the corresponding numerical value of C by means of (10). The values of C are shown in Tables IV–VII.

TABLE IV

Calculation of C for Type B

Zone 0°

	h, *H*	*i*, *I*	*j*, *J*	*k*, *K*
$\sqrt{\pi}\bar{R}_0$	19·74	27·06	33·43	32·30
$S\cos\lambda$	3·47	10·35	18·12	15·30
t	5·69	2·615	1·845	2·11
ξ	0·1815	0·463	1·05	0·675
C	365	500	298	514

Zone 20°

	e, *E*	*f*, *F*	*g*, *G*	*l*, *L*	*m*, *M*	*n*, *N*
$\sqrt{\pi}\bar{R}_0$	18·43	34·98	25·09	15·33	35·81	37·36
$S\cos\lambda$	2·68	14·84	14·86	2·68	20·20	20·22
t	6·88	2·36	1·69	5·72	1·775	1·848
ξ	0·1485	0·543	...	0·1805	1·75	1·04
C	327	745	...	221	133	378

* The notation following is that of *M.N.*, **98**, 662, 1938.

TABLE V

Calculation of C for Types A and F

	Type A					Type F				
	$\sqrt{\pi}\bar{R}_0$	$S\cos\lambda$	t	ξ	C	$\sqrt{\pi}\bar{R}_0$	$S\cos\lambda$	t	ξ	C
h, H	20·70	2·36	8·77	0·1155	417	29·84	2·04	14·63	0·0687	882
i, I	33·97	12·18	2·79	·420	841	36·77	12·13	3·02	·377	1037
j, J	34·94	14·88	2·35	·547	740	41·70	15·13	2·76	·427	1253
k, K	28·62	8·84	3·24	·345	655	27·17	9·28	2·93	·393	557
e, E	18·00	1·23	14·63	·0687	320	29·61	0·45	65·5	·0153	870
f, F	27·09	10·98	2·47	·504	475	33·33	10·56	3·16	·356	882
g, G	21·21	6·95	3·05	·372	350	28·07	6·74	4·16	·256	692
l, L	20·02	6·81	2·94	·391	303	25·48	7·07	3·60	·303	543
m, M	34·00	16·55	2·055	·719	529	38·98	17·18	2·27	·582	870
n, N	29·82	12·53	2·38	·536	548	30·30	13·43	2·26	·586	524
b, B	14·96	2·45	6·11	·1685	210	29·27	3·71	7·89	·129	829
c, C	24·21	5·14	4·71	·223	531	25·53	4·16	6·14	·1675	615
d, D	17·92	2·00	8·96	·113	313	19·56	1·25	15·65	·0642	380
p, P	16·67	8·67	1·92	·875	98	25·09	9·53	2·63	·457	433
q, Q	27·43	16·26	1·69	...	...	32·64	17·39	1·88	·951	335
r, R	20·34	13·13	1·55	...	...	25·02	14·48	1·73	...	...

TABLE VI

Calculation of C for Types G and K

	Type G					Type K				
	$\sqrt{\pi}\bar{R}_0$	$S\cos\lambda$	t	ξ	C	$\sqrt{\pi}\bar{R}_0$	$S\cos\lambda$	t	ξ	C
h, H	32·56	0·774	42·07	0·0238	1056	26·97	0·785	34·4	0·0291	734
i, I	34·64	11·02	3·14	·359	942	40·51	12·33	3·28	·3395	1318
j, J	33·45	16·36	2·04	·730	502	37·79	18·23	2·07	·705	671
k, K	25·80	12·13	2·13	·660	339	27·50	13·45	2·045	·725	346
e, E	29·81	0·516	5·78	·1785	835	34·82	1·02	34·1	·0294	1204
f, F	36·22	12·13	2·99	·382	1011	37·70	13·04	2·89	·400	1063
g, G	28·42	10·84	2·62	·460	557	36·57	11·52	3·17	·354	1056
l, L	28·32	3·10	9·14	·1108	784	35·59	4·01	8·88	·114	1239
m, M	37·13	15·74	2·36	·543	841	39·56	18·05	2·19	·623	841
n, N	31·80	14·45	2·55	·479	912	37·88	16·58	2·28	·578	824
b, B	28·09	2·60	18·04	·0556	2190	35·40	3·87	9·15	·1105	1225
c, C	39·23	7·24	5·42	·191	1436	36·50	7·04	5·18	·201	1225
d, D	24·75	6·24	3·97	·270	534	26·05	5·88	4·43	·239	605
p, P	28·92	4·59	6·30	·163	795	33·38	6·20	5·38	·193	1030
q, Q	43·30	14·43	3·00	·380	1436	39·29	17·11	2·29	·573	894
r, R	36·51	13·43	2·72	·435	955	40·32	16·00	2·52	·488	1076

It is to be noticed that in the combined regions *g, G* of Table IV and *q, Q* and *r, R* of Table V the values of ξ—and, consequently, of C—are indeterminate; in these instances the values of t are less than 1·772, or $\pi^{1/2}$, so that $\bar{R}_0 < S\cos\lambda$; the inequality arises from a deficiency of the larger radial speeds to be expected in a normal distribution.

TABLE VII

Calculation of C for Types A to M and B to M

	Types A to M					Types B to M				
	$\sqrt{\pi}\bar{R}_0$	$S\cos\lambda$	t	ξ	C	$\sqrt{\pi}\bar{R}_0$	$S\cos\lambda$	t	ξ	C
h, H	26·80	0·091	294·5	0·0034	718	24·66	0·643	38·4	0·0260	610
i, I	38·23	11·75	3·25	·344	1170	35·09	12·03	2·92	·395	930
j, J	37·41	16·53	2·26	·587	795	36·27	17·69	2·05	·730	586
k, K	27·70	11·63	2·38	·535	471	29·38	12·97	2·26	·588	488
e, E	29·70	0·492	60·4	·0166	870	28·42	1·23	23·1	·0438	790
f, F	34·62	11·80	2·93	·393	900	34·66	12·34	2·81	·416	882
g, G	30·19	9·70	3·11	·363	713	29·29	10·78	2·72	·435	615
l, L	28·82	4·71	6·12	·168	790	24·80	4·35	5·70	·179	590
m, M	37·78	17·00	2·22	·607	784	37·12	17·92	2·07	·705	645
n, N	34·20	14·87	2·30	·568	686	34·71	16·36	2·12	·667	600
b, B	27·87	3·57	7·81	·1303	751	27·32	4·37	6·25	·164	708
c, C	32·34	5·99	5·40	·192	973	31·69	6·18	5·13	·203	924
d, D	22·83	4·33	5·27	·197	484	21·58	4·95	4·36	·243	416
p, P	29·50	6·84	4·31	·246	773	28·72	6·79	4·23	·251	734
q, Q	36·98	16·40	2·26	·587	784	35·86	17·34	2·07	·705	605
r, R	31·61	14·74	2·145	·650	515	31·07	16·11	1·93	·859	353

5. The least-squares solutions of equation (6) to determine P, Q and R have been obtained for each spectral type and for each galactic zone, and also for all stars of spectral types A to M and B to M in each zone.

From (8) and (9) we obtain the appropriate values of G_0 and q; from (7) we then determine p and hence, by (5), the semi-minor axis, $1/H$, in km./sec. The ratio, K/H, of the axes of the velocity ellipsoid is given by

$$\frac{K}{H}=\left(\frac{p}{p+q}\right)^{1/2},$$

which, with the value of $1/H$ previously found, determines the value of the semi-major axis, $1/K$, in km./sec.

The solutions are shown in Table VIII, together with the number, N, of stars used.

The fourth columns under the headings A, F, G, K give the total number of stars of each type, and the values of G_0, $1/K$, $1/H$ and K/H are simple means of the three zone-values. For types A to M and B to M the probable errors are given in each zone for G_0 and K/H; the values of G_0 in the fourth columns are the means obtained by weighting the zone-values according to their probable errors; the values of $1/K$, $1/H$ and K/H in the fourth columns are simple means of the three zone-values.

The numbers in parentheses in the fourth columns are Nordström's values of the corresponding quantities, to which reference will be made later.

Considering the individual spectral types we notice from Table VIII that the B-type stars in Zone 0° show little evidence of preferential motion

TABLE VIII

Values of G_0, $\frac{1}{K}$, $\frac{1}{H}$ *and* $\frac{K}{H}$

	B		A				F			
Zone	0°	20°	0°	20°	45°	All	0°	20°	45°	All
N	281	253	152	254	237	643	120	163	175	458
G_0	286°·5	19°·3	7°·5	22°·2	12°·4	14°·0 (357°·9)	356°·3	349°·4	311°·2	339°·0 (339°·7)
$1/K$	21·3	22·0	29·0	23·8	31·4	28·1 (24·2)	35·2	30·4	30·6	32·1 (33·2)
$1/H$	19·6	16·3	21·8	17·5	10·7	16·7 (14·8)	25·1	23·9	18·6	22·9 (20·0)
K/H	0·921	0·743	0·754	0·737	0·340	0·610	0·713	0·786	0·610	0·703

	G				K			
Zone	0°	20°	45°	All	0°	20°	45°	All
N	76	138	173	387	238	366	385	989
G_0	316°·3	348°·2	327°·8	330°·8 (339°·4)	335°·6	301°·8	323°·5	320°·3 (342°·2)
$1/K$	33·4	31·0	51·8	38·7 (38·9)	35·4	35·8	39·1	36·8 (34·2)
$1/H$	17·3	26·7	27·1	23·7 (23·8)	16·7	29·1	28·9	24·9 (27·6)
K/H	0·519	0·859	0·523	0·634	0·473	0·812	0·739	0·675

	A to M				B to M			
Zone	0°	20°	45°	All	0°	20°	45°	All
N	619	981	1068	2668	900	1234	1164	3298
G_0	340°·5 ± 2°·4	332°·2 ± 6°·9	338°·8 ± 4°·3	339°·5 ± 1°·4 (344°·4)	335°·9 ± 6°·5	344°·2 ± 14°·1	333°·0 ± 6°·0	335°·6 ± 2°·0 (340°·1)
$1/K$	33·7	30·1	37·2	33·7 (31·7)	29·5	28·3	36·7	31·5 (29·0)
$1/H$	20·9	26·4	22·1	23·1 (23·5)	20·8	24·4	19·6	21·6 (22·9)
K/H	0·619 ± 0·037	0·879 ± 0·028	0·594 ± 0·056	0·697 ... (0·745)	0·702 ± 0·063	0·862 ± 0·064	0·534 ± 0·094	0·699 ...

(the value of K/H is close to unity and, as a consequence, the direction of the vertex is hardly determinate); the A-type stars in all three zones and the B-type stars in Zone 20° give the longitude of the vertex about 40° higher than that, 335°, obtained in the general solution for stars of all types, with—at the same time—quite normal values for the ratio of the ellipsoidal axes. Preferential motion is shown clearly by types F, G, K and by types A to M and B to M, with the exception in Zone 20°, where the ratios of the axes of the ellipsoid are approximately 5/6—a value considerably higher than in the other zones; this seems a curious result for which, if it is real, there seems to be no explanation.

The longitudes of the vertex determined from the stars of types A to M and types B to M are 339°·5 and 335°·6 ; the values for the separate zones are mutually consistent and the probable errors for the combined zones are small. As compared with Shapley's value of 327° for the longitude of the galactic centre, the longitude of the vertex found in the present investigation is about 10° higher ; the value found by Eddington * from the proper motions of the Boss stars (which include practically all the stars in the usual radial velocity investigations) is still higher at 347° ; Nordström's values from radial velocities are 344° and 340° for types A to M and B to M respectively, as shown in Table VIII.

Nordström's investigation † is, I think, the most recent, and so I have compared his results (shown in parentheses in Table VIII, where comparisons are possible) with those of the present investigation. Moreover, Nordström used very nearly the same number of stars and possibly the material was almost identical. Nordström, it should be remarked, based his analysis on the general velocity ellipsoid with, theoretically, three unequal axes. Except in his solutions for types B and G the direction of the largest axis is in, or very near to, the galactic plane, so that his values of G_0 and $1/K$ should be directly comparable with mine ; I have used the mean of his values for the shorter axes for purposes of comparison with my values of $1/H$. Nordström's solution for stars of types A to M shows that the two smaller axes are practically equal so that, in this case, the comparison of our results obtained by two totally different methods is entirely justifiable ; it will be seen from Table VIII that our values of the several ellipsoidal constants are in good agreement. It is to be noted that Nordström uses

$$f(U, V, W) \equiv \frac{U^2}{{\sigma_1}^2} + \frac{V^2}{{\sigma_2}^2} + \frac{W^2}{{\sigma_3}^2} = 1$$

as the equation of the velocity ellipsoid, but as his frequency function is taken to be

$$e^{-\frac{1}{2}f(U, V, W)}$$

the identification of the semi-axes in the two systems is given by

$$\frac{1}{K^2} = 2{\sigma_1}^2, \qquad \frac{1}{H^2} = 2{\sigma_{2,3}}^2$$

where $\sigma_{2,3}$ is the mean of σ_2 and σ_3—according to the convention adopted above. Accordingly, his published values of σ_1, etc. require to be multiplied by $\sqrt{2}$ for comparison with my values of $1/K$ and $1/H$.

6. *Summary.*—The paper deals with the statistical application of a new method, based on radial speeds, for determining the values of the semi-major and semi-minor axes, $1/K$ and $1/H$, of the velocity ellipsoid (with two equal axes) and the longitude, G_0, of the vertex.

* *M.N.*, 71, 4, 1910.

† *Lund Medd.*, Ser. II, Nr. 79, 1936; the relevant information is to be found on pp. 161, 163.

Solutions have been obtained for each of the spectral types B, A, F, G and K, all types from A to M and all types from B to M in each of three galactic zones.

For types A to M and B to M the mean value of K/H for stars in all three zones is 0·70 in each instance, and the respective values of G_0 are $339^\circ{\cdot}5$ and $335^\circ{\cdot}6$.

University Observatory,
Glasgow, W. 2 :
1938 *November* 26.

A STUDY OF GALACTIC ROTATION, BASED ON THE VELOCITIES OF THE PLANETARY NEBULÆ.

G. L. Camm, formerly Skynner Student in Astronomy, Balliol College, Oxford.

(Communicated by Professor E. A. Milne)

1. *The Scope of the Paper.*—The planetary nebulæ have several advantages over other bodies as objects from which to study galactic rotation. Their spectral lines are suited to the determination of radial velocities, and the objects themselves are all found near the galactic plane. But their special value is in the large area over which they lie, when projected on to the plane of the galaxy. These advantages have already been appreciated, in particular in papers by Berman * and Ogrodnikoff ; † but it is questionable whether these writers have made the best possible use of the material. An alternative method is used here to obtain more, and more direct, information as to how the speed of rotation is related to the distance from the galactic centre.

The galaxy is assumed to rotate in concentric circles, with a speed depending only on the radius of the circle ; the most direct procedure is therefore to calculate for each planetary its distance from the galactic centre, and (from its radial velocity) its angular speed of rotation about the centre. After taking average values of radii and angular velocities for nebulæ in neighbouring circles, a curve is drawn, giving the relation between speed of rotation and galactic radius.

From this curve a theoretical value is found for the radial velocity of each planetary ; this is seldom in agreement with the observed value, and gives rise to a velocity-dispersion, over and above the mean motion. This velocity-dispersion, as measured by the mean square residual velocity, is reduced by making slight corrections to the constants of the problem, of which provisional values had been assumed. Such constants are the distance and direction of the galactic centre, the components of solar motion, and a constant K-term. The velocity-dispersion, after these corrections have been made, has a smaller value than has previously been obtained for the planetary nebulæ.

As an alternative to a constant K-term, a correction is also made in which the K-term for each object is directly proportional to the distance from the Sun. Such a form was suggested by Milne,‡ as a feature of an expanding universe, and he estimated the constant of proportionality. With this value, the constant derived from the radial velocities of the planetaries is in good agreement. As both forms of K-term lead to the same final value of the

* *Lick Obs. Bull.*, **18**, 57, 1937.

† *Poulkovo Obs. Circ.*, **21**, 15, 1937.

‡ *Proc. Roy. Soc.*, A, **160**, 20, 1937.

mean square residual velocity, the observations do not decide which is the more probable interpretation.

The linear speed of rotation at the distance of the Sun cannot be determined from the radial velocities, but it can be evaluated from the proper-motions. These have been considered as having systematic errors, by Vorontsov-Velyaminov * and by Ogrodnikoff.† At any rate, they show remarkable discrepancies when used to determine the speed of rotation at the Sun, and the speed here finally adopted is much below the generally accepted value. The linear speed at the Sun's distance having been found, a curve is drawn to show the variation of linear speed with galactic radius.

It is assumed that the mean rotation now determined corresponds to circular orbits, described under the gravitational attraction of the whole galaxy ; hence it is possible to find the variation of the force with galactic radius. The galaxy is usually supposed to consist of a thin circular disc of matter, with a massive nucleus at the centre. By adjusting the masses of the two parts, it is possible to get a theoretical gravitational field which corresponds very closely to the field of force deduced from the observations.

2. *The Uncertainty of the Distances of the Planetary Nebulæ.*—The most serious obstacle encountered in this, or any other, treatment of the planetary nebulæ arises in the estimation of their distances. The method of treating the problem of galactic rotation, briefly outlined above, will apply, whatever principle be used to determine distances. Indeed, from one point of view, it is a method which minimizes the effect of errors in distance, for the error in assigning the distance of a nebula from the galactic centre is nearly always far less than the corresponding error in the distance from the Sun.

Three tables of distances have already been published, by Zanstra,‡ Vorontsov-Velyaminov § and Berman.|| Apart from the lack of agreement between them, all three have the same defect—at least, so far as this work is concerned—that the radial velocities, interpreted by means of galactic rotation, have already been used to determine distances.

It was therefore considered necessary to evaluate a fourth set of distances, which, if possible, should be independent of the radial velocities. Briefly, the method is to use the angular diameters as well as the apparent magnitudes, and to treat them as being equally reliable indicators of distance.

The surface brightnesses, it is found, indicate that the planetaries can be divided into two distinct groups, so it is not likely that both groups have the same mean absolute magnitude, or the same mean linear diameter. By assuming a linear relation between absolute magnitude and linear diameter, we obtain a sliding scale which permits both quantities to change continuously on passing from one group to the other.

No allowance is made for interstellar absorption, or for the effects of selection, as the method is too crude to warrant such corrections. The effect of interstellar absorption on the diameters and magnitudes is far from obvious ; it would be expected that such absorption would reduce the

* *Z. f. Astroph.*, **8**, 198 and 207, 1934.
† *Poulkovo Obs. Circ.*, **21**, 29, 1937.
‡ *Z. f. Astroph.*, **2**, 331, 1931.
§ *Z. f. Astroph.*, **8**, 204, 1934.
|| *Lick Obs. Bull.*, **18**, 73, 1937.

observed diameters in a way at least comparable with the reduction in brightness, but it will be seen in Table I that there are many nebulæ of large angular diameter and faint apparent magnitude. This suggests that, though the nebulæ are near the galactic plane, they are little affected by interstellar absorption.

TABLE I

The Distances of the Planetary Nebulæ

N.G.C. (or R.A.)	m	a	S	Distances in parsecs, estimated by		
				Camm	Vorontsov-Velyaminov	Berman
40	9·5	60	23·4	670	1000	1220
$0^h\ 22^m.8$	13·3	5	21·8	6220	4170	7010
246	9·4	240	26·3	240	460	1410
650–1	11·4	157	27·4	420	2510	4570
II 1747	13·9	13	24·5	3610	4790	4270
I 289	12·3	45	25·6	1200	2630	3350
I 351	12·4	8	21·9	3980	2760	5500
II 2003	12·6	5	21·0	5470	3020	8800
1501	12·6	56	26·3	1060	4170	3390
1514	10·8	120	22·3	1700	1320	1550
1535	9·9	40	22·9	940	660	1720
Jonckheere 320	12·3	11	22·5	3190	3470	4260
I 418	10·6	14	21·3	2040	2290	1800
2022	12·4	28	24·6	1710	3310	4570
II 2149	10·5	15	21·4	1920	870	2250
II 2165	11·5	9	21·3	3150	2880	4610
Jonckheere 900	11·8	12	22·2	2780	2760	4300
2371–2	12·6	54	26·3	1080	3630	4740
2392	8·5	47	21·9	670	420	860
2438	11·8	68	26·0	830	1660	3920
2440	10·6	54	24·3	840	2000	2640
2452	13·3	22	25·0	2290	3020	4700
2610	13·6	38	26·5	1580	4790	8750
II 2448	11·5	8	21·0	3370	1820	2920
2792	13·5	10	23·5	4070	4570	5400
2818	13·0	40	26·0	1420	3630	7520
2867	9·7	8	19·2	2300	790	1900
II 2501	11·3	2	17·8	6430	1660	2550
3132	8·2	30	20·6	830	400	780
II 2553	13·0	4	21·0	6730	360	3890
3211	11·8	8	21·3	3560	2090	2850
3242	9·7	40	22·7	910	580	1640
II 2621	9·5	2	16·0	3730		1470
3587	11·1	203	27·6	330	2290	3630
$11^h\ 24^m.0$	11·4	15	22·3	2260		2090
3918	8·4	10	18·4	1510	4400	1220
4361	11·7	81	26·2	720	1320	3470
II 3568	10·8	18	22·1	1820	1900	2340
II 4191	12·0	5	20·5	4880		4070
5189	11·0	20	22·5	1750		2430
CD $-50°$ 8073	12·1	10	22·1	3280	2400	5300
5315	13·0	5	21·5	5920	3630	5750
II 4406	10·6	20	22·1	1640	1200	2430
5873	13·3	3	20·7	8430	4170	11600

TABLE I—*continued*

N.G.C. (or R.A.)	m	a	S	Distances in parsecs, estimated by Camm	Vorontsov-Velyaminov	Berman
5882	10·5	7	19·7	2950	1140	1780
$15^h\ 26^m{\cdot}2$	12·5	24	24·4	1930	2880	3000
6058	13·6	25	25·6	2160	4170	3460
6072	14·1	50	27·6	1350	6020	12300
II 4593	11·1	15	22·0	2150	1000	2000
6153	11·5	2	18·0	6790	1820	2780
6210	10·0	20	21·5	1480	790	1720
II 4634	11·1	20	22·6	1790	2630	3330
II 4637	13·6	2	20·1	11220	4790	4800
II 4642	13·4	2	19·9	10760	2760	12300
6309	12·4	19	23·8	2250	1900	4570
6369	14·2	28	26·4	2130	7240	8050
$17^h\ 35^m{\cdot}8$	13·6	5	22·1	6550	4790	7240
CD −29° 13998	12·0	3	19·4	6400	2290	3950
6439	14·7	5	23·2	7830	5250	12500
6445	12·7	50	26·2	1160	3980	5000
$17^h\ 47^m{\cdot}9$	13·8	2	20·3	11690	5240	7180
$17^h\ 49^m{\cdot}2$	13·6	5	22·1	6550	4790	5250
$17^h\ 53^m{\cdot}3$	11·4	2	17·9	6610	1740	2090
6543	8·7	22	20·4	1090	520	1080
6537	12·5	5	21·0	5370	2880	4670
6563	13·6	50	27·1	1280	5250	10800
6565	12·8	10	22·8	3680	3980	7350
6572	9·2	16	20·2	1440	760	1230
6567	11·7	11	21·9	2880	2000	3990
6578	14·6	8·5	24·2	5350		5500
II 4699	11·9	5	20·4	4760	2160	6790
$18^h\ 13^m{\cdot}0$	12·9	6·5	22·0	4940	3470	4360
6620	14·9	5	23·4	8050	9110	10000
6629	12·8	16	23·8	2680	2190	3890
6644	12·2	2·5	19·2	7310	2510	6370
II 4732	13·3	2	19·8	10520	4170	9640
II 4776	12·6	8	22·1	4110	2880	5830
CD −32° 14673	10·9	4	18·9	4280	1380	5300
I 1295	15·0	120	30·4	730	9120	3000
6720	9·0	83	23·6	500	660	1640
6741	11·7	9	21·5	3270	2000	3910
$18^h\ 58^m{\cdot}7$	13·4	5	21·9	6340	4370	12700
6751	12·9	21	24·5	2250	2510	4030
6772	14·2	75	28·6	1000	6310	13200
I 1297	11·8	2	18·3	7350		4430
II 4846	12·7	2	19·2	9200	3020	6610
6778	13·4	25	25·4	2110	3980	6250
6781	12·0	106	27·1	610	2880	3280
6790	11·4	2	17·9	6610	1740	4650
6803	11·3	5·5	20·0	4000	1740	2640
6804	12·8	63	26·8	990	4170	3600
6807	13·8	2	20·3	11690	5250	12600
BD +30° 3639	9·6	5	18·1	2780	760	1050
6818	9·6	22	21·3	1300	870	2380
6826	9·2	27	21·4	1070	520	1050

TABLE I—*continued*

N.G.C. (or R.A.)	m	a	S	Distances in parsees, estimated by Camm	Vorontsov-Velyaminov	Berman
6833	13·8	2	20·3	11690	5250	9680
6842	13·6	50	27·1	1280	4790	3530
6853	8·2	480	26·6	130	300	1040
6879	13·6	5	22·1	6550	2400	7180
6881	14·7	5	23·2	7830	6610	4570
6884	12·0	7·5	21·4	3860	3020	6890
6886	12·3	9	22·1	3630	2510	7240
6891	12·1	15	23·0	2520	1740	2750
6894	13·8	44	27·0	1450	6920	6310
II 4997	11·4	2	17·9	6610	1740	2340
6905	12·1	44	25·3	1190	2190	3870
7008	13·3	86	28·0	820	4170	3800
7009	7·9	44	21·1	630	440	930
7026	12·5	25	24·5	1880	3160	3020
7027	9·8	18	21·1	1520	1100	2130
7048	11·3	60	25·2	860	1660	3470
II 5117	13·3	2	19·8	10520	4170	7010
$21^h\ 29^m{\cdot}1$	12·7	5	21·2	5600	3160	5650
7139	13·8	86	28·5	860	6310	10400
II 5217	11·5	7·5	20·9	3500	3020	3060
7293	7·5	900	27·3	75	180	1050
$22^h\ 32^m{\cdot}2$	15·0	30	27·4	2200		3000
7354	13·3	32	25·8	1740	3470	4830
7408	12·8	72	27·1	890	3310	3000
1470	8·1	70	22·3	490	2090	840
7635	9·9	205	26·5	290	520	900
7662	8·7	32	21·2	880	550	1200
$23^h\ 21^m{\cdot}9$	14·0	10	24·0	4410		4780

3. *The Surface Brightnesses.*—The apparent magnitudes used here are taken from the table at the end of Berman's paper,* and the angular diameters are the major angular diameters, given by Vorontsov-Velyaminov.† Both quantities are known for 111 nebulæ ; for a further 12, the angular diameters are given as less than two seconds of arc, and these will be considered actually to be two seconds.

The following symbols will be used repeatedly :—

m, the apparent magnitude of the nebula.
M, the absolute magnitude.
a, the major angular diameter, in seconds of arc.
D, the major linear diameter, in astronomical units.
r, the distance from the Sun, in parsecs.

Between these there are the relations:

$$M = m + 5 - 5 \cdot \log_{10} r, \tag{1}$$

$$D = r \cdot a. \tag{2}$$

Hence we define the surface brightness, S, by the equation

$$S = M + 5 \cdot \log D = m + 5 + 5 \cdot \log a. \tag{3}$$

* *Lick Obs. Bull.*, **18**, 73, 1937. † *Russ. Astron. J.*, **11**, 54, 1934.

The surface brightness is found for each nebula, and the frequency curve is given in fig. 1. The ordinate at any value S is the number of nebulæ for which the surface brightness lies between $(S-1)$ and $(S+1)$. The curve shows two distinct maxima, and can readily be resolved into two curves, each symmetrical about a well-defined maximum. This suggests that there are

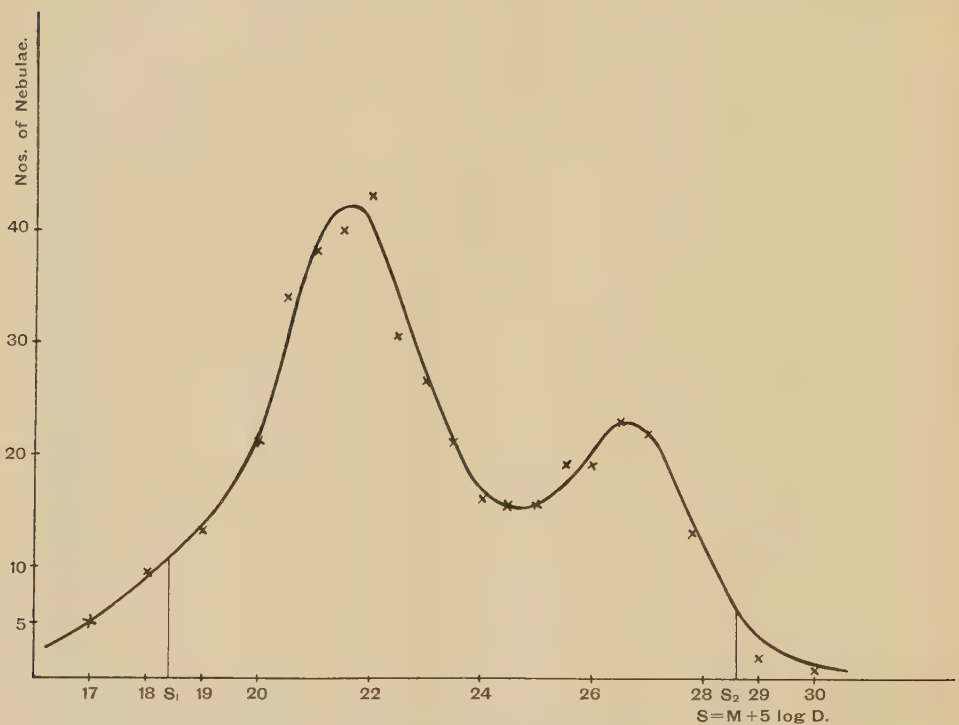

Fig. 1.—*The frequency distribution of the surface brightnesses of planetary nebulæ.*

two distinct types of nebula, but it must first be shown that this peculiarity is not due to the selection of the material.

The spectrum of a planetary nebula is so distinctive that any nebula, sufficiently bright to be seen, will be recognized, however small its diameter may be. The material will not therefore be deficient in nebulæ of small angular diameter, but will contain, as we know, at least twelve nebulæ of which the angular diameters should be smaller. If these are reduced from 2″ to 1″, and the frequency of surface brightness again examined, the curve to the right of the first maximum is unaltered. To the left of this point the fall is at first steeper, but the curve extends further towards small values of S. The evidence for two types of nebula still remains.

The faintest planetary included is of the fifteenth magnitude, and the material is likely to be deficient beyond the fourteenth. If all nebulæ fainter than the fourteenth magnitude are omitted, the first maximum and minimum are unaffected, but the second maximum is reduced. Thus it is probable that, were the faint planetaries better represented, the second maximum would be accentuated, and the natural division would be more pronounced.

In view of this division, it can hardly be supposed that both types have the same mean linear diameter, or the same mean absolute magnitude.

If the distance of a planetary were known, then on a diagram relating absolute magnitudes and linear diameters, the nebula would be represented by a single point. As the distance is unknown, the best that can be done is to draw for each nebula the curve of constant surface brightness, defined by (3), and this curve must pass through the required point. A number of curves of constant surface brightness are given in fig. 2, shown dotted. Further, it might be supposed that the nebulæ all satisfy some relation,

$$D = f(M). \tag{4}$$

Were this relation known, the curve (4) could also be drawn, and the points of intersection with the curves (3) would determine the true values of D and M. If the relation (4) holds only approximately, then an error will be introduced, corresponding to a slight displacement of each point from its true position along the curve (3). An error of this kind must occur in any attempt to assign distances by a statistical method, since it corresponds to the departure of an individual value from a mean value.

The relation (4) is now supposed to be of the form

$$D = aM + b. \tag{5}$$

This form is chosen for its simplicity ; it has the property that, if a is taken to be zero, the linear diameters are constant—which was the basic assumption made by Berman ; if $1/a$ is zero and b/a is finite, absolute magnitudes are constant—which was the basic assumption made by Vorontsov-Velyaminov. Thus our procedure includes those of these two authors as particular cases.

4. *The Determination of Distances.*—The method of estimating distances is now, in principle, straightforward, but it is first necessary to find suitable values of the parameters, a and b. Here a new principle is adopted, namely that, though the nebulæ cannot all have the same linear diameter and the same absolute magnitude, the dispersions in linear diameters and in absolute magnitudes shall both be as small as possible.

Referring again to fig. 2, we shall choose that transversal, $D = aM + b$, on which the dispersion of the points of intersection is a minimum. However, a distinction must be drawn between a minimum arising on account of the frequency distribution of fig. 1, and a minimum which is approached as D tends to zero, and which is due to the shrinkage of the scale. This distinction is preserved by reducing the dispersion to a dimensionless quantity, and by seeking values of a and b which will give a minimum value of the quantity

$$\Sigma(D - \overline{D})^2/(D_1 - D_2)^2. \tag{6}$$

In this, $\overline{D}$ is the mean linear diameter, and D_1 and D_2 are linear diameters corresponding to particular values, S_1 and S_2, of the surface brightness.

This process is illustrated in fig. 2 and fig. 2A ; in fig. 2, the particular curves of constant surface brightness, S_1 and S_2, are drawn as full lines, and the straight lines shown are three possible positions of the line given by (5).

In fig. 2A, the three straight lines are reproduced, each on a different scale, and the scales are chosen so that the intercept between the curves S_1 and S_2 is the same for all. The dispersion of the points along any line in fig. 2A corresponds to the value of (6) for the same line in fig. 2.

The values of S_1 and S_2 are chosen from the frequency curve, fig. 1; the ordinate at S_1 is a quarter of the first maximum ordinate, and the ordinate

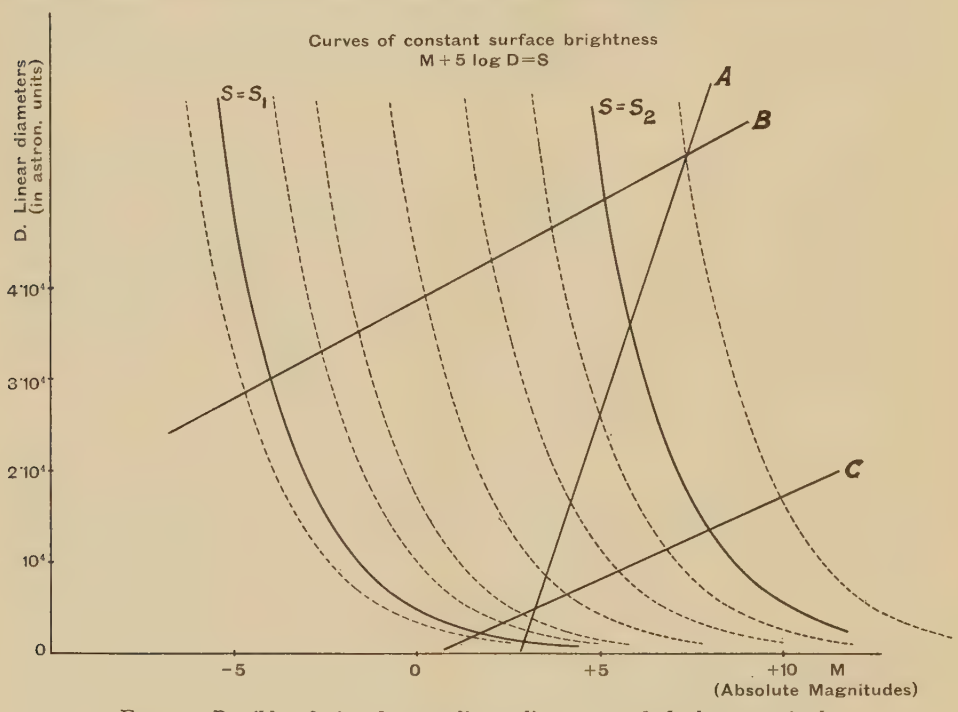

FIG. 2.—*Possible relations between linear diameters and absolute magnitudes.*

at S_2 is a quarter of the second maximum. More than 90 per cent. of the values of S are between S_1 and S_2.

The quantity (6) is a function of a single variable, u, given by

$$u = 5 \,.\, \log_{10} a - b/a.$$

The condition that (6) should be minimum is

$$U \equiv N\left[1 - (\overline{D} + 5a\eta)\overline{\left\{\frac{1}{D + 5a\eta}\right\}}\right] + \frac{\Sigma(D - \overline{D})^2}{(D_1 + 5a\eta)(D_2 + 5a\eta)} = 0. \qquad (7)$$

Here, N is the number of nebulæ, η denotes $\log_{10} e$, and $1/(D + 5a\eta)$ is the mean value of $1/(D + 5a\eta)$. The solution of (7) is determined by trial and error, and U has been calculated for seven values of the variable u. In every case the two separate terms of U are of the order 10, and their difference is less than 0·1; the solution of the simultaneous equations (3) and (5) for D is only correct to three significant figures, but the value of U is susceptible to errors in the fourth significant figure. The zero of U must therefore be found

by assuming a linear relation between U and u in this region, and determining the relation from the seven sets of values, by the method of least squares. Thus it is found that the value of u which will satisfy (7) is 15·525, so that a and b are connected by

$$5 \cdot \log_{10} a - b/a = 15{\cdot}525. \qquad (8)$$

One further condition is necessary to determine the separate values of a and b, and for this, following Vorontsov-Velyaminov, it is assumed that the

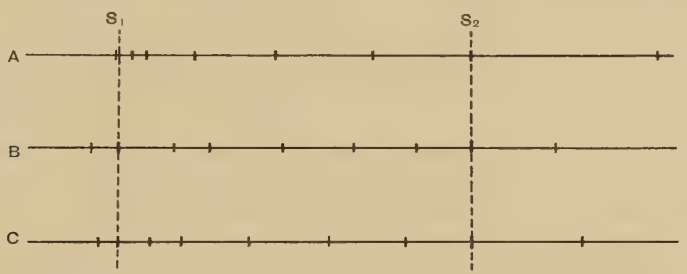

FIG. 2A.—*The transversals of fig. 2, when the intercept between the curve S_1 and S_2 is made constant.*

mean absolute magnitude $\bar{M}$ of the planetaries is +0·2. This value was obtained from the radial velocities—a step which it had been hoped to avoid. No weight is laid on the value +0·2—indeed the mean absolute magnitude finally obtained is +0·13—but it must be admitted that the final distances will no longer depend on apparent magnitudes and angular diameters only.

As a part of the determination of U, the quantities $\bar{D}$ and $\overline{1/(D+5a\eta)}$ were evaluated for $a = 5000$ astr. units, and four different values of b, and also for $a = 10{,}000$ astr. units, and three different values of b. From the relations

$$\bar{D} = a\bar{M} + b,$$

$$\delta\bar{M} = -5\eta\{\overline{1/(D+5a\eta)}\}\delta b,$$

the values of $\bar{M}$ are determined for these two values of a, and the values of b given by (8). Assuming a linear relation between $\bar{M}$ and a over this range, we find that $\bar{M}$ will be +0·2 when a takes the value 8820 astr. units. The corresponding value of b, as given by (8), is 37,060 astr. units. The relation (5) is now rewritten as

$$D = M \cdot 8820 + 37{,}060. \qquad (9)$$

At this stage it may be as well to summarize the three principles from which the distances are found. The two alternative hypotheses of constant linear diameters and constant absolute magnitudes are replaced by the relation (5). The two parameters of this relation are not arbitrary, but must give a mean absolute magnitude of +0·2. From the one-parameter system of lines, we choose the line along which the dispersion of points, as measured by the quantity (6), is a minimum.

The absolute magnitude of each planetary was now determined from (3) and (9). The mean absolute magnitude comes out as +0·13, which is rather brighter than had been expected. However, as Berman's value of the mean

absolute magnitude is −0·88, a value of +0·13 is considered satisfactory. The dispersion in absolute magnitudes is 1·9 magnitudes, which may be considered rather large.

One very noticeable feature among the absolute magnitudes is that nebulæ of exceptionally large angular diameter are always found to be exceptionally faint. This is a consequence of the attempt to avoid the enormous range of linear diameters which was found by Vorontsov-Velyaminov.*

From the absolute magnitudes, the distances were calculated by means of (1); the distances, in parsecs, are given in the fifth column of Table I. The first column gives the N.G.C. number, or the R.A., of the nebula; the second and third contain the observational data, the apparent magnitudes given by Berman,† and the major angular diameters, in seconds of arc, taken from Vorontsov-Velyaminov's catalogue.‡ The fourth column gives the surface brightness, as defined by (3). In the sixth and seventh columns are listed the distances assigned by Vorontsov-Velyaminov § and by Berman.

The outstanding differences arise in the case of objects of exceptionally large angular diameter, of which the distances, as estimated by this method, are very small. For the purpose of studying galactic rotation, this particular discrepancy is not serious, since the distances of these objects are comparatively small, whatever method is used to obtain them.

In fig. 2B are given the correlation diagrams, in which the distances found by Vorontsov-Velyaminov and by Berman are plotted against those determined in this paper. In both cases the dispersion is very large; apart from the peculiarity of nebulæ of large angular diameter, there are no systematic differences in the comparison with Berman. On the other hand, Vorontsov-Velyaminov's distances rather tend to fall short. Since they are based on apparent magnitudes only (whereas Berman has made use of the angular diameter, the radial velocity, and the apparent magnitude of each nebula), such a systematic difference is not surprising. The difference is even greater in the comparison of the two given sets of distances. They have 116 objects in common, and in 102 cases Berman's distance is the greater.

Although our agreement with Berman is so poor, it might be added that the processes described in § 5 have also been carried out with the use of Berman's distances, and the curve corresponding to fig. 3 is almost coincident with the curve obtained from our own distances.

5. *Properties of Galactic Rotation Derived from the Radial Velocities.*— The radial velocities of 102 planetary nebulæ are given by Campbell and Moore,‖ and these were combined with the distances just obtained, in order to examine galactic rotation.

It is supposed that the galaxy is rotating in concentric rings in its own plane; the angular velocity of each ring, ω, is measured in the direction of decreasing galactic longitude, and is a function of R, the radius of the ring, only. No allowance is made for the fact that the Sun is not exactly in the

* *Z. f. Astroph.*, **8**, 202, 1934.
† *Lick Obs. Bull.*, **18**, 73, 1937.
‡ *Russ. Astron. J.*, **11**, 54, 1934.
§ *Z. f. Astroph.*, **8**, 204, 1934.
‖ *Publ. Lick Obs.*, **18**, 213, 1932.

galactic plane. The sole effect of this is that the term "galactic centre," as subsequently used, refers to the point of intersection of the axis of rotation with a plane, normal to it, through the Sun. The longitude of the galactic

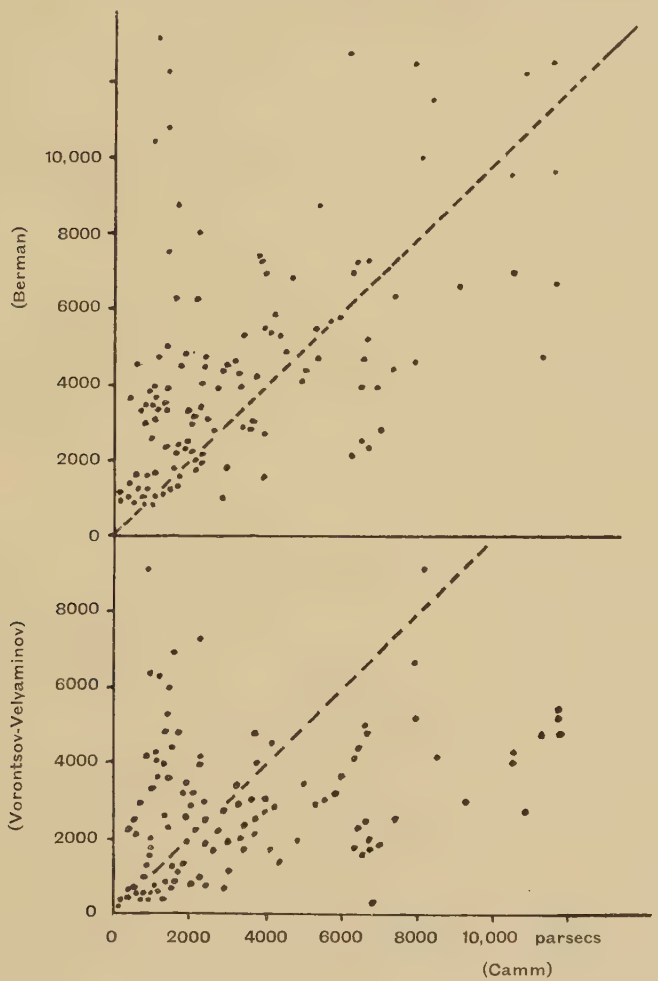

FIG. 2B.—*The correlation of distances.*

centre, l_0, is provisionally assumed to be 325°, and R_0, the distance from the Sun, to be 10,000 parsecs.

The radial velocities, ρ, were all corrected for solar motion, which was assumed to be 19·5 km./sec., towards the apex, R.A., 18^h, dec. $+30°$. Then for a nebula at a distance R from the axis of rotation, and of galactic co-ordinates (l, b), the corrected radial velocity, ρ_c, is given by

$$\rho_c = R_0[\omega(R) - \omega(R_0)] \sin (l - l_0) \cos b.$$

This expression, given by Bottlinger,* is easily derived from the assumptions

* *Berlin-Babelsberg Veröff.*, **10**, Heft 2, 1933.

made, and is exact, in the sense that it involves no approximations.* For simplicity it is more conveniently written:

$$\rho_c = f(R, R_0) \sin (l - l_0) \cos b. \qquad (10)$$

However, this formula is obtained by considering a fluid motion, in which the velocity corresponding to any point is quite definite at any instant; it will not be exact for statistical motion, in which there is a velocity-dispersion superposed on a mean motion. This, in itself, is not serious, for in the process of averaging, the effect of the velocity-dispersion will be much reduced. But a more serious error may occur when (10) is used in the more convenient form

$$f(R, R_0) = \rho_c \operatorname{cosec} (l - l_0) \sec b. \qquad (11)$$

If $\sin (l - l_0)$ is small, the possible error in (10) will be greatly magnified in (11). In consequence, (11) can only be safely applied to nebulæ for which $\sin (l - l_0)$ exceeds $\sin 15°$ in absolute value; there are 76 such nebulæ. For these, $f(R, R_0)$ was evaluated from (11), and R was found from the relation

$$R^2 = R_0^2 + r^2 \cos^2 b - 2R_0 r \cos b \cos (l - l_0). \qquad (12)$$

The results were grouped according to the distance R, and the average value of R and $f(R, R_0)$ was found for each group. A curve was drawn, similar to that in fig. 3, to show the relation between $f(R, R_0)$ and R.

The slope of this curve at $R = R_0$ should be numerically equal to $2A$, where A is the constant derived by Oort.† The value of A from this curve is 0·0095 km./sec./parsec, which should be compared with the value 0·0155, in the same units, obtained by Plaskett and Pearce.‡

It was this second value of A which Vorontsov-Velyaminov used to derive his set of distances; Ogrodnikoff, using those distances, derives the value of A as 0·0090. Berman's value, in the same units, is 0·0140.

There seems to be one possible explanation for our unusually small value of A; the application of Oort's approximate method is equivalent to replacing the curve of fig. 3 by a straight line. Clearly, over a large range of R on either side of the value R_0, the slope of the best straight line is much steeper than the slope of the tangent at R_0; this effect will be increased in this particular case, for 70 per cent. of the objects used are at distances less than R_0 from the galactic centre, and in this region the slope varies from 0·0190 to 0·2000 km./sec./parsec.

The preliminary curve similar to fig. 3 has another peculiarity, for

* The first approximation to it, in the case of objects near the Sun, is the first term of an expansion in Taylor series. The difference $(R - R_0)$ is replaced by $r \cdot \cos (l - l_0) \cdot \cos b$, and the expression reduces to the form given by Oort, namely, $Ar \cdot \sin 2(l - l_0) \cos^2 b$. For more distant objects the expansion must be made to more terms, and it is no longer sufficient to replace $(R - R_0)$ by $r \cos (l - l_0) \cos b$. The resulting expression, correct to the sixth harmonic, has been given by Miss Hayford in the *Lick Obs. Bull.*, **16**, 56, 1932.

† *B.A.N.*, **3**, 276, 1927.

‡ *Publ. Dom. Ap. Obs.*, **5**, 300, 1933.

$f(R, R_0)$ is definitely negative at $R = R_0$, when, of course, it should be zero. The true explanation is that the solar motion, for which the radial velocities have been corrected, is not the value determined from the nebulæ themselves. At first sight, however, it suggests that the galactic centre has not been

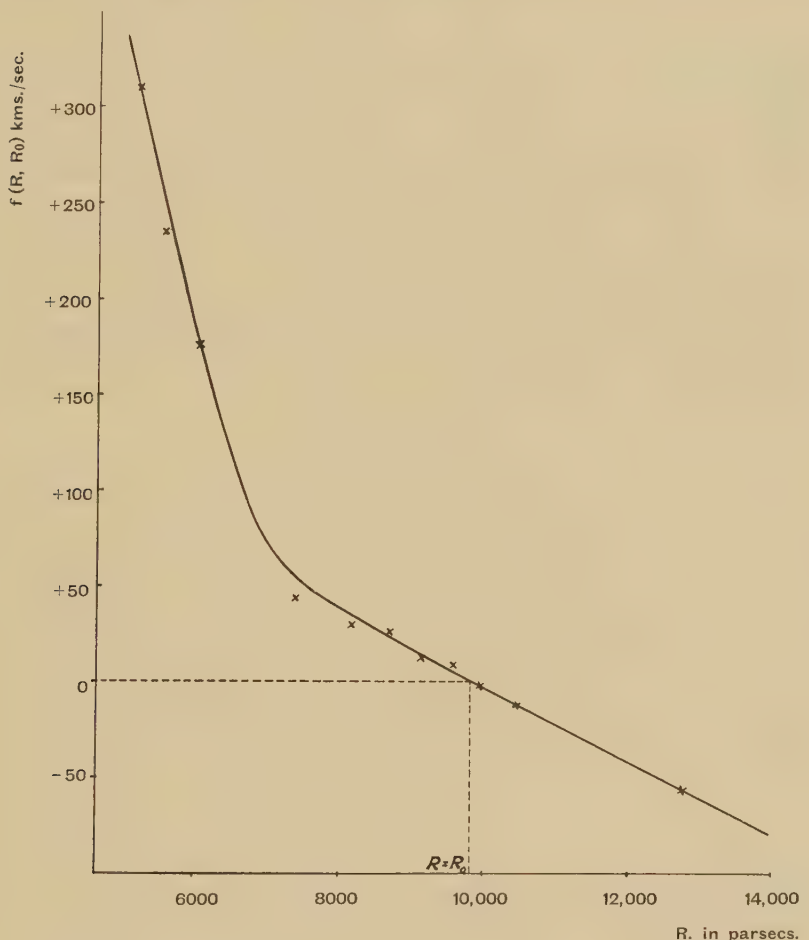

FIG. 3.—*The relation between* $f(R, R_0)$ *or* $R_0[\omega(R) - \omega(R_0)]$ *and* R.

accurately located; hence the first correction to be applied was a slight displacement in the position assumed for the galactic centre.

6. *The Distance and Direction of the Galactic Centre.*—In any attempt to locate the galactic centre, it is obvious that the planetaries in the neighbourhood of the Sun will have little or no weight, so that, in the first instance, the corrections are determined from the fifteen nebulæ, of which the distance from the Sun exceeds 5000 parsecs.

The method used assumes that the curve of $f(R, R_0)$ is correct if distances are measured from the true centre. This is now supposed to be at a distance $(R_0 + \delta R_0)$, in the direction of galactic longitude $(l_0 + \delta l_0)$. Equation (10) is now written:

$$\rho_c - f(R, R_0)\sin(l-l_0)\cos b - \delta R_0 \frac{\partial}{\partial R_0}\{f(R, R_0)\}\sin(l-l_0)\cos b$$
$$- \delta l_0 \frac{\partial}{\partial l_0}\{f(R, R_0)\sin(l-l_0)\}\cos b = 0. \quad (13)$$

In this, R is a function of R_0 and l_0, as defined by (12). Applying (13) to the fifteen planetaries, we form the normal equations, and solve for δR_0 and δl_0.

The longitude of the galactic centre is now altered to 333°, which is the value obtained for the planetaries by Oort,* and independently by Berman.†

The revised distance of the galactic centre is estimated at 10,400 parsecs, which is rather in excess of Berman's value of 9360 ± 220 parsecs, and also of the value, 9500 parsecs, given by Ogrodnikoff.‡

As the order in which the corrections are applied may well lead to inaccuracies, the above method of correction was applied later, after the redetermination of solar motion, to 90 objects. The final values of l_0 and R_0 were:

$$l_0 = 332^\circ\ 24' \pm 9',$$
$$R_0 = 9830 \pm 110 \text{ parsecs.}$$

7. *The Determination of Solar Motion.*—The peculiarity, already mentioned, that $f(R, R_0)$ is not zero at $R = R_0$, still persists after we have applied the correction to the position of the galactic centre. The discrepancy may now be attributed to an inaccurate value of the solar motion. The motion of the Sun relative to the rotating ring of nebulæ of radius R_0 can be conveniently resolved into three components, u, v, w; w is towards the galactic pole, and u and v are in the galactic plane, in the directions of longitude 333° and 63°. If ρ denotes the observed, uncorrected radial velocity, (10) can be written:

$$\rho - f(R, R_0)\sin(l-l_0)\cos b + u\cos(l-l_0)\cos b + v\sin(l-l_0)\cos b$$
$$+ w\sin b = 0. \quad (14)$$

In the same way (11) now becomes:

$$f(R, R_0) = \rho\ \mathrm{cosec}\,(l-l_0)\sec b + u\cot(l-l_0) + v + w\ \mathrm{cosec}\,(l-l_0)\tan b.$$

The process of averaging, to determine the points on fig. 3, followed by further averaging in drawing a smooth curve to fit them, will reduce, and may even eliminate, errors due to the components u and w, but the error due to v is the same for every value of $f(R, R_0)$, and is exactly the displacement which was found in $f(R, R_0)$ at $R = R_0$. This is provisionally adopted as the value of v, and the whole curve is translated parallel to the axis of f, until $f(R_0, R_0)$ is zero.

One effect of taking average values is that the range of R for which the curve is drawn does not include the nebulæ at the greatest and least distances from the galactic centre. At the outer limit, the curve can be continued

* *B.A.N.*, **3**, 278, 1927.
† *Lick Obs. Bull.*, **18**, 65, 1937.
‡ *Poulkovo Obs. Circ.*, **21**, 29, 1937.

smoothly beyond the last point which determines it without serious error. However, on account of the extremely rapid variation of $f(R, R_0)$ for values of R less than 7000 parsecs, it is impossible to find a reliable value at 4000 parsecs, which is the inner limit of distance. Thus the residual radial velocity of the nebula nearest the centre is indeterminate.

On the other hand, the material can be increased at this stage by including a further fifteen nebulæ. These are nebulæ in the sectors from galactic longitude 138° to 168°, and 318° to 348°; because of the large values of cosec $(l - l_0)$ in these regions, they were considered unreliable for determining $f(R, R_0)$. Now that this function is known, it is possible to obtain theoretical values for their radial velocities, and so determine the residual velocities.

Values of u, v, w were found by solving 90 equations of the type (14). The process was repeated twice, since at each stage the curve of $f(R, R_0)$ was slightly modified. The final values, given in Table II, were determined simultaneously with a K-term, and a final correction for the galactic centre. Table II also gives the values of u, v, w for the planetary nebulæ, as deduced from the solar motion found by Wirtz,* by Strömberg,† and by Ogrodnikoff.‡

TABLE II

The Components of Solar Motion, as determined from the Planetary Nebulæ

	u km./sec.	v km./sec.	w km./sec.
Wirtz	11·2	28·2	7·2
Strömberg	8·4	23·6	13·4
Ogrodnikoff	17·2	32·8	..
Camm	14·4 ± 1·2	26·7 ± 3·6	−9·6 ± 9·1

The indeterminate nature of the value of w is explained by the small galactic latitudes of all the objects. Since w is the component of solar motion towards the galactic pole, the effect of w on the radial velocities is always very small.

8. *The K-term.*—As has already been pointed out, the final determination of the constants must evaluate them all simultaneously. For this reason, the final values of R_0, l_0, u, v, w, already given, were found from 90 equations of the form

$$\rho - f(R, R_0) \sin (l - l_0) \cos b - \delta R_0 \frac{\partial f}{\partial R_0} \sin (l - l_0) \cos b$$

$$- \delta l_0 \frac{\partial}{\partial l_0} \{f \cdot \sin (l - l_0)\} \cos b + u \cos (l - l_0) \cos b + v \sin (l - l_0) \cos b$$

$$+ w \sin b - K = 0. \quad (15)$$

The value of K is found to be $+1{\cdot}4 \pm 2{\cdot}8$ km./sec., and is to be compared with Wirtz's value, +2 km./sec., and that found by Ogrodnikoff, $6{\cdot}4 \pm 2{\cdot}9$ km./sec.

With this K-term, and the final values of the constants, the final curve of $f(R, R_0)$ was drawn, and is given in fig. 3. The root-mean-square residual

* *A.N.*, **215**, 204, 1922.

† *Ap. J.*, **61**, 371, 1935.

‡ *Poulkovo Obs. Circ.*, **21**, 24, 1937.

radial velocity for 90 nebulæ is 33·8 km./sec.; if the six largest residuals are rejected, the root-mean-square residual is reduced to 27·0 km./sec. Vorontsov-Velyaminov * evaluates the same quantity, and obtains 38·8 km./sec. for 100 nebulæ, and, rejecting the ten largest residuals, it is reduced to 27·6 km./sec. It can therefore be claimed that the use of the curve for $f(R, R_0)$ enables us to account for the observed radial velocities more nearly than other methods.

9. *An Alternative Form of K-term.*—It has been suggested by Milne † that, in addition to rotating, the galaxy is also expanding : the supposed law of expansion is that a star at a distance R from the galactic centre should move outwards with a velocity kR, and the actual value of k suggested in that paper was 5 km./sec. per 10,000 parsecs.

The effect of this expansion on the relative motion of a nebula at a distance r from the Sun is to give the nebula an additional speed of recession, kr. Thus the value of k could be determined by replacing the constant K in (15) by the term kr. Clearly, for most of the objects from which galactic rotation has been studied, the distances from the Sun are too short to give a reliable value of k, but among the planetary nebulæ there are values of r exceeding 10,000 parsecs, and a determination is possible.

With K replaced by kr, the 90 equations of the type (15) were solved, and the value of k was found to be $+7{\cdot}3 \pm 8{\cdot}2$ km./sec. per 10,000 parsecs—which is in good agreement with the theoretical value. All the other constants are slightly altered, and their probable errors are all increased. On the other hand, the root-mean-square residual velocity is negligibly reduced —from 33·81 to 33·78 km./sec. It is thus very difficult to decide from the observations whether this form of K-term has any advantage over the simple constant term. On theoretical grounds, of course, it is much the better form, since there is a physical interpretation of it, whereas it is much more difficult to account for a constant K-term.

10. *The Proper-Motions of the Planetary Nebulæ.*—The proper-motions of 21 nebulæ have been determined by van Maanen.‡ These were used to find the linear speed of rotation at the distance of the Sun. The two elements of proper-motion were combined to give μ_l, the proper-motion in galactic longitude. Then $4{\cdot}74 \,.\, r \,.\, \cos b \,.\, \mu_l$ is the linear speed in km. per second, parallel to the galactic plane, and transverse to the line of sight. The formula corresponding to (10) was found to be

$$f(R, R_0)\{R_0 \cos (l - l_0) - r \cos b\}/R_0 + u \sin (l - l_0) - v \cos (l - l_0) - 4{\cdot}74r \,.\, \cos b \mu_l - r \cos b \,.\, \omega(R_0) = 0. \qquad (16)$$

Since the curve for $f(R, R_0)$ is known, $\omega(R_0)$ is the only unknown in this equation. If all 21 objects are included, the value of $R_0\omega(R_0)$ is 162 km./sec. The root-mean-square residual velocity, in linear measure, is 50 km./sec. ; two of the objects have residual velocities of 130 km./sec. In view of the small number of nebulæ, two such large residuals are improbable, and these two objects were rejected.

* *Z. f. Astroph.*, 8, 207, 1934. † *Proc. Roy. Soc.*, A, **160**, 20, 1937.
‡ *Ap. J.*, 77, 191, 1933.

From the remaining 19 nebulæ, $R_0\omega(R_0)$ was found to be 195 ± 43 km./sec. This is much lower than the value of 275 km./sec., obtained by Plaskett and Pearce.*

The mean peculiar motion is now 32·6 km./sec., which compares well with the value of 33·8 km./sec., from the radial velocities.

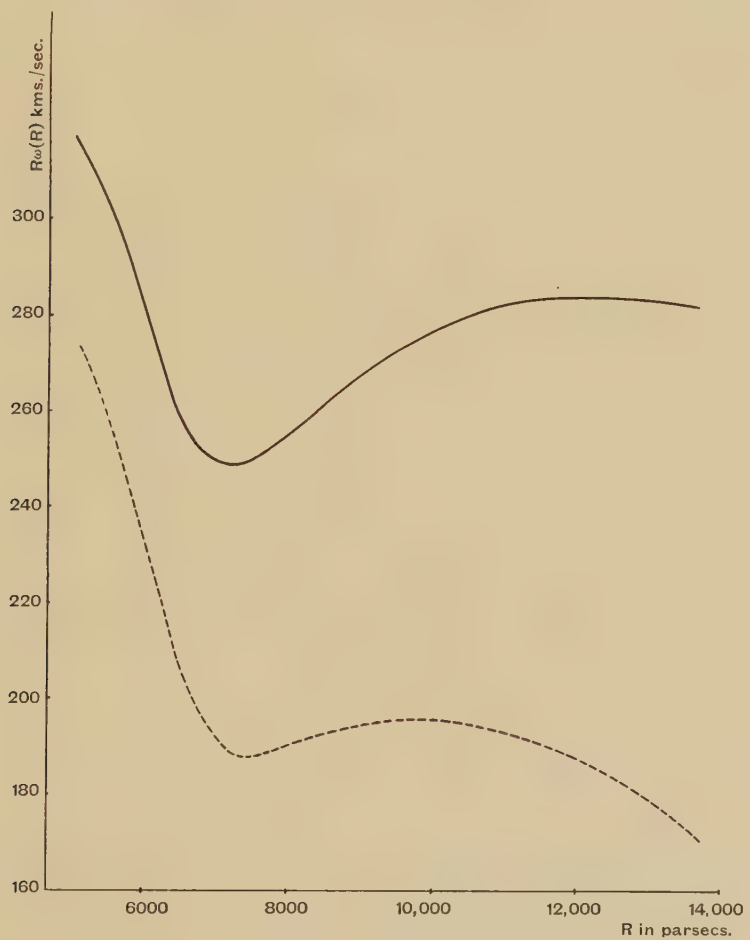

FIG. 4.—*The variation of the linear speed of rotation, $R\omega(R)$.*

Although it would be difficult to justify the step, it may be pointed out that, if the object with the greatest peculiar motion is again omitted, the value for the 18 nebulæ rises to 262 km./sec. It can only be concluded that, with the great uncertainties of the proper-motions, 21 objects are not sufficient to give a reliable value of $R_0\omega(R_0)$.

The variation of linear speed can now be found, for we have

$$R\omega(R) = [f(R, R_0) + R_0\omega(R_0)]R/R_0.$$

This relation between $R\omega(R)$ and R is given in fig. 4; the full curve is the

* *Publ. Dom. Ap. Obs.*, 5, 301, 1936.

result of taking $R_0\omega(R_0)$ to have the usual value of 275 km./sec., and the dotted curve comes from our value, 195 km./sec.

11. *The Gravitational Attraction of the Galaxy.*—On the assumption that the rotation, of which we have now found the variation, corresponds to circular orbits described under the gravitational attraction of the whole galaxy, then $\Omega(R)$, the gravitational potential due to the galaxy at a point in the galactic plane, at a distance R from the centre, must satisfy

$$\frac{d\Omega}{dR} + R\{\omega(R)\}^2 = 0. \qquad (17)$$

If we adopt 275 km./sec. as the value of $R_0\omega(R_0)$, we obtain the full curve of fig. 5, showing the variation of gravitational force with distance. This curve has one obvious peculiarity, for in the region of R less than 7000 parsecs, the curve falls more rapidly than M/R^2. If the mass of the galaxy is distributed symmetrically about the centre, this rapid fall is impossible, for no such distribution of attracting matter can give a fall steeper than M/R^2. The cause of this discrepancy can be traced to the errors in fig. 3. If the root-mean-square residual velocity is calculated separately for each group—that is, for each point in fig. 3—it is found that for R exceeding 8200 parsecs, the greatest value is 33·4 km./sec. On the other hand, for the three points for which R is less than 8200 parsecs, the mean peculiar motion of the group rises from 36·6 to 49·0 km./sec. Thus the curve of $f(R, R_0)$ is rather uncertain for R less than 8200 parsecs. In passing from fig. 3 to fig. 5, the ordinates are squared, and as they are greatest in the region where they are least certain, the probable errors in fig. 5 will be very large in the region of R less than 8200 parsecs. This is probably the explanation of the too rapid fall of the curve in the region of 7000 parsecs.

As a first approximation to the spatial distribution of matter, it was supposed that the galaxy consisted of a thin circular disc of uniform density, together with a massive nucleus at the centre of the disc. However, if the gravitational force of this distribution of matter be evaluated, it is found that it cannot have a point of inflexion, such as is found in the natural curve of fig. 5.

The next most simple form of distribution is one in which the density of the disc decreases uniformly outwards. If ν is the density of the ring of radius r, and if c is the radius of the whole disc, the density then varies according to the law:

$$\nu = \nu_0(1 - r/c).$$

The values of the three constants, c, the radius of the disc, M_1, its mass, and M_0, the mass of the nucleus, are at our disposal, and are chosen in order to get the best agreement with the natural curve. The value of c has no great effect on the shape of the curve, and is assumed to be 15,000 parsecs. The dotted curve of fig. 5 is almost the best fit for this value of c. The mass of the disc comes out as $1{\cdot}01 \times 10^{11}$ Suns, and the mass of the nucleus, $0{\cdot}76 \times 10^{11}$ Suns. The total mass is thus $1{\cdot}77 \times 10^{11}$ Suns, which is comparable with the value of $1{\cdot}65 \times 10^{11}$, given by Plaskett and Pearce.*

* *Publ. Dom. Ap. Obs.*, 5, 303, 1936.

In order to find how close is the agreement between these two curves, it is interesting to deduce the curve of fig. 3 from the theoretical curve of fig. 5. It is then found that, for R greater than 10,000 parsecs, the observed and theoretical curves of fig. 3 do not differ by more than 3 km./sec. ; for smaller values of R the difference is somewhat larger, but at 8600 parsecs it is no

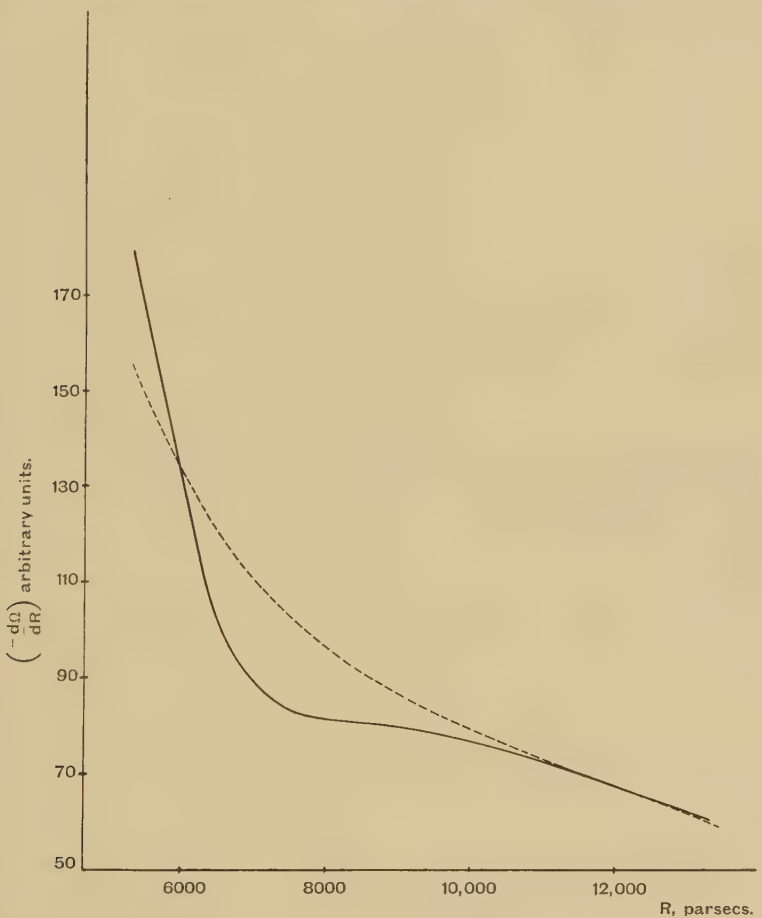

FIG. 5.—*The variation of the gravitational attraction*

more than 16 km./sec., and the greatest difference, occurring at 7300 parsecs, is 40 km./sec.

12. *Summary*.—The radial velocities of the planetary nebulæ have been analysed in an unusual way, in order to determine how the angular speed of rotation of the galaxy varies with galactic radius.

As the treatment required a knowledge of the distances of the nebulæ, these have been estimated by a rather crude, but consistent, method, in which apparent magnitudes and angular diameters are treated as being equally reliable indicators of distance.

The analysis of the radial velocities yielded values for the constants of solar motion, the distance and direction of the galactic centre, and the K-term.

The variation of the angular speed of galactic rotation with distance is shown graphically.

The proper-motions have also been examined, and it is shown how they can be used to determine the linear speed of rotation at the Sun's distance. In this case the proper-motions are too few to make an accurate estimate.

The linear speed at the Sun's distance is assumed, and the variation of the gravitational attraction of the galaxy is deduced. This variation is very similar to that arising from a thin circular disc, the density of which decreases uniformly outwards, together with a massive nucleus at the centre. The best agreement between this model and the observed radial velocities of the planetaries is obtained when a mass of $0{\cdot}76 \times 10^{11}\odot$ is assigned to the nucleus, and a mass of $1{\cdot}01 \times 10^{11}\odot$ is assigned to the disc; these give a total galactic mass of $1{\cdot}77 \times 10^{11}\odot$.

The whole investigation has only been possible because the exact expression for the relative radial velocity due to galactic rotation has been used throughout. Over so great an area of the galactic plane, approximate expressions would be inadequate.

My grateful acknowledgments are due to Professor H. H. Plaskett and Dr. H. Zanstra for their very useful criticism and suggestions; I am especially indebted to Professor E. A. Milne, who has most willingly given me help, encouragement and advice.

Oxford:
1938 *November.*

NOVA HERCULIS 1934: CONTOURS AND INTENSITIES OF ABSORPTION AND EMISSION BANDS DURING THE FIRST THREE MONTHS OF 1935.

E. G. Williams, M.A.

(Communicated by the Director, Solar Physics Observatory, Cambridge)

With the emergence of the second, more displaced, absorption system at the end of 1934 December, the spectrum of Nova Herculis entered on a phase of high complexity. The second absorption components were soon followed by a third set and, for some lines, several others. At the same time the number of elements giving lines was large, so that blending became general throughout the spectrum. Moreover, the comparatively simple forms of the absorption and emission contours typical of the first phase, which have been fully dealt with in a previous article,* were succeeded by contours on which it would be difficult to generalize at first sight.

These considerations have led to the following approach to the photometry of the spectrum. Firstly, attention has been confined to a few representative lines, chiefly those for which blending is least serious. Secondly, typical dates have been chosen from the very extensive series of observations available, and for these intensity diagrams covering several short spectral ranges have been prepared. These diagrams demonstrate better than could any words the character, variations and complexity of the nova bands. Thirdly, the more obvious features of the diagrams are discussed generally and for the different elements. This discussion is supplemented by intensity measures where necessary, but it will be obvious from the nature of the spectrum that high accuracy is not only unobtainable but usually unnecessary.

It is felt that such a survey of the contours is essential before any future analysis of the more complex and finer details of the spectrum can be profitably undertaken.

The Intensity Diagrams

The spectra were obtained and the photometer tracings made at the Solar Physics Observatory, Cambridge. Typical examples of each have been illustrated and the method of reduction explained in two earlier papers.* † The present diagrams (figs. 1 to 8) are drawn on a uniform scale. The abscissæ are reduced to displacements, expressed in kilometres per second from the normal position of the principal line in the region illustrated, with short vertical lines erected on the axis at intervals of 1000 km./sec. Ordinates are intensities, with horizontal lines at each 0·2 of the intensity in the continuous spectrum.

* E. G. Williams, *M.N.*, **97**, 612, 1937. † *M.N.*, **95**, 573, 1935.

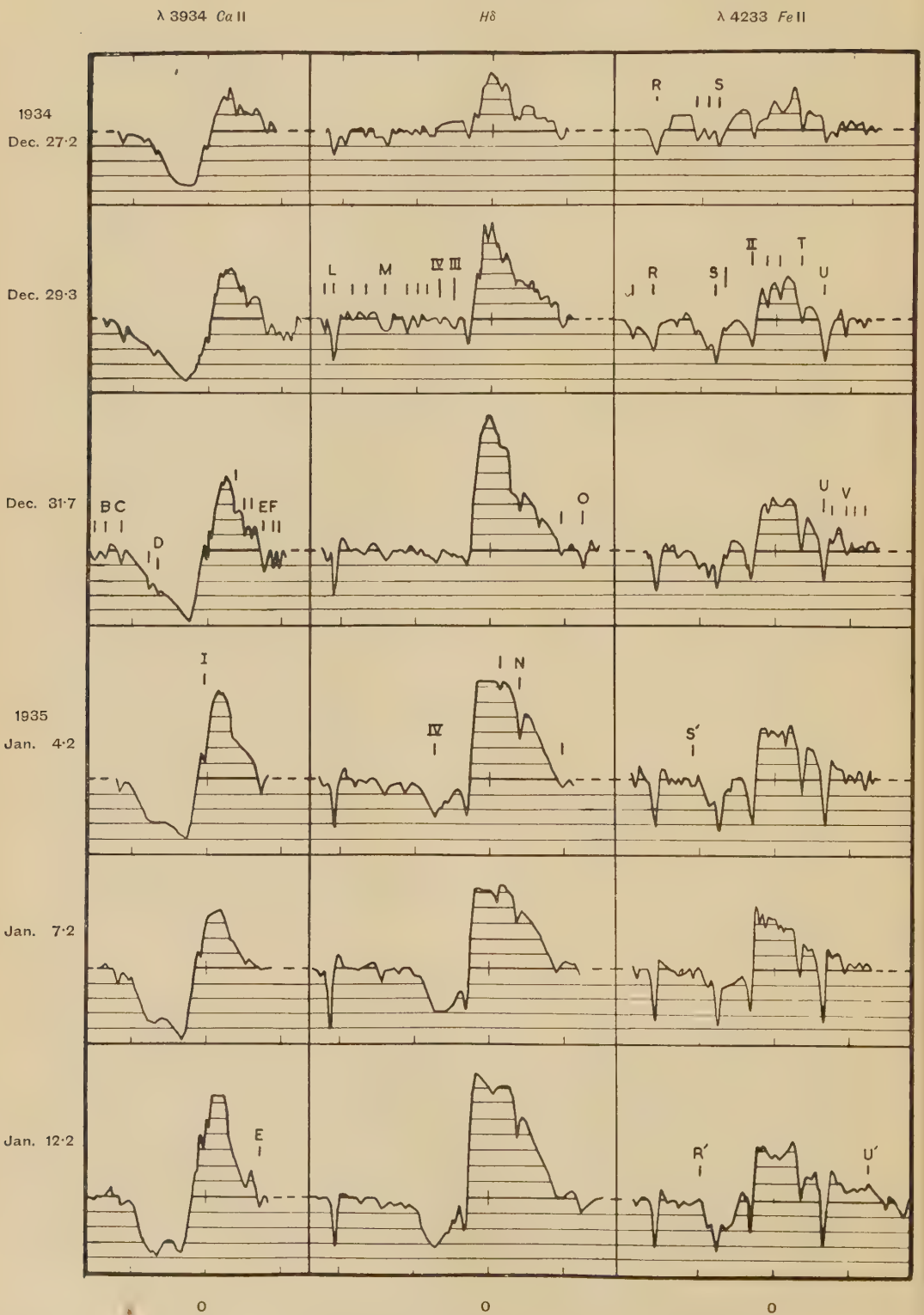

FIG. 1.—*The displacements are marked off at intervals of* 1000 *km./sec.*

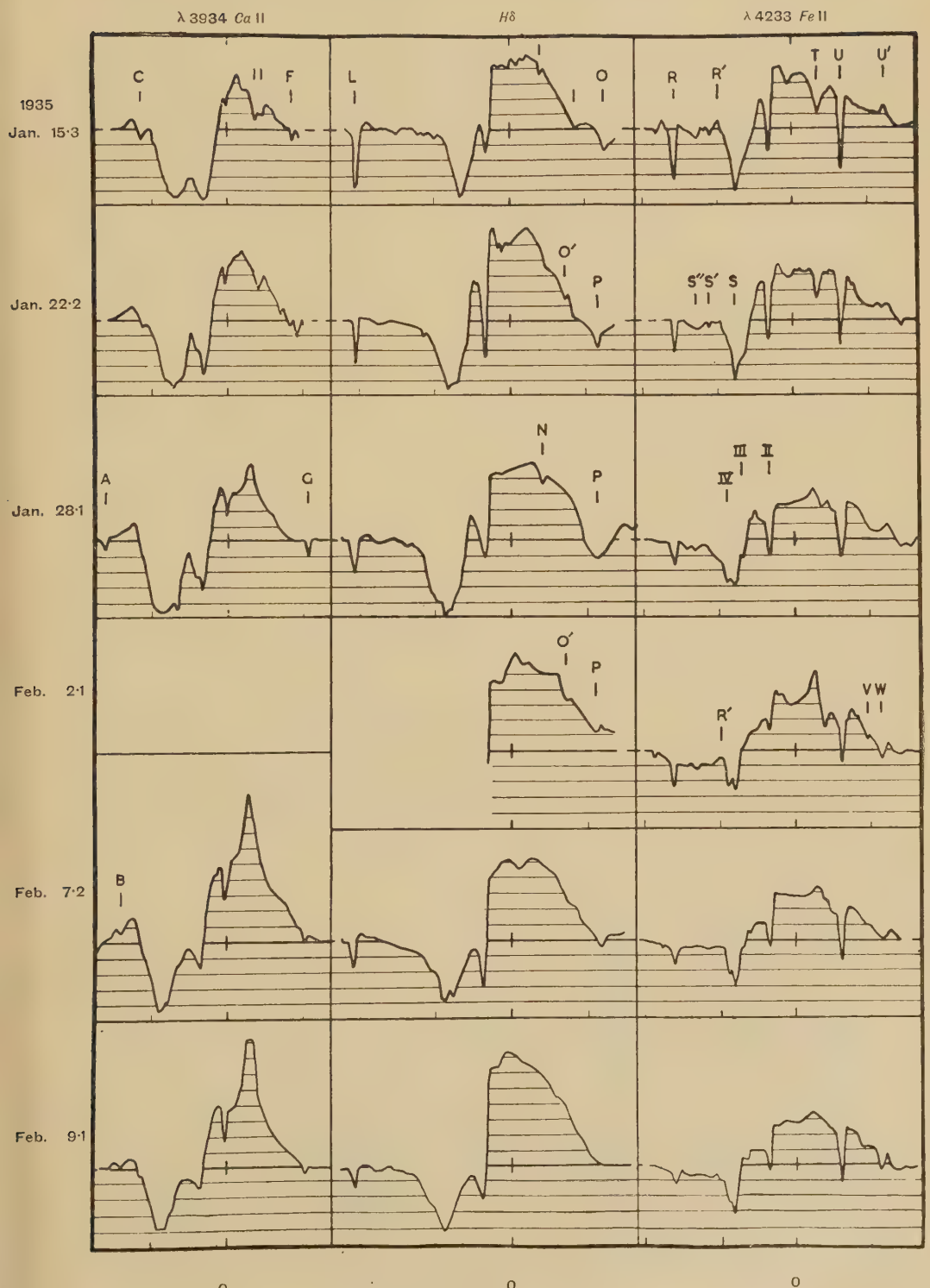
λ 3934 Ca II
Hδ
λ 4233 Fe II
1935
Jan. 15·3
Jan. 22·2
Jan. 28·1
Feb. 2·1
Feb. 7·2
Feb. 9·1
C
H
F
L
I
O
R
R′
T
U
U′
O′
P
S″
S′
S
A
G
N
III
II
IV
VW
B
0
0
0

FIG. 2.

TABLE I

List of Lines appearing in the Diagrams

(All belong to Absorption Component II unless otherwise stated)

Designation	Line	Identification	Intensity *	Remarks
A	3916·3	Zr^+ La^+ V^+	3	
	3918·5	*Fe*	1	
B	3920·3	*Fe*	1	
C	3922·9	*Fe*	2	
	3927·9	*Fe*	2	
D	3929·9	V^+, *Fe*	4	
	3933·7	Ca^+	25	
	3942·5	*Fe*	1	
	3944·0	*Al*	1	
	3945·2	Cr^+, *Co*	1	
E	3947·5	*O*, *Fe*	4	
F	3949·0	*Fe*, La^+	1	
	3950·4	Y^+	1	
G	3952·0	V^+	3	
H				Normal position for O^+ λ 3919·3 (with C^+ $\lambda\lambda$ 3919–21).
H′				Approximate position for Component VI of O^+ and C^+ lines.
I				Interstellar line.
J				Undisplaced position for O^+ line λ 3945.
J′, *J″*				Approximate positions for Components VI and VIII of O^+ λ 3945.
K′, *K″*				Approximate positions for Components VI and VIII of O^+ λ 3954.
	4075·8	Ce^+	2	
L	4077·7	Sr^+	6	
	4080·9	*Fe*, Ce^+	1	
	4083·2	Ce^+	1	
M	4086·7	La^+	2	
	4090·5	Zr^+	1	
	4092·6	*Co*, *V*	1	
	4095·0	*Ca*, *Fe*	—	
	4101·7	*Hδ*	4	
	4107·5	*Fe*	0	
N	4110·7	*Cr*, *V*, Cr^+	2	
	4118·6	*Fe*	2	
O, *O′*	4122·7	Fe^+	3, 1 :	*O′* refers to Component III–IV.
P	4128·7	Fe^+	1·5	With λ 4128·1 Si^+?
Q, *Q′*				O^+ lines $\lambda\lambda$ 4070–72–75, normal position and displaced 950 km./sec. (Component VIII).

* Intensities from McLaughlin.

TABLE I—*continued*

Designation	Line	Identification	Intensity *	Remarks
R	4211·9	Zr^+	1	
R′	4215·5	Sr^+	5	1st head of 2nd *CN* band occurs at 4216·0.
	4215·5	Sr^+		Red maximum.
	4222·6	Ce^+	1	
S, *S′*, *S″*	4224·9	V^+, Cr^+	2	
	4226·7	*Ca*	4	Components II, III and IV. The red maximum almost coincides with the violet maximum of λ 4233.
	4233·2	Fe^+	5	
	4236·0	*Fe*	1	
T	4238·7	La^+, *Fe*	1	
	4242·4	Cr^+	3	This nearly coincides with λ 4233 red maximum.
U				
U′	4246·8	Sc^+	6	
	4246·8	Sc^+		Red maximum.
V	4248·8	V^+	—	
	4250·8	*Fe*	2	
	4252·6	Cr^+	0	
W	4254·3	*Cr*	0	
Y	4261·8	Cr^+	3	Absorption Component IV.
Z	4254·0	O^+		Undisplaced emission.
	4267·2	C^+		Absorption displaced 400 km./sec. (Component VI) falls in this position.

Though the continuous background has been drawn in with considerable care, using wide ranges on either side of the region of measurement, there are cases where its position is by no means certain. This is particularly true of the later dates. Uniformity of procedure for any one line has been aimed at. On the other hand, grain irregularities have given comparatively little trouble, and the large majority of minor features shown may be regarded as real, except perhaps for a few of the later plates when the spectrum width had perforce to be made narrow.

The three regions principally studied are centred on the K line, *Hδ* and λ 4233 *Fe* II. These are pictured for 31 dates. In addition, *Hβ*, λ 4924 *Fe* II and λ 4444 *Ti* II are illustrated for a number of selected dates. Table I gives data on lines within the limits of the first three regions which are identifiable from the published lists. The position of features tabulated is marked in the diagrams by short vertical lines above them, and enough of these are designated by letters to render identification of all easy. Roman numerals indicate the system to which absorption components of the principal line of the region belong.

* Intensities from McLaughlin.

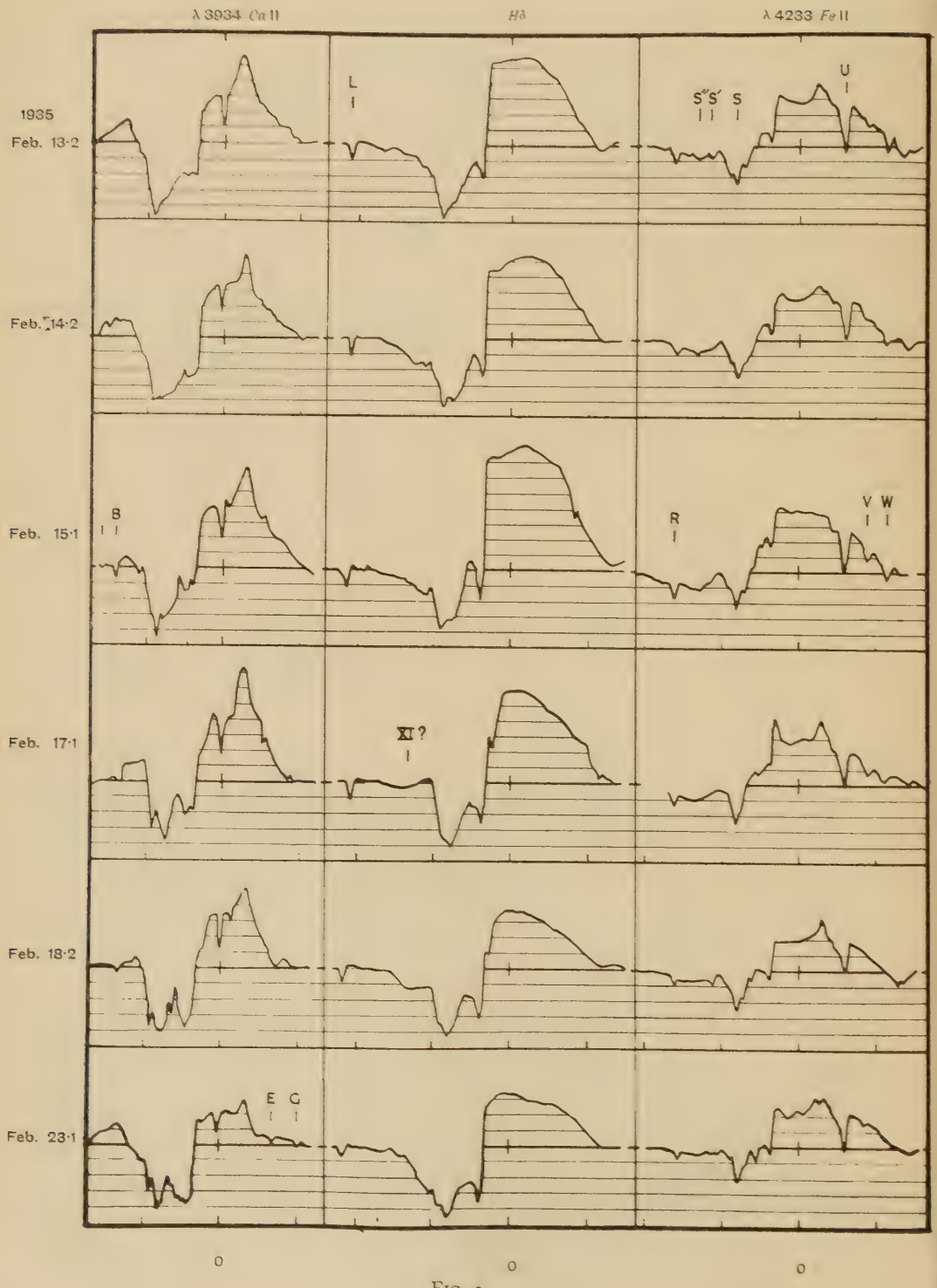
λ 3934 Ca II
Hδ
λ 4233 Fe II
1935
Feb. 13·2
Feb. 14·2
Feb. 15·1
Feb. 17·1
Feb. 18·2
Feb. 23·1
L
S″ S′ S
U
B
R
V W
XI ?
E G
0
0
0

Fig. 3.

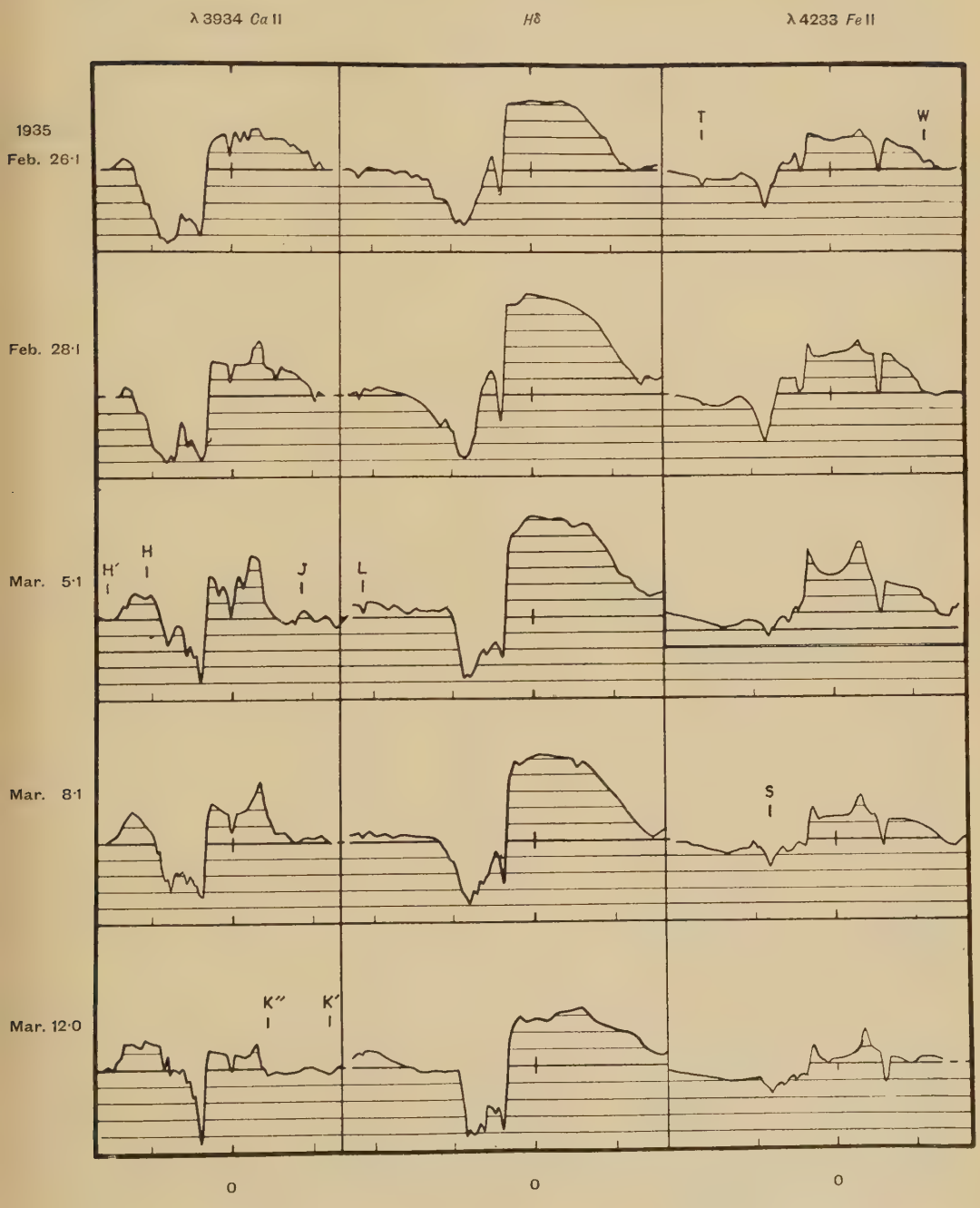
λ 3934 Ca II
Hδ
λ 4233 Fe II
1935
Feb. 26·1
Feb. 28·1
Mar. 5·1
Mar. 8·1
Mar. 12·0
T
W
H′
H
J
L
S
K″
K′
0
0
0

FIG. 4.

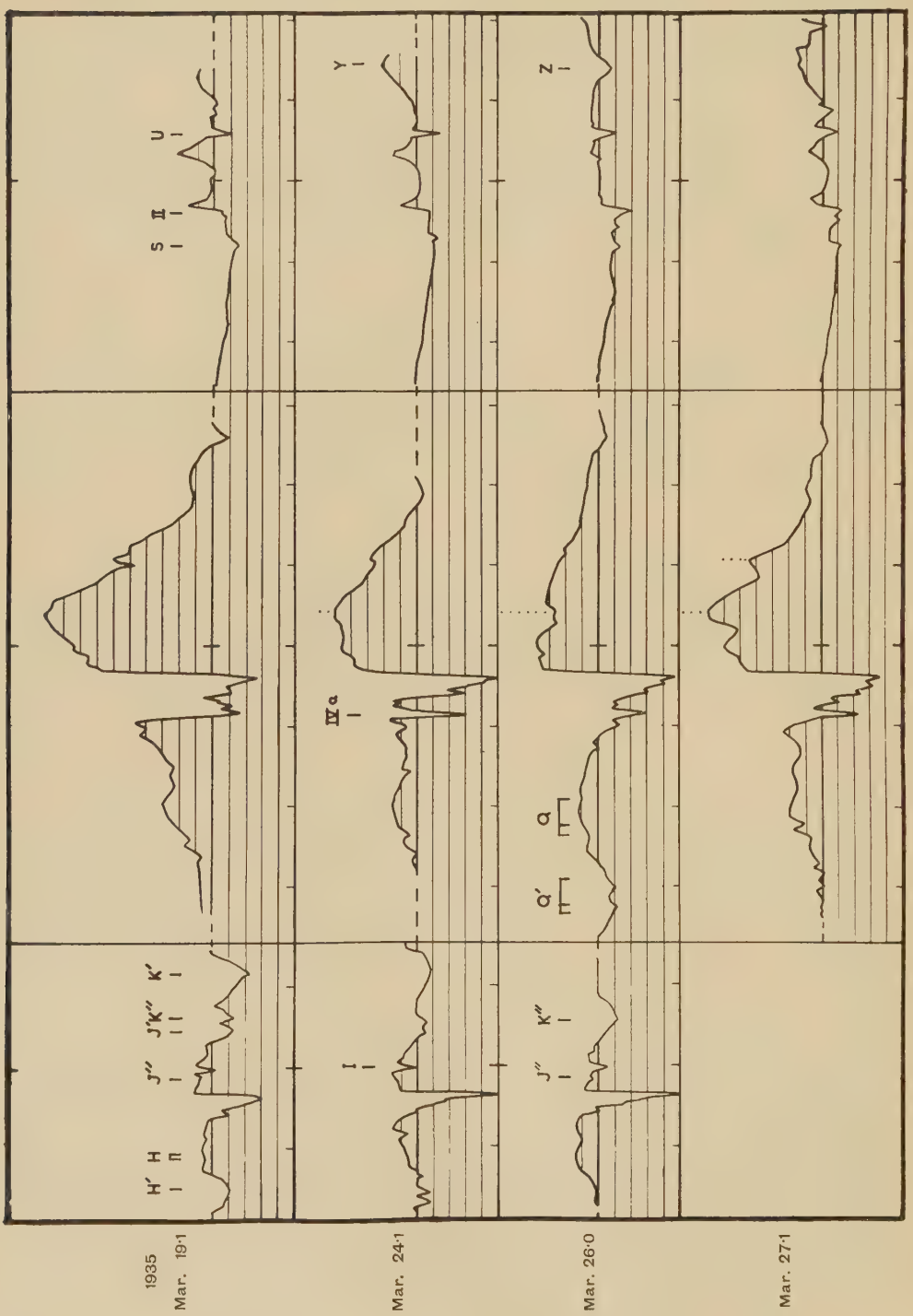
λ 3934 Ca II
Hδ
λ 4233 Fe II
1935
Mar. 19·1
Mar. 24·1
Mar. 26·0
Mar. 27·1
H′ H
J″ J′K″ K′
IIIa
J″ K‴
Q′ Q
S II U
Y
Z
0
0

FIG. 5.

FIG. 6.

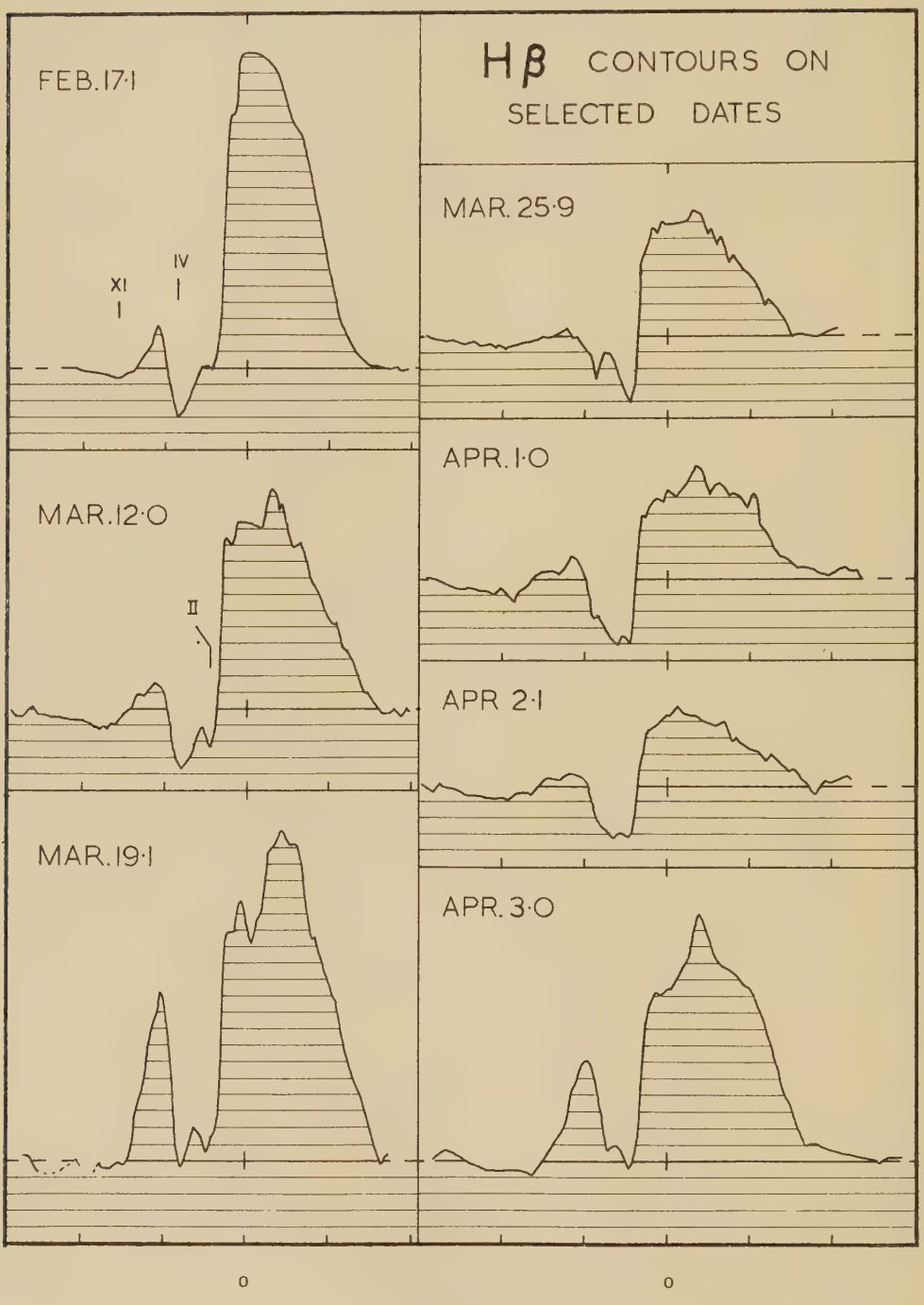
Hβ CONTOURS ON SELECTED DATES
FEB. 17·1
XI
IV
MAR. 25·9
APR. 1·0
MAR. 12·0
II
APR 2·1
MAR. 19·1
APR. 3·0
0
0

Fig. 7.

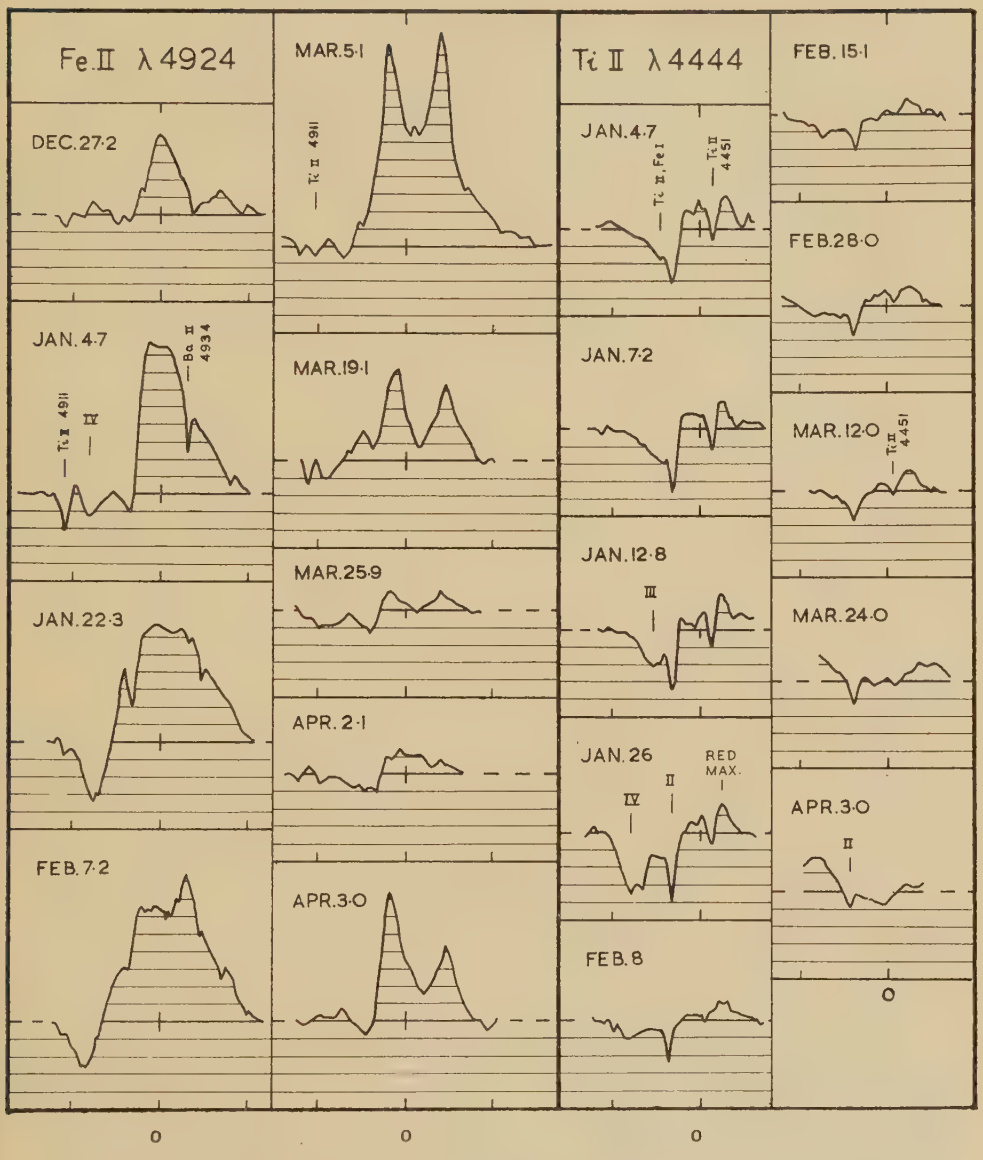

FIG. 8.—*Some of the irregularities in λ 4924 after March 5 may be due to Components VI, VIII of λ 4922 He.*

General Description of the Line Structure

In what follows we shall adopt the designation of absorption components given by McLaughlin in his valuable work.*

Throughout the majority of the diagrams the same general structure exists, and the contours for February 7 may be taken to illustrate typical features. Those of the K line, *Hδ* and λ 4924 *Fe* II are comparatively

* *Pub. Obs. U. Michigan*, 6, 107, 1937.

free from interference by other lines, but that of λ 4233 *Fe* II exhibits considerable blending and is best ignored at the first approach.

Each contour consists of a broad emission band roughly centred on the undisplaced position of the line. In K the interstellar component closely marks this position. On the redward side the intensity falls away somewhat smoothly to that of the continuous spectrum, but on the violet side both emission and underlying continuous are heavily cut into by absorption. This absorption begins abruptly with the intense Component II of displacement −348 km./sec. The line is sharp in hydrogen and iron, but relatively less so in calcium. This component persists throughout the period under study. Practically all the numerous sharp lines in the spectrum are Absorption II components of various elements.

The powerful broad absorption to the violet of Component II, into which it emerges, has two cores, McLaughlin's Absorptions III and IV. The deepest part of this structure varies in position from day to day. Its violet extremity appears to be displaced about 1080 km./sec. Beyond this K shows emission while *H*δ shows more absorption. The latter, though appearing as a wing to the strong line, is probably associated with Component XI, which was not noticeable in March.

It is noteworthy that in none of the lines does the most displaced part of the red emission extend as far from the normal position as does the violet absorption, nor as far as the violet emission in K.

Superimposed on the broad emission and displaced about 300 km./sec. on the redward side of the zero position, a comparatively sharp emission maximum presents a striking feature. This maximum, which corresponds to that observed in the forbidden oxygen lines, is very strong in K and prominent in *Fe* II, but is merely suggested in *H*δ. On most dates the last-named line shows no trace of the maximum. It is probable that the similar and almost equally displaced violet maximum, such as shows in the [*O* I] lines, is masked by Absorption II, which falls close to the position it should occupy.*

Though the sequence of changes is complicated the general development is relatively clear. On December 27 all absorption lines, of which there are a large number, corresponding to a late F-type, are weak, with the single exception of the *Ca* II lines. Rapid changes take place and the absorption lines become fewer in number. Absorption II is the strongest component and the emission is of the "peaked" type. Absorptions III and IV emerge, earliest in hydrogen, and their blend rapidly becomes predominant. The emission becomes less peaked and broadens. The red maxima appear in some lines. Odd cores appear in the heart of the absorption band, where there are day-to-day changes and even fluctuations between absorption and emission.

* This close coincidence of the violet maximum and the underlying absorption line shifts the *apparent* maximum in the former to a longer wave-length, and accounts for the smaller separation found by Bobrovnikoff (*Perkins Obs. Contr.*, No. 2, 1935) for *Fe* II maxima in the visual region than for [*O*], where there is no confusing absorption.

The strong III–IV absorption dies out, though II remains prominent; in calcium and hydrogen II merges on its violet side with what remains of the broader absorption. The intensity of emission in the metallic lines rapidly decreases and large irregularities in contour appear in the hydrogen emission. As the nova starts its big light decrease at the beginning of April, hydrogen alone is strong in absorption, but the two displaced maxima have become pronounced in iron.

Results of Line Measurement

Emission Contours.—In the case of *Hβ*, *Hδ*, λ 4924 and K, the blends which actually interfere are not usually strong and it is possible to allow

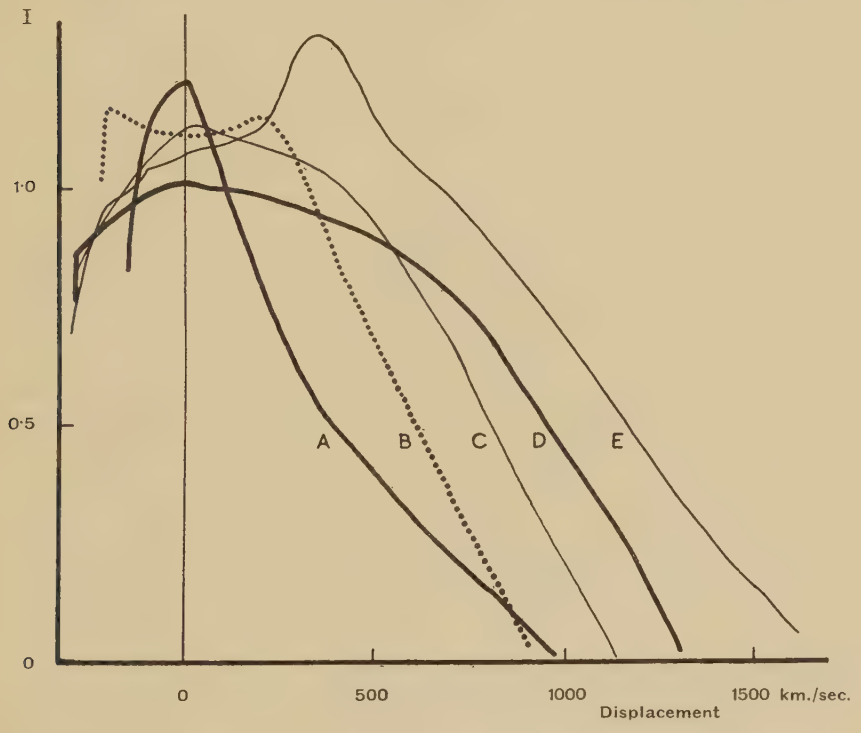

FIG. 9.—*Mean emission contours for Hδ. (Mean Hβ is shown in place of Hδ after March 8 on account of the irregularities in the latter line): A, Dec. 27–31; B, Jan. 4–15; C, Jan. 22–Feb. 18; D, Feb. 23–Mar. 8; E, Hβ contour, Mar. 12–Apr. 3.*

for them in determining mean shapes over several dates. Such mean contours of the redward emission over different time-intervals are illustrated for *Hδ* and K in figs. 9 and 10, which show clearly how the lines broaden and become less peaked with time. The intensities are mean values with respect to the continuous spectrum.

Comparison of different lines on the same plate proves that the intensity distribution in the redward emission is not identical for hydrogen and the metallic atoms. This is still true when the effect of the red maxima has

been eliminated. The following ratios are from measures made at the point where the band-intensity is $0{\cdot}5P$, P being the intensity in the undisplaced position, with the following results :—

Width-ratio at $0{\cdot}5P$ $\begin{cases} H\delta/\mathrm{K} & \text{Jan. 28 to Feb. 28, } 1{\cdot}27 \pm 0{\cdot}18. \\ H\delta/\lambda\ 4924 & \text{Dec. 27 to Mar. 5, } 1{\cdot}27 \pm 0{\cdot}12. \end{cases}$

For K, on dates earlier than January 28, apparent absorption interferes at the undisplaced position, a peculiarity that will be commented on later.

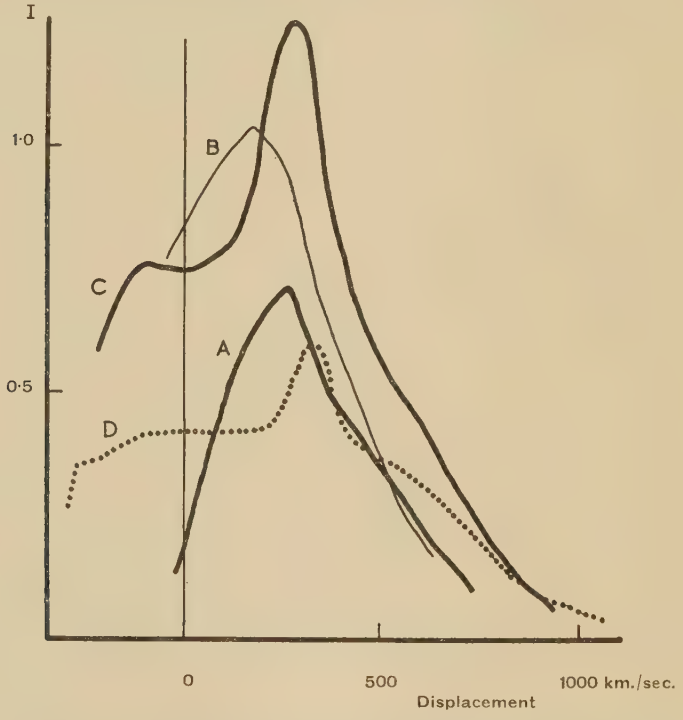

Fig. 10.—*Mean contours of emission in the K line. A, Dec. 27–31; B, Jan. 4–22; C, Jan. 28–Feb. 18; D, Feb. 23–28.*

Similar width-ratio for the extreme redward edges of the bands yield $H\delta/\mathrm{K} = 1{\cdot}16$; $H\delta/\lambda\ 4924 = 1{\cdot}05$. Thus $H\delta$ has a greater tendency to be flat-topped than K, and *Fe* II is intermediate. Apart from a closer equality of K and $H\delta$ for the three December plates, there is little evidence of change in the ratios with time.

The contour for $H\beta$ is satisfactorily similar to that for $H\delta$ during the period December 27 to March 19, though the large intensity of $H\beta$ with respect to the continuous background and the difficulty of drawing in this background, which is curved on the tracings, prevent high measuring accuracy. To compare the lines, the widths as measured on 13 dates have been expressed in terms of the $H\delta$ width at half the peak intensity, P. Mean values follow.

Intensity in Band		0·9*P*	0·7*P*	0·5*P*	0·3*P*	0·1*P*
Width	*Hδ*	47	73	100	134	171
	Hβ	53	74	95	120	178
Average difference		23	13	9	17	16

This agreement shows that there is a decided change from the pre-maximum period when the width-ratio *Hβ*/*Hδ* at 0·5*P* was 1·38.*

After the middle of March the intensity distribution in the two lines differs, and for *Hδ* mean shapes have little meaning owing to rapidly changing irregularities. It has been found impossible to ascribe these to blends, such as λλ 4097, 4103 *N* III, λλ 4089, 4116 *Si* IV or λ 4128 *Si* II. There are, however, suggestions of progressive shifts in one or two of the *Hδ* band maxima which are indicated by dotted lines in the intensity diagrams. These may result from shifting absorption features.

True Intensity Variations.—As far as possible the normal emission band and the red maximum have been measured and treated separately, the contour of the broad normal band being drawn in under the maximum, giving a base from which the intensity of the latter could be measured. For the normal band the intensity measured is not the total emission but that of the line in its undisplaced position. As previously pointed out,† this represents a mean for the emitting material in a plane through the nucleus normal to the line of sight, and is an easily determined datum for inter-comparison of lines. The tabulated values are not total emissions but represent the magnitude difference between the line intensity in the undisplaced position (or at the displaced maximum) and the intensity per $\Delta\lambda/\lambda$ of continuous spectrum at λ 5300 in a $5^{m}\cdot0$ star. The peak intensity was compared with the continuous intensity at the same wave-length, this was compared from the star's colour curve with the intensity at λ 5300, and a further correction was made to reduce to a constant stellar magnitude. The relative energies in the continuous spectrum, with respect to which the line intensities were measured, have been derived from the published magnitude and colour-temperature observations.‡

True intensities for several of the stronger lines are plotted, together with light-curves, in figs. 11 and 12, and are listed for a number of dates in Table II, where the adopted nova magnitude and temperature are also given. The curve for the [*O* I] line, λ 6300, has been obtained from Merrill's data,§ with an approximate allowance for the effect of a central emission component on his tabulated figures. The data for the *Fe* II lines is incomplete because in the earlier stages the red maximum for λ 4924 coincides with *Ba* II absorption, and that for λ 4233 is close to a *Cr* II line; also the undisplaced emission dies out early in March.

* *M.N.*, **97**, 612, 1937. See also *Observatory*, **61**, 214, 1938.

† *M.N.*, **97**, 621, 1937.

‡ Magnitudes: Beer, *M.N.*, **95**, 538, 1935; Grouiller, *Pub. Obs. Lyon*, **1**, fasc. 16, 1935; Campbell, *Harvard Bull.*, **898**, 20, 1935. Temperatures: Petrie, *Ap. J.*, **81**, 483, 1935; Beileke and Hachenberg, *Zs. f. Ap.*, **10**, 366, 1935; Greaves and Martin, *M.N.*, **96**, 425, 1936; Oehler, *Zs. f. Ap.*, **12**, 281, 1936.

§ *Ap. J.*, **85**, 62, 1937.

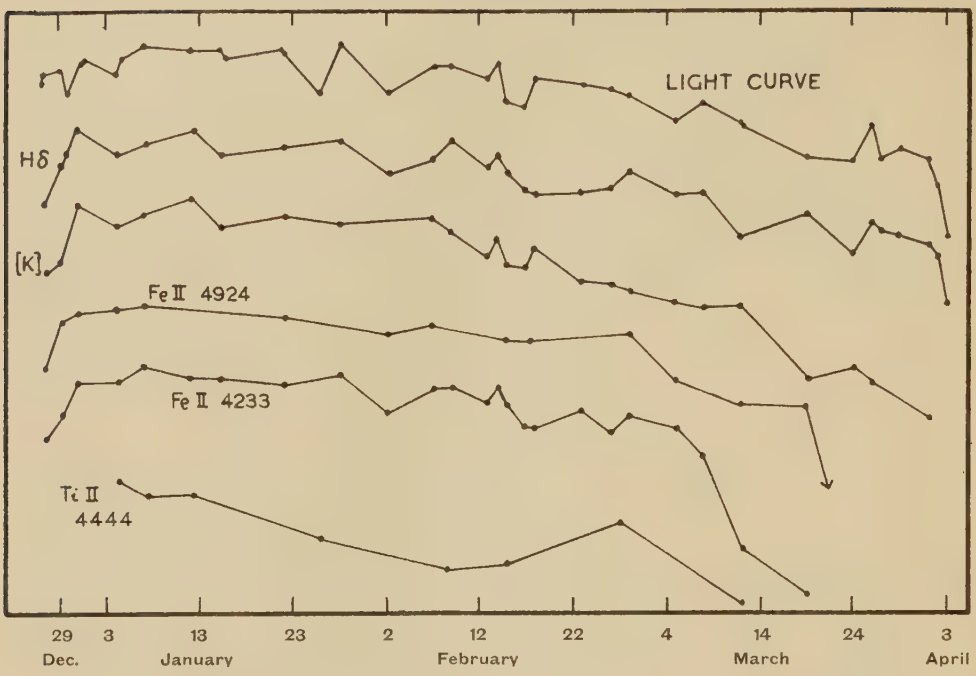

FIG. 11.—*True intensity variations in the normal emission lines, expressed in magnitudes for comparison with the light-curve.*

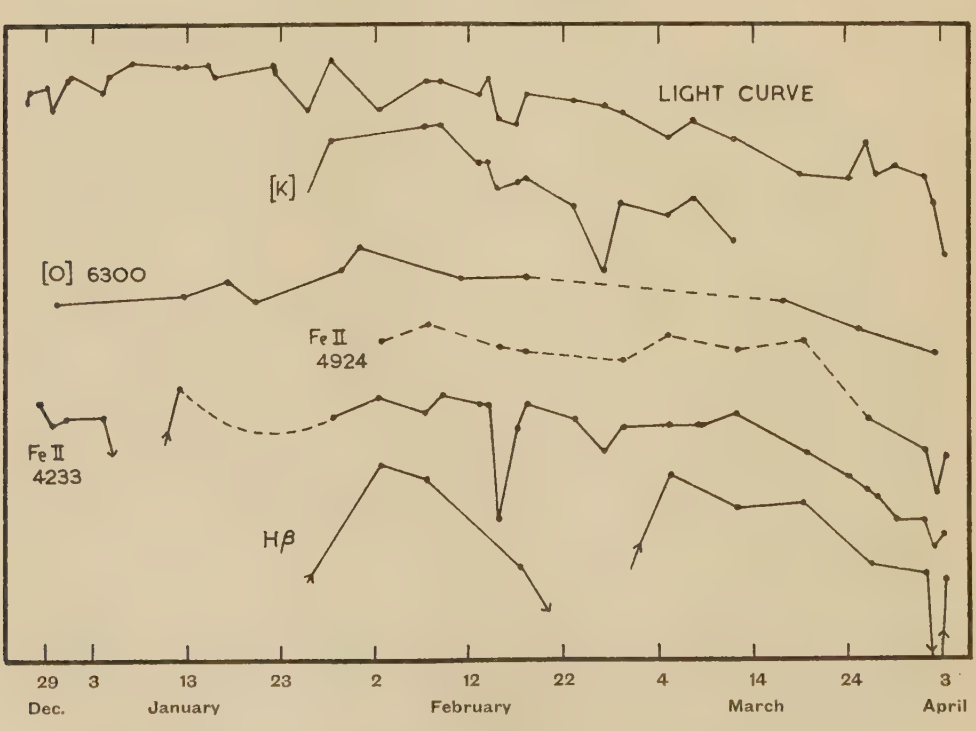

FIG. 12.—*True intensity variations in the displaced red maxima, expressed in magnitudes for comparison with the light-curve.*

TABLE II

True Intensities and Emission Ratios

Intensities are expressed as magnitude differences between peak intensities and $\Delta\lambda/\lambda$ of the continuous spectrum at λ 5300 in a 5·0 magnitude star. Negative values indicate fractional line intensities. The ratios are energy ratios.

				Normal Band						Red Maximum *		
Date	m_v	T	$H\delta$	K	*Fe* II 4924	*Ti* II 4444	$\frac{H\beta}{H\delta}$	$\frac{4924}{4233}$	$H\beta$	K	4924
1934 Dec. 27·2	3·0	7500	1·6	1·6 :	1·9		3·10	2·9	—	—	
29·3	2·7	8000	2·5	1·7 :	2·8		5·25	3·6	—	—	
31·2	2·6	9600	3·2	3·0 :	3·0		2·59	2·6	—	—	
1935 Jan. 4·2	2·8	9500	2·7	2·6	3·1	1·3	4·48	2·5	—	—	
7·2	2·2	9300	2·9	2·8	3·2	1·0	3·54	2·0	—	—	
22·3	2·4	8700	2·8	2·7	2·9		3·40	2·3	—	—	
Feb. 2·1	3·2	11000	2·3		2·6		2·38	2·9	1·7		1·4
7·2	2·6	10500	2·6	2·7	2·8		2·15	2·0	1·3	2·6	1·8
15·1	3·4	10500	2·3	1·7	2·4	−0·4	2·89	2·2	—	1·2	1·3
17·1	3·5	10500	1·9	1·6	2·4		2·81	3·3	−0·5	1·3	1·2
28·0	3·2	12500	2·4	1·2	2·6	0·1	2·52	2·1	—	0·9	1·0
Mar. 5·1	3·8	13500	1·8	0·9	1·6		1·82	2·6	1·4	0·7	1·5
12·0	3·8	15000	0·9	0·8	1·0	−1·2	3·21		0·7	0·1	1·2
19·1	4·6	16500	1·4	−0·8	1·0		1·32		0·8		1·4
25·9	3·9	15000	1·2	−0·8	—		1·38		−0·4		−0·2
Apr. 1·0	4·6	16500	0·8	−1·3	−2·3		0·87		−0·7		−0·9
2·1	5·2	18700	0·6		−1·6		0·49		−2·9		−1·8
3·0	6·2	23000	−0·5		−2·1		1·25		−0·8		−1·0

A dash indicates that emission was not detected.

* On March 19, the only date when this emission is prominent at $H\delta$, the ratio $H\beta/H\delta$ is 2·2.

Fig. 11 presents substantial agreement with the results of Whipple and Payne-Gaposchkin * for total emissions. Many of the irregularities of the light-curve are reflected in the lines, though there is by no means a one-to-one correspondence. There is, however, little evidence for their contention that when the nova brightness decreases in a minor oscillation the emission-line intensity increases with respect to that of the continuous spectrum. Of the lines examined, $H\delta$ most nearly follows the visual magnitude, and in the mean the fluctuations of this line are of the same size as those in the light-curve. Those for λ 4233 are rather larger than those for λ 4924.

The additional information of fig. 12 is for the red maxima, and here there is much less correspondence with the visual magnitude. The [*O* I] line shows no intensity correlation with the short-period fluctuations of the light-curve. This line is relatively stable; the variations in K, and particularly in $H\beta$, are much greater. Three abrupt intensity minima are noticeable.† The first, February 15, in K follows a drop in the light-curve; the drop in λ 4233 *Fe* II needs checking since λ 4924 does not

* *Harvard Circ.*, No. 414, 1937.

† These may occur in all the red maxima, but the data do not suffice to define them.

show it;* the second, February 26, though unmarked in the light-curve is prominent in λ 4233 and strong in K; the third and most remarkable, found in all three maxima studied on April 2, coincides with the commencement of the rapid fading of the nova. The intensity of the red maxima, however, recovers on April 3 nearly to its April 1 value. In λ 4233 *Fe* II this is mostly due to the violet maximum of λ 4243·97 [*Fe* II].

A rough idea of the relative *total* intensities of normal emissions and displaced maxima is given by the following summary, which refers to the period (early February) when the maxima were at their strongest; the total emissions for both normal and displaced emission are on the same scale.

Line	Normal Redward Emission	Displaced Red Maximum	Chromosphere (Mitchell)
Hβ	100	2 :	200
K	24	5·1	200
λ 4924 *Fe* II	30	2·8	30
λ 4233 *Fe* II	16	1·6	30
λ 4444 *Ti* II	3 :	*	30
λ 6300 [*O* I]	?	3·5	—

* There is a red maximum for Ti^{+}, but it is blended and unmeasurable.

It will be noticed that the intensity distribution between different atoms is very different in the two sources. With respect to the iron lines, the [*O* I] line and K are considerably stronger in the displaced maxima, whereas hydrogen is very much weaker.

Emission Line Ratios.—For the 18 dates listed in Table II *Hβ* was measured as well as *Hδ*. The energy ratio between these two lines gives an idea of the Balmer decrement. It decreases rather steadily from a mean of 3·6 early in January to less than unity at the end of March. The *Hβ*/*Hδ* ratio found for the pre-maximum stage of the nova was 1·8.

These values compare with 9·5 found for RS Ophiuchi,† 2·1 for N Lacertæ 1936,‡ and 3·45 derived theoretically for electron capture, by Cillié.§

On 12 dates when blends permit determination, the *Fe* II mean ratio λ 4924/λ 4233 is, in the normal emission 2·57 ± 0·31, and in the red maximum (excluding the plate of February 15 when λ 4924 shows a strong maximum and λ 4233 none) 1·82 ± 0·29. The value found for the pre-maximum phase was 1·2. The ratio for the maxima must be accepted with reserve, as day-to-day changes in displacement suggest that absorption blends, though hidden, may remain.

In general, comparison of K and H is impossible, since H is confused with *Hε*. The particular case of the displaced emission maxima is an

* Professor Stratton has suggested that the low maximum on this date may be due to coincidence with a displaced absorption line *Cr* II 4242·4.

† Wilson and Williams, *Ap. J.*, **80**, 344, 1934. A minimum value of 3·9 was found when space absorption was allowed for.

‡ McKellar, *Pub. Dom. Ap. Obs.*, **6**, 347, 1937.

§ *M.N.*, **96**, 771, 1936.

exception, for, in the period dealt with, this feature occurs rarely, if at all, in hydrogen lines of shorter wave-length than $H\gamma$, so that the whole of the sharp emission band superimposed on the broad blend can be ascribed to calcium. This assignment is confirmed by Stratton's unpublished wave-length measurements; assuming that the peak in the blend belongs to calcium, the mean velocities for H and K, from 13 plates, agree within 4 kilometres per second.*

From plates on the 11 dates when the maxima were prominent in calcium and apparently absent in hydrogen we derive the energy ratio $H/K = 1{\cdot}42 \pm 0{\cdot}26$. In obtaining this result the peak intensity in the maxima, over and above that in the underlying emission, has been measured in terms of the continuous spectrum at the same wave-length, and a uniform factor, 1·02, has been applied to correct for the different energy values in the continuous at K and H. Though the result must be accepted with some reserve, because of density differences in the spectra at the two wave-lengths and of uncertainties in defining both the limits of the displaced maxima (*i.e.* normal emission contour uncertain) and the continuous background used as a standard for measurement, it creates the impression that the maximum in K was less intense than that in H.

There is the possibility that the extra intensity in H may be accounted for by excitation from $H\epsilon$ radiation, since the calcium line can absorb from this hydrogen line when the relative velocity between the atoms concerned is -120 km./sec.

Absorption.—Little more has been attempted than to study line-depths. A good idea of relative intensities is obtained by reflecting the redward emission over the violet side and finding the percentage absorption from this background. This procedure is not entirely reliable, since we have no guarantee that the unabsorbed emission band is symmetrical about the zero position. But it is the best that can be done. When emission is visible also on the violet extremity of a line, the assumed background has been made to join up with this.

Let a be the fractional absorption, produced by a spherically expanding gas layer, from the radiation of the same apparent wave-length originating behind it. Let C be the intensity of the continuous spectrum and N that of the normal emission band at the same wave-length as the absorption line. If absorption takes place from the nuclear radiation only, the observed line-depth is aC. As was pointed out in a previous note,† it frequently happens that a, determined on this assumption, turns out greater than unity. This implies that part of N is also absorbed, *i.e.* that the absorption occurs in layers outside those producing the emission band. For $H\beta$ and $H\delta$ this is true of the bulk of the measures for the III–IV absorption blend as well as those for Component II.

In general, even when the source of N is behind the absorbing layer, only a fraction b of N will be absorbable, b being a function of the radii,

* The K displacements are some 20 km./sec. larger in early February and some 29 km./sec. smaller early in March than those of H.

† *Observatory*, **49**, 331, 1936.

velocity distribution, etc., of the emitting and absorbing layers. The full contributory depth aN is reached only if the radius of the absorbing layer is very large compared with that of the source of the line emission.

TABLE III

Absorption Line Percentage Depths

	Component II *								Component III–IV					
Date	*Hβ*	*Hδ*	K	*Fe* II 4233	*Ti* II 4444	*Sc* II 4247	*Cr* II 4242	*Sr* II 4078	*Hβ*	*Hδ*	K	*Fe* II 4924	*Ti* II 4444	λ 4214
1934														
Dec. 27·2	24	34	82	32		24	24	35	8	5	33 :	—		—
29·3	48	58	88	50		57	23	56	38	26	48 :	—		—
31·7	36	57	96	56		49	32	58	31	36	50 :	16 :		—
1935														
Jan. 4·2	52	76	89	68	67	67	43	63	50	61	61	40	14	8
7·2	59	76	97	67	78	75	34	78	57	67	73	61	33	10
12·2		75	84	64	73	69	29	61		75	89		43	9
15·3		63	97	51 :		68	17 :	78		92	91			11
22·3	54	75	82	54 :		56	20	55	84	88	90	79		13
26·0					80								71	
28·1		61	94 :	45		45	10	42		100	90			12
Feb. 2·1	71	68		20 :		41	14 :	31				53		24
7·2	71	79	98 :	45		46		35		82	91	67		11
9·1		73	100 :	41	50	46	2 :	26		87	80		22	15
13·2		71	76 :	40		37	—	19		95	95			16
14·2		73	73 :	35		30	—	23		92	81			16
15·1	81	75	74 :	24	42	35	—	23		85	91		27	21
17·1	79	76	74 :	24		31	—	24	88	88	82	53		17
18·2		77	87 :	44		25	—	17		87	83			13
23·1		80	83 :	51		34	—	14		92	85			10
26·1		63 :	85	39		28	—	10		79	92			11
28·1	74	69	100 :	41	37	33	—	11	94	87	80	68	17	15
Mar. 5·1	91	78	81	34		21	—	14	86	87	51	39		22
8·1		76	91	41		25	—	7		87	67			17
12·0	95	92	91	43	30	31	—	4	90	87	27	43	8	20
19·1	100	100	77 †	43	23	26	—	—	75	69	5 :	—	—	18
24·0		100	100	40	28	32	—	—		76	—	—	—	15
26·0	96	97	100	50	32	26	—	—	75	71	—	—	—	20
27·1		98		39		22	—	—		70	—	—		15
29·1		95		24		20	—	—		65	—	—		10
Apr. 1·1	91	100	83	28	25	22	—	—	74	66	—	—	—	15
2·1	79	91		23	19	27	—	—	72	55	—	—	—	13
3·1	76	79			18		—	—	66	50	—	—	—	

A dash indicates that the line was not detected.

* These depths should probably be somewhat reduced when Component III–IV is strong to allow for wing overlap.

† This low value is probably produced by a strong violet maximum in nearly the same position. Both *Hδ* and *Fe* II show intense red maxima on this date, though in K it is concealed by a very strong component of λ 3945 *O* II at the same wave-length. In λ 4924 the violet component is stronger than the red in spite of absorption.

In Table III line intensity is expressed as the percentage of $C+N$ that is apparently absorbed.

The line-depth variations are exhibited in figs. 13 and 14. With the exception that calcium K (Absorption II) remains strong to the end, their

behaviour is similar to that found for estimated total intensities by McLaughlin.* The tabulated values and the curve for *Fe* II show percentage depths derived on the assumption that the violet maximum in the

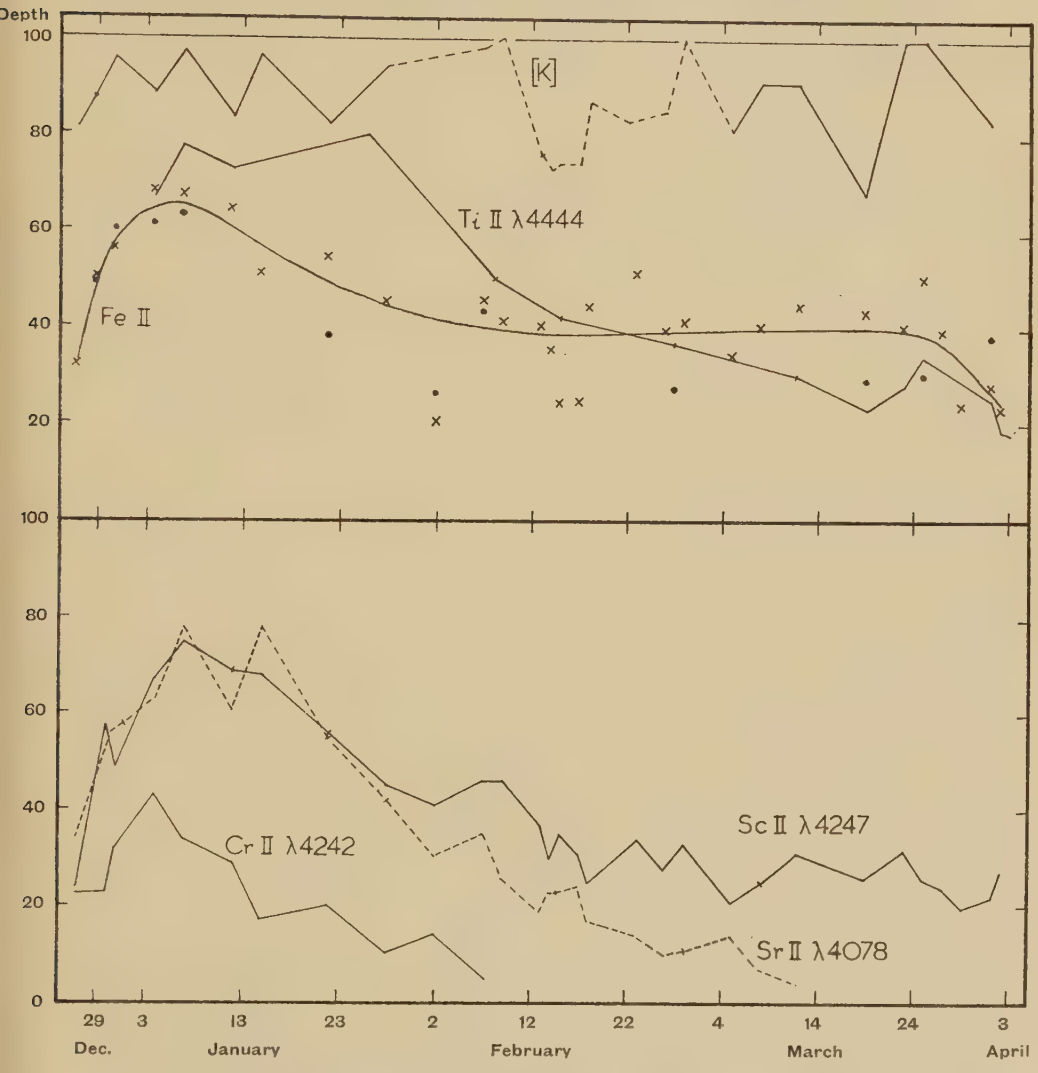

FIG. 13.—*Variations in absorption-line percentage depth for Component II. The Fe II curve, in which crosses represent λ 4233 and dots λ 4924, is not as reliable as the others. The broken part of the K curve is also uncertain.*

line is equal in strength to the red one. This accounts for the difference between my curve and McLaughlin's for visually estimated intensities.

A few points connected with Absorption II deserve mention. For the two *Sr* II resonance lines total absorptions have been obtained. When

* *Pub. Obs. U. Michigan*, **6**, 146, 1937.

grouped the measures show the following progressive change in the intensity ratio λ 4078/λ 4216 :—

	No. Plates	E.W. of λ 4078	Ratio
Dec. 27–31	3	0·50 A.	0·90
Jan. 4–12	3	0·66	0·97
Jan. 15–28	3	0·53	1·27
Feb. 7–13	3	0·23	1·31
Feb. 14–18	4	0·17	1·31
Feb. 23–28	3	0·08	1·77

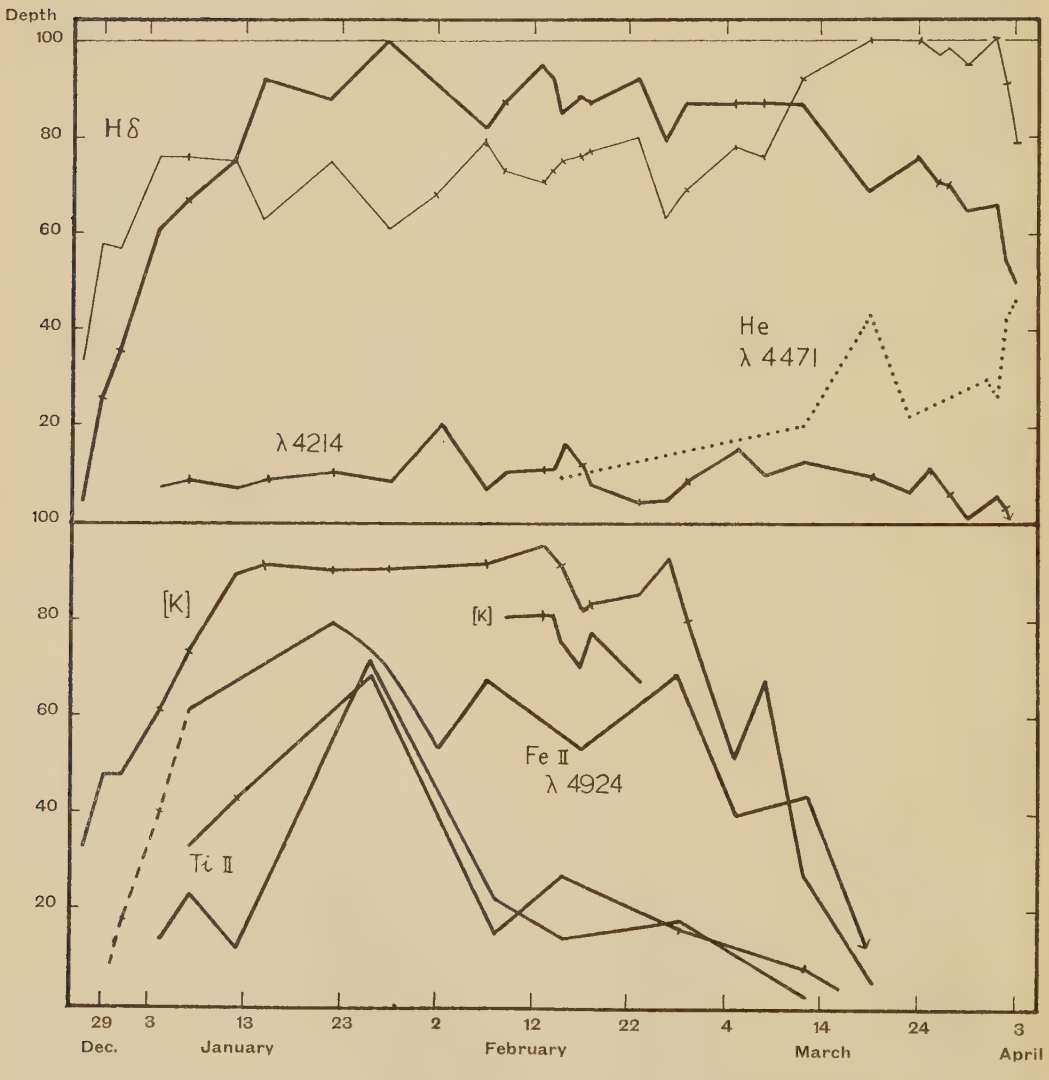

FIG. 14.—*Variations in absorption-line depth. The heavy lines represent the III–IV component, the two curves for K and λ 4444 Ti II being for different cores in this band. The thin line for Hδ is Component II, and the dotted curve is Component VI of He. That marked λ 4214 is identified either with Component III–IV of λ 4227 or, more probably, with Component XI of λ 4233 Fe II.*

For the Sun * the intensity of λ 4078 is 0·27 A. and the ratio is 1·21. Both lines reach their maximum intensity on January 7. Though it is possible that some of the early excess strength of λ 4215·5 is caused by its close coincidence with the head of the *CN* band at λ 4216·0, a real change in the *Sr* II ratio seems indicated. McLaughlin finds evidence for *CN* at λ 3883 till December 31 only. There is also a *Cr* II line at λ 4217·1, but this is probably too weak to influence the blend as stronger lines of the same multiplet are unrecorded by McLaughlin.

The persistence of the neutral calcium resonance line λ 4227 right through till April with great strength in February is noteworthy. Another neutral line of unusual persistence is λ 3838 *Mg* I (McLaughlin). The blend of the *Ca* I line with the more displaced component of λ 4233 *Fe* II makes intensity measures impossible. In late March the line appears to be shallow and very broad.

For *Hβ* the mean depth is 15 per cent. less than *Hδ*, but this is doubtless largely an instrumental effect.

The III–IV components, which are shown by heavier lines in fig. 14, are usually about 3·5 times as wide as II. Using this value, the ratio of total intensities is obtained. Arranged in decreasing order of $\frac{\text{III, IV}}{\text{II}}$, for the period when both sets of lines are fully established, we find:

Fe II, 5·0 ; *Hδ*, 4·3 ; K, 3·6 ; *Ti* II, 2·1 ; *Sc* II and *Cr* II ; *Sr* II.†

The mean depth derived for *Hβ* exceeds that for *Hδ* by only 3 per cent. The difference between the variations of *Fe* II and *Ti* II is peculiar. The curve for iron has an extended maximum, while titanium has a somewhat phenomenal peak around January 26.

Another curious feature, just detected by McLaughlin, is what may, from its position, be ascribed either to the III–IV component of λ 4227 *Ca* I or to Component XI of λ 4233 *Fe* II. Its development towards the end of January is clearly shown in the diagrams. Later the feature attains an extraordinary width, and remains when all III–IV components, other than hydrogen, have faded. This and the late development suggest *Fe* II as origin, in which case the displacement is −1350 km./sec. No corresponding band can, however, be traced at λ 4924. The diffuseness is such that the line would normally be missed on visual inspection of a plate, though photometer tracings show it to have a depth of 10 to 20 per cent. Component XI of *Hβ* is readily discernible in the diagrams, where its "centre" is pushed out to about −1700 km./sec. by emission.

Abnormal Features.—Until after January 22 the edge of the K absorption band encroaches on the emission to the redward side of the undisplaced position so that the point of greatest intensity in the emission has considerable positive displacement (*cf.* fig. 10). It might be thought that

* Woolley, *Ann. Solar Physics Obs. Cambridge*, **3**, pt. 2, 1933.

† McLaughlin (*loc. cit.*), lists *Sc* II and *Cr* II lines belonging to Component III–IV, but none for *Sr* II.

this was a wing effect due to the very great number of calcium atoms above the photosphere. In that case calcium H would be less broad than K. The evidence from H is not conclusive either way. On December 27 and 29 hydrogen contributes but slightly to the absorption blend. Taking the Component II position as line-centre, the violet wing width-ratio K/H for these dates is 1·67 at $r=0{\cdot}5$ and 1·27 at $r=0{\cdot}9$, while the extreme wing-widths, which alone provide the test, seem to be closely equal. The redward absorption edges, as measured by the position of the apparent maximum in the emission, are also equally displaced for H and K, though a blending absorption line on H complicates matters. On balance the evidence suggests turbulent motions producing actual inward velocities, though it is curious that the hydrogen lines do not show the same feature. For them the undisplaced position is marked by the emission peak.

On dates after mid-March the III–IV absorption in $H\delta$ is bounded on its violet side by emission, the intensity of which sometimes exceeds half that of the continuous spectrum. This emission is shown much more strongly in $H\beta$, where it is quite distinct after February 15. There are, moreover, clear indications of it in $H\delta$ on even earlier dates, when it shows as a hump in the extensive violet absorption wing. See especially January 28 (with a suspicion of the same thing in λ 4233) and February 17.

There is little doubt that this is the extremity of the emission band remaining unabsorbed, since the displacement of its violet edge agrees with that of the extremity of the redward part well within the accuracy of determination. This is true also for the occasional violet emission found in λ 4924.

A similarly displaced violet emission is also sometimes seen in the K line, where it is outstanding on February 17. Ionized calcium, however, shows a more interesting and persistent emission not shown by the other atoms. This, which first appears about January 12, has a usual outer limit around −1500 km./sec. and an apparent maximum at −1260 km./sec. Occasionally it extends to −1600 km./sec. It has no counterpart on the redward wing of K. On January 28, a typical date, the *maximum* in this emission is 400 km./sec. more displaced than the *extremity* of the redward K emission, and equally displaced with that in $H\beta$, which is the broadest line measured. The feature is confirmed as due to calcium by its presence in H.

The correspondence in position of this emission with absorption Component XI is fairly good, and the most reasonable explanation seems to be that a high-velocity approaching cloud emits in ionized calcium while it absorbs in other lines.

Relation of Absorption II to Displaced Emission Maxima.—It happens that the displacement of Absorption II nearly coincides with that of the violet maximum in lines showing the displaced emission. Let M be the intensity in this maximum at the wave-length of the absorption line, and R the measured residual intensity at the line centre. If the maximum originates outside the absorbing layer, the percentage line depth, freed of the effect of M, is $100\left(1-\frac{R-M}{C+N}\right)$ (where C and N have the values given on p. 109). If,

however, the geometrical relationship is such that absorption from the maximum occurs, the line depth is $100\left(1-\frac{R}{C+N+M}\right)$.

Calcium K is the only line suitable for a test between the two possibilities.* Absorption II is strong, and the displaced emission becomes so during February. Indeed, the effect of the violet maximum can be clearly seen in the diagrams. When the red one first appears the residual intensity in II immediately jumps to higher levels and a distinct shoulder appears on the steeply descending absorption contours (see February 17 and 23 particularly).

No red maximum is seen in K before the January 28 plate. From December 27 to January 22 the mean value of $100\left(1-\frac{R}{C+N}\right)$ is 89·4 (8 dates). For 6 dates after February 26 for which the red maximum is again absent † it is 90·0. Hence there is little real change in the line depth throughout the period of observation. On the 11 dates when the red maximum is clearly present the mean value of $100\left(1-\frac{R-M}{C+N}\right)$ is 87·4, while for the same dates $100\left(1-\frac{R}{C+N+M}\right)$ is only 74·5.

Thus the evidence is against absorption by Component II from the displaced maxima.

Discussion

In this section some of the more important data which may help towards a physical interpretation of the middle phases of the nova phenomenon are collected and briefly discussed.

(1) The normal hydrogen emission band has a contour tolerably well represented by curves derived theoretically by Chandrasekhar.‡ On his Mechanism A (repulsion of atoms from the stellar boundary with a force exceeding gravity) three curves are given corresponding to $\beta=2$, 3 and 4 in the expression $i(r) \propto p^r v^\beta$. In the part of the band to the red of the normal frequency, where he allowed fully for occultation, these three curves bear a distinct resemblance to the observed mean contours for $H\delta$, with $\beta=2$ for the period December 27–31 and $\beta=4$ for the period February 23 to March 8. This agreement suggests that the normal emission arises from outwardly accelerated atoms forming an atmosphere immediately surrounding the star, this atmosphere being comparable in depth, at least in the earlier stages, with the photospheric radius.§

* Even here, to obtain M we must assume that the violet and red maxima are similar in intensity and contour and are equally displaced. For the [*O*] lines, in which there is no complicating absorption, Merrill (*Ap. J.*, **82**, 413, 1935) and Bobrovnikoff (*Perkins Obs. Contr.*, No. 2, 1935) found the mean displacement to be −21 km./sec. Merrill's observations show the violet component of both [*O*] and long wave-length *Fe* II lines as a little stronger than the red. Such an assumption for K would slightly increase the derived depths.

† But omitting March 19. See note to Table III. ‡ *M.N.*, **94**, 522, 1934.

§ It should be mentioned that Chandrasekhar assumed that the atoms left the photosphere with zero velocity.

There is a progressive increase in the band-width, exceeding 50 per cent. in the three months of observation. On Chandrasekhar's assumptions this implies that the ejection velocity increases.

(2) The very persistent and relatively sharp lines of Absorption Component II absorb from this emission and hence originate outside it. For about a week after first appearance, while the lines are strengthening, the steepest part of the redward emission contour is less displaced than this absorption, and though the occultation effect is partly responsible for this, the absorbing atoms are evidently being recruited from the inner emission.

This absorption, doubtless, represents a rather dense gas shell cast off from the photosphere soon after light maximum. Since the lines are relatively narrow the velocity spread is small. McLaughlin * points out that the spectrum is such as we might expect for an absorbing shell far from the nucleus. Lines of *H*, *Ca* II, *Fe* II and *Ti* II remain till masked by emission, when the nova fades away. It may be noted that these, as well as those studied of *Sc* II, *Sr* II and *Cr* II, can all arise from ground or metastable levels. Our observation that around March 20 the calcium and hydrogen lines were quite black suggests that at that time the emission originated from an area small in comparison with the size of the absorbing shell.

(3) The intense, broad absorption band (Components III, IV) which develops after the main emission band has begun to widen, absorbs from it and must therefore also originate at a level effectively exterior to this emission. This concept of the absorption lying at a higher level than the emission was indicated by Sayer's work on Nova Aquilæ † and was also suggested for Nova Herculis by Whipple and Payne-Gaposchkin.‡ For the first seven weeks of its existence the limits of the really intense part of the absorption correspond in displacement with the steep, outer part of the emission contour.§ This absorption is therefore attributed to atoms which have streamed outwards through the emission region and attained their limiting velocity.

After about February 3 the absorption no longer keeps in step with the accelerating emission. In hydrogen and calcium the contour of the emission develops a relatively flat top, which extends, and the displacement of the sloping sides shows that the velocities of the atoms responsible are chiefly greater than 800 km./sec. The band extremity eventually reaches 1600 km./sec. displacement.

At this stage the base of the III–IV absorption has evidently parted from the photosphere, and the absorption, no longer recruiting atoms, begins to die out. In the new, high-velocity stream, which is responsible for the normal band in March, emission overpowers absorption, so that in both *Hβ* and K the violet end of the emission band, beyond the surviving deep III–IV absorption, is nearly as intense as the redward wing. The iron and titanium lines do not appear in this high-velocity stream; hence their normal emission fades away with the III–IV absorption system.

* *Pub. Obs. U. Michigan*, **6**, 149, 1937.

† *Harvard Circ.*, No. 406, 1935. ‡ *Proc. Nat. Acad.*, **22**, 199, 1936.

§ The mean "centre" of the absorption is at −750 km./sec., while the steep part of the emission contour is within the limits +400 to +1200 km./sec.

McLaughlin attributes III–IV, as well as II, to expanding shells. This may be effectively correct for the cores measured by him, but it seems likely that as long as the emission velocity corresponds to that of the absorption band these shells must be regarded as outward moving condensations in an atmosphere continually replenished by material ejection from the photosphere.

(4) The two displaced emission maxima, seen superimposed on the normal emission, are relatively much weaker in hydrogen than in calcium, forbidden oxygen and iron. In iron their combined total intensity is one-tenth that of the normal band. Evidence from the K line places them exterior to, or rather not within, the Absorption II shell, so that the low hydrogen intensity may be due to screening by the inner envelopes from the relatively high excitation required for Balmer emission.

When the nova fades in April, rather sharp emission lines become conspicuous. Both Adams and Joy,* and McLaughlin,† have inferred that these replace the Absorption II lines. It seems more probable, however, that they are the continuation of the violet component of the original displaced maxima. Thus, on March 27 the velocity of Absorption II was −393 km./sec. (−395, Merrill,‡ D lines, March 25·0; −391, Adams and Joy, March 25·0; −395, McLaughlin, March 29·3). During March the daily increase in velocity was about 0·75 km./sec. The absorption was last seen on April 3, and on April 4 had been replaced by emission lines with displacement −354 km./sec. (McLaughlin, −355; Adams and Joy, −352, for permitted lines only), that is, some 45 km./sec. less than the extrapolated displacement for Absorption II on the same date.

Meanwhile, the violet component of the forbidden oxygen lines, which represents displaced maxima untroubled by blending absorption, had also shown increasing velocity. The half-separation of the two components may be used to find the acceleration, and yields the value 1·06 km./sec./day (January–March),§ while five observations by Merrill ‖ give a normal place, March 21·4, −345 km./sec., for the violet maximum. The expected displacement for April 4 is thus −(345 + 15) = −360 km./sec., which agrees much more closely with −354 for the observed emission on that date.

The violet component was displaced −368 km./sec. on April 15 and −410 km./sec. on May 20.¶ Both these velocities are consistent with the 1·1 km./sec./day acceleration.

Whipple and Payne-Gaposchkin ** have identified the source of these maxima with the two bodies observed visually by Kuiper, while McLaughlin associates them with Shell II. It is possible that these two views are reconcilable and that the maxima represent cloud-like condensations in the shell. Comparison of the velocity of the violet maximum in the [*O* I] lines with

* *Ap. J.*, **84**, 14, 1936.

† *Pub. Obs. U. Michigan*, **6**, 198, 1937.

‡ *Ap. J.*, **82**, 413, 1935.

§ From measures by Merrill (*loc. cit.*) and Bobrovnikoff (*Perkins Obs. Contr.*, No. 2, 1935), both of whom used much larger dispersion on the [*O*] lines than McLaughlin.

‖ *Ap. J.*, **82**, 413, 1935.

¶ Adams and Joy, *Ap. J.*, **84**, 14, 1936.

** *Proc. Nat. Acad.*, **22**, 195, 1936.

the velocity of Absorption II shows that, from January 16 till the end of March, the ratio between the two is closely constant at 0·88. Thus, if both emission and absorption arise from the same spherical expanding shell, the angle between the direction of motion of the two supposed clouds and the line of sight is $\cos^{-1} 0{\cdot}88 = 28°$. With a mean separation for the two components of 700 km./sec. the relative tangential velocity is 700 tan 28° = 380 km./sec. = 80 astronomical units per year. The parallax of the nova derived by the writer from the interstellar line intensity was 0″·0027.* Hence, the expected angular rate of separation of the sources of the maxima is 80 × 0·0027 = 0″·216 per year. According to Kuiper,† the observed rate for the two bodies observed visually is 0″·26. The very reasonable correspondence suggests that the pair of displaced lines originate one from each of two clouds expanding as part of the spherical shell. The clouds themselves emit negligible continuous spectrum, since otherwise it would be impossible to have completely black lines, such as are observed, in Absorption II.

A difficulty arises, however, when the later radial-velocity measures are considered. Kuiper's discussion of the double-star observations points definitely towards a constant rate of angular separation after the discovery of duplicity. The spectroscopic evidence, on the other hand, shows definite deceleration after the great minimum. Wyse ‡ states that the first trace of the nebular [*O* III] emission appeared on April 11, and that the displacement was still the −400 km./sec. of the earlier violet emission. Later recorded velocities are as follows: −375 km./sec., June 8–9, Adams and Joy; −290, from 5 plates grouped round August 4, by Beer; § −275, September 10, −275, October 8 and −235, November 11, all by Adams and Joy. McLaughlin's measures were made on the band edges instead of the maxima, but they also show some decrease in displacement with time. Finally, on a photometer tracing of the N_1 line from a Cambridge plate of 1936 October 10, two points which may be considered as maxima separated by a slight dip have a relative displacement of only 375 km./sec. The total width of the nebular bands on this plate is essentially the same as it was in April 1935.

These later spectra do not present maxima as clearly defined as those of the pre-minimum phase, and it is possible that we are recording changes in the intensity distribution throughout the nebula rather than velocity changes. Also, as Stratton has pointed out,‖ there are differences of structure between different lines. Thus λ 4363 shows one central maximum, while according to Adams and Joy a plate taken 1936 February 7 by Merrill still shows the violet component of the [*O* I] line λ 6300 displaced "about 8 angstroms" or −380 km./sec. Further attempts to reconcile these inconsistencies can profitably await separation of the double star on the spectrograph slit.

* *M.N.*, **95**, 573, 1935. A trigonometric parallax has been obtained by Stearns (*Pub. A.A.S.*, **9**, 55, 1937). His value is −0″·005 ± 0·012.

† *Ap. J.*, **86**, 102, 1937.

‡ *P.A.S.P.*, **47**, 204, 1935.

§ *M.N.*, **96**, 236, 1936.

‖ *Observatory*, **60**, 197, 1937.

Summary

1. The primary purpose of the paper is to exhibit by means of contour diagrams the differences between and changes in form of several typical and relatively unblended lines. The period covered is that between the emergence of the second absorption system at the end of December and the rapid fading of the nova in April.

2. For hydrogen and calcium mean emission contours are determined. The forms of these approximate to curves derived theoretically by Chandrasekhar on the assumption of outward acceleration in an atmosphere maintained by continuous ejection. All lines gradually broaden from December to April, the total width-increase exceeding 50 per cent. $H\delta$ is broader than K with the iron lines intermediate.

3. $H\beta$ and $H\delta$ are compared. Until March their intensity distribution in emission is similar within the errors of observation; after that pronounced and inexplicable differences appear. During the period of observation the true intensity ratio $H\beta/H\delta$ decreases from 3·6 to less than unity.

4. The displaced emission maxima are treated as sources independent of the normal central band. Intensity variations for both sources are shown diagrammatically. The normal emission in $H\delta$ follows the light curve rather closely, and the magnitude fluctuations in the line equal those in the continuous. There is much less correspondence for the displaced maxima. The red component is strongest in H and K, followed by forbidden oxygen. It is abnormally weak in hydrogen.

5. Intensity changes in the two main absorption components are studied. The total absorption of the more displaced band is four times that of the sharp component though their depths are comparable. The connection between absorption and emission is discussed and several abnormal features are commented on.

6. The observations afford support for a picture of the nova in which the main emission arises from an expanding atmosphere continuously ejected from a pulsating and highly expanded photosphere, while the strong, broad absorption is produced at a higher level in this same atmosphere. The narrow absorptions originate in a detached expanding shell. The evidence suggests that the two displaced emission maxima represent outward moving condensations in this shell on opposite sides of the nucleus. These emit line-radiation only. Though it is tempting to identify these clouds with the two nuclei observed visually at a later date, the spectroscopic evidence for deceleration after the great minimum is difficult to reconcile with the observed constant rate of separation for the double star.

It is a pleasure to record my gratitude to Professor Stratton for his numerous and valued suggestions and comments, and for the interest he has shown in all stages of the work. I am much indebted also to Dr. Brück, who very kindly made numerous photometer tracings for me after I had left Cambridge.

Radcliffe Observatory,
Pretoria.

NEW MEASURES OF THE WAVE-LENGTHS OF THE CALCIUM LINES K AND H.

J. Evershed, F.R.S.

In *Monthly Notices*, **90**, 189, the wave-length of K and H in the carbon-iron arc at atmospheric pressure was determined from the nearest secondary standards of iron as follows :—

K 3933·663, H 3968·470.

The close accordance of the different series of measures, including both prism and grating spectra, appeared to show that these values could not be in error by as much as one unit in the third decimal, and no change exceeding this would seem possible unless the secondary standards of iron published by the International Astronomical Union in 1928 should be revised.

These values, however, are not in good agreement with the interferometer measures of the lines made in 1932 by the late Mr. C. V. Jackson at the Imperial College.* In this work the calcium lines were produced by a small quantity of $CaCo_3$ in a carbon arc *in vacuo*, and the measures were referred to the krypton standards between $\lambda\lambda$ 4273 and 4502. The mean values from 15 sets of observations, when corrected to atmospheric pressure, were

K 3933·666, H 3968·472.

The successful working of the liquid prism spectrograph, using ethyl cinnamate as the dispersing medium, has yielded arc spectra of iron and calcium on a scale of about 2 mm. to the angstrom with two transmissions through the prism, and between 3 and 4 mm. with four transmissions. The refracting angle of the prism is 63°, and the effective aperture for this part of the spectrum about 8 cm. The calcium lines in these spectra are very narrow, and the iron lines also are narrow and well defined, excepting the four strong lines near K, which have a central narrow absorption line. I have measured these spectra with a re-designed micrometer to see if any modification of the figures quoted above would result from the increased resolving power and scale of the spectra, and with improved methods of measuring.

The Micrometer consists of a Hilger screw mounted on an iron base-plate and furnished with a long self-adjusting nut. The screw has a millimeter pitch, which is uniform throughout the length used of about 10 cm., and there appear to be no sensible periodic errors. Attached to the nut is a brass plate, 12 by 6 cm. : of this, 4 cm. of its width overhangs the nut on the outer side, and in this portion a slot is cut, 10 cm. long by 1 cm. wide. Below this is an equally long mirror, reflecting light upwards through the slot. The glass negative to be measured is stuck to the plate by three small lumps of optical

* *M.N.*, **93**, 98, 1932.

cement, the spectrum image being placed centrally along the slot and adjusted parallel to the screw.

To prevent the nut rotating when the screw is turned either way a round steel arm is attached to it directed downwards, and bearing against a straight edge fixed on the base-plate and adjusted parallel to the screw. It is held against the straight edge by a 100-gramme weight at the end of a short arm, also attached to the nut. The end of the screw is polished flat, and bears against an optically worked sapphire thrust block. It is held against this by a spring acting on a shoulder on the screw shaft at the drum end of the screw, according to the design of Messrs. Hilger.

It will be seen from this short description that friction is reduced to a minimum. The screw simply moves the nut carrying the photograph, the only friction other than the screw bearings and the nut itself is the sliding of the steel arm against the straight edge. The result is that backlash on reversing the motion is very nearly abolished, and wear on screw and nut is inappreciable.

The rest of the instrument is designed to facilitate measuring by the positive on negative method, or by the usual scheme of bisecting the spectrum lines with a fine straight line or lines engraved on glass. For either purpose an adjustable frame is attached to solid cast-iron supports above the screw, and this can be raised or lowered rapidly through 2 cm. screw movements being provided for fine adjustments. This frame carries alternatively either the positive spectrum plate attached with optical cement, or a glass reticule on which two parallel fine lines are engraved, $\frac{1}{4}$ mm. apart and 7 mm. long.

For the wave-length measures the glass reticule is used, and this is lowered to within about 0·3 mm. of the negative, and carefully adjusted by means of the appropriate screws until the engraved lines are as nearly as possible parallel with the spectrum lines.

The viewing microscope consists essentially of a telescope of 22 cm. focus, fitted with an additional object-glass of the same focal length to form a collimator. This gives a flat field of excellent definition, and the small difference of focus of the reticule and the negative (0·3 mm. on a focal distance of 220 mm.) is of no account. The two are seen in perfect focus together. This optical combination is shortened, and the eyepiece brought to a convenient angle for viewing the spectrum, by a right-angle prism and a small plane mirror. The glass reticule when adjusted is clamped firmly above the negative : the microscope therefore does not need to be immovably fixed, as would be the case were the reticule placed as is usual in the focus of the eyepiece. It is in fact mounted on a slide, and can be moved about by hand parallel to the screw for the purpose of adjusting the negative accurately parallel before beginning the measures.

Method of Measuring.—The positive on negative method is inconvenient for wave-length measures because of the very large intervals involved. The screw would need to be twice the usual length to deal effectively with the intervals. I have therefore adopted the following scheme for reducing to a minimum the errors involved in bisecting a spectrum line with the engraved line of the reticule.

The lines in these prismatic spectra are very nearly straight, the curvature being compensated by an appropriate curvature of the spectrograph slit.

In the diagram, 1, 2, and 3 represent three successive positions of a spectrum line with reference to the shorter lines of the reticule. A movable mask in the eyepiece of the microscope allows one to concentrate attention first at A, where readings are taken at each successive position ; then, moving the mask, a similar set of readings is made at B. The number of settings for each position is usually three. Consequently the final position of a line

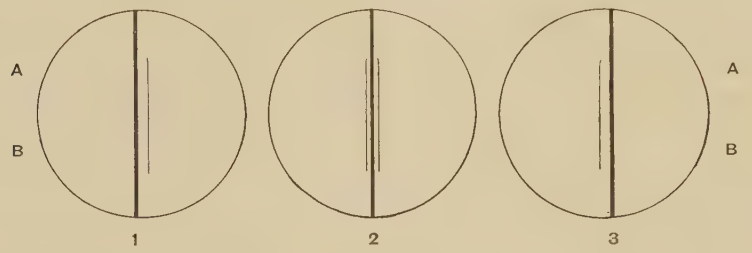

depends on the mean of 18 settings. The spectrum is, however, always measured twice, red to the right and red to the left, or 36 settings altogether for each line.

It is a very great advantage to have the engraved lines shorter than the spectrum lines, and not occupying more than one-third the diameter of the field of view of the microscope, for then it is possible to measure very faint and narrow lines which would be completely hidden when covered by the engraved line ; but it is easy to see the line projecting beyond the engraved line, and to place it in alignment in positions 1 and 3, and to place it central in position 2 with very considerable accuracy. I find it an advantage also in bisecting the stronger lines to observe the alignment at the same time.

Methods of Reduction.—In all prismatic spectra hitherto measured, including those obtained with glass prisms or with ethyl cinnamate as the dispersing agent, it is found that the rate of increase of scale with decrease of wave-length is very nearly constant over a range of 60 angstroms. In other words, $\frac{\delta\lambda}{\delta m}$ plotted against λ is sensibly a straight line. In measuring a low-dispersion solar spectrum, extending over many hundreds of angstroms, and plotting this relation over the whole range, it becomes apparent that the curvature over even 100 A. is inappreciable. I have therefore adopted a linear relation for converting measured intervals into wave-length. The wave-length of K and H is in this way derived from the nearest secondary standards, one on either side of these lines. These were

$$\begin{matrix}3930{\cdot}299\\3935{\cdot}815\end{matrix} \text{ for K} \quad \text{and} \quad \begin{matrix}3967{\cdot}423\\3969{\cdot}261\end{matrix} \text{ for H.}$$

Professor Fowler has suggested to me that it would be more satisfactory to adopt the Cornu-Hartmann interpolation formula in reducing the measures, for the results would then depend on all of the secondary standards measured, and not merely the two nearest lines ; also, as the straight-line formula can

only be approximate, the error might be appreciable in the case of K, where the nearest secondary standard on the violet side is over 3 A. distant. With Professor Fowler's kind advice and assistance, several sets of measures have been reduced by both methods, but with no appreciable differences in the values obtained ; and it was shown also that with the straight-line formula no error would be introduced in the wave-length of K as great as 0·001 A. ; and in H, where the two lines used in the simpler method are very close to the calcium line, the error would be much smaller. The Hartmann formula would, however, be of use in checking or improving the relative wave-lengths of all the secondary standards measured, and in this connection we found that the only line which appears to require a small correction is the line tabulated at 3940·882.

As a further check on the two methods of reduction I measured ten prominence spectra, selected for the excellent quality of the comparison arc lines of iron and calcium. These were obtained with solid glass prisms of 10 cm. effective aperture, and have a scale between H and K of 1·2 mm./A., or about 1/3rd the dispersion obtained with four transmissions through the liquid prism.

The measures were reduced using the simpler method, and independently by Dr. Comrie using the Hartmann formula, which involves 8-figure logarithms, and a very considerable amount of computation. In this case the following secondary standards of iron were measured, the constants in the formula being determined from those marked with an asterisk :—

3920·260*	3956·681
3930·299	3966·066
3935·815	3967·423
3940·880	3969·261
3948·779*	3977·745*
3949·958	

In Table I, I give the results of this comparison. The columns headed C and E are the fractional wave-lengths determined respectively by Comrie using the Hartmann formula, and the writer using a large scale graph to find the required conversion factors.

In addition to K and H, I measured a faint *Fe* line at λ 3932, which does not appear to be subject to pole effect, and the line at 3940 which appeared to require a correction. At the foot of each column I give the mean values of the two methods and the probable errors derived from the residuals of the individual measures. The mean values from all the 10 plates reduced by the Hartmann formula have been tested by means of an error curve in the usual way, but the only line requiring an appreciable correction is H, which required to be increased by 0·0025 A., making it equal to my value.

Two points are to be noted in this table : first, the agreement of the two methods of reduction, and, second, the very much larger range of values for the H line computed by the Hartmann formula compared with the simpler method depending only on the two neighbouring lines. This results in a probable error for H nearly three times larger for the Hartmann method.

Table I

No.	K 3932 C	K 3932 E	K 3933 C	K 3933 E	3940 C	3940 E	H 3968 C	H 3968 E
1	·628	·626	·663	·661	·883	·881	·466	·470
2	·630	·630	...	...	·880	·881	·462	·469
3	·628	·631	·660	·662	·880	·880	·464	·467
4	·629	·631	·663	·663	·880	·879	·467	·469
5	·625	·626	·662	·662	·878	·878	·466	·467
6	...	...	·662	·662	·883	·882	·459	·465
7	·629	·630	·662	·662	·883	·882	·466	·471
8	·629	·630	·659	·660	·882	·882	·466	·469
9	·628	·628	·665	·665	·882	·882	·474	·468
10	·630	·633	·663	·663	·882	·881	·469	·473
Means	·628	·629	·662	·662	·881	·881	·466	·469
P.E. ±	·0003	·0005	·0004	·0003	·0002	·0001	·0011	·0004

This difference is not due to errors of computation, as the wave-lengths showing the largest discordances have been checked.

On the whole, I consider this series of measures gives reliable mean values of wave-length, notwithstanding the comparatively small scale of the spectra. The greatest deviation from the mean for K is 0·003 A., and for H in column E it is 0·004 A. In Jackson's interferometer measures of 15 plates the greatest deviations are also 0·003 A. for both K and H. A slight instability in these lines appears to be indicated.

Table II

Mean Results of New Measures of K and H in Iron-carbon Arc in Air

Series	No. of Measures	K	H
1	Mean of 6 spectra, approx. scale 4 mm./A.	3933·663 ± ·0004	3968·468 ± ·0001
2	Mean of 10 spectra, approx. scale 2 mm./A.	·663 ± ·0001	·469 ± ·0002
3	Mean of 10 spectra, approx. scale 1·2 mm./A.	·662 ± ·0004	·469 ± ·0004
	Adopted values	3933·663	3968·469
	Previous values, *M.N.*, **90**, 189, 1929	·663	·470

In Table II, I have collected the mean values from all the new measures without giving individual results. In series 1 and 2 with high dispersion, the separate values are rather more accordant than those shown in Table I, as was to be expected. In series 1 the greatest deviation from the mean for K is 0·002 A., and for H it is less than 0·001 ; and for series 2 it is 0·003 for K and 0·002 for H. These variations are larger than can be accounted for by errors of measurement. In series 2, the plates giving the lowest and highest values for K were re-measured with results not differing at all in the third decimal. Such small differences may of course be due to the gelatine film on drying not recovering the exact form it had before development. If,

however, it is a real variation in the relative positions of the calcium and iron lines, then one would expect H to vary in the same direction as K in any single photograph. This is in fact usually the case, though H is less affected than K, as the following comparison of mean values indicates:—

High Dispersion Spectra

		K	H
Mean of 9 measures, K exceeding	3933·6630	3933·6642	3968·4696
Mean of 6 measures, K less than		3933·6620	3968·4688
	Difference	·0022	·0008

Low Dispersion Spectra

Mean of 3 measures, K exceeding	3933·6630	3933·6638	3968·4700
Mean of 7 measures, K less than		3933·6615	3968·4688
	Difference	·0023	·0012

Approximately, therefore, when K increases in wave-length by 0·002 A. H increases by 0·001 A. Assuming the secondary standards of iron to be perfectly stable lines, it may be that K and H are very slightly subject to pole effect. In working the iron-carbon arc for these spectra the lower pole is of steel, and the upper one a rod of carbon, 5 mm. thick, which contains sufficient traces of calcium to give very narrow lines, but the length of the arc cannot easily be controlled; it may vary from a few mm. to 1 or 2 cm. with 5 to 6 amperes on a 100-volt circuit. It follows that some of the spectra may have been obtained with a short arc very near to the poles, and others near the centre of a long arc.

The mean values of the three series in Table II are in quite satisfactory agreement, and they confirm the values previously published, the only difference being a correction to H of −0·001 A. The difference between these results and the interferometer measures already referred to is 0·003 A. for both K and H, the interval 34·806 A. between the two lines being the same in both.

If the lines are subject to pole effect, I can only suggest that in Jackson's work the pole pieces were very close together in the vacuum arc, for this might tend to give larger values, but the difference may also be connected with the different standards used.

If the adopted mean values are corrected by subtracting the pressure shift of one atmosphere, and are then compared with the measures of these lines in the Revision of Rowland, the following differences are obtained :—

	K	H
Arc reduced to vacuum	3933·661	3968·467
Centre of Sun (1928 scale)	·684	·494
Sun − vacuum arc	+0·023	+0·027

My direct measures of the shift of the solar lines gave K +0·020 and H +0·023.

I may once more call attention to this large shift of the high-level calcium lines at the centre of the Sun, approximately three times the Einstein effect, whilst at the limb it is reduced to +0·015 A., according to my direct measures.

Supplementary Measures.—In addition to K and H a few other lines were measured in these spectra. The mean wave-lengths are given in Table III as follows :—

TABLE III

Mean λ	Element	Number of Measures	Greatest Deviation from Mean
3928·091	*Fe*	2	0·000
3932·628	*Fe*	9	0·002
3933·602	*Fe*	3	0·002
3940·881	*Fe*	10	0·003
3944·014	*Al*	6	0·002
3949·957	*Fe*	5	0·001
3961·529	*Al*	6	0·002

The lines 3932 and 3940 are from Table I. 3933 is a faint iron line very close to K, and only measurable in three plates where the iron lines are strong and K very weak. The aluminium lines show in these spectra as well-defined narrow lines.

Summary.—High dispersion spectra in the H and K region obtained with the liquid prism spectrograph, and others of less dispersion obtained with glass prisms, have been measured with a newly designed micrometer for the accurate determination of the wave-lengths of the calcium and other lines in the open arc, and for comparison with interferometer measures of H and K.

A description is given of the micrometer and of the method of measurement. The computation of wave-lengths was made by the Cornu-Hartmann interpolation formula for many of the measures and compared with a simpler graphical method.

Tables are given showing the results for calcium, aluminium and some of the iron lines. The wave-lengths of the calcium lines are in very close agreement with those previously published by the author, but differ appreciably from the interferometer measures by the late C. V. Jackson. Possible causes of this difference are mentioned.

The adopted wave-lengths of K and H reduced to zero pressure are compared with the values given in the Revision of Rowland's Table for the Sun, showing a shift to red of these lines at the centre of the Sun which is three times the Einstein effect.

AN IMPROVED LIQUID-FILLED PRISM.

F. J. Hargreaves.

Owing to the difficulty of obtaining homogeneous blocks of highly dispersive glass large enough to form prisms of from 4 to 6 in. effective aperture, numerous experiments have been made by Mr. J. Evershed with a hollow prism filled with a highly dispersive non-volatile liquid. Ethyl cinnamate has been used with very considerable success, and also a solution of 2-methyl naphthalene in 1-methyl naphthalene. Neither liquid has any of the disadvantages of carbon disulphide.*

The prism with which these experiments were made was described by Mr. Evershed in *M.N.*, **89**, 175, 1928, and I wrote an account in *The Observatory*, 1936 Oct., of difficulties which were encountered owing to the fact that the walls of the prism were cemented together more or less rigidly, and of the remedy that was found for these difficulties. I also said that although a remedy for a defective prism of this type had been found, it was desirable to find a mode of construction which would be free from the causes of distortion inherent in the "cemented-box" type.

Such a construction has been devised and found to be satisfactory in practice. The essential feature is that the glass plates constituting the refracting sides of the prism are joined at their edges to the remainder of the "box" by a flexible connection in the nature of camera bellows, and that three external abutments or stops are provided for each plate, against which the plate is held solely by the pressure of the dispersing liquid within the cell. Thus the only forces acting on the plates (apart from gravity) are the pressure of the liquid and the reactions at the abutments. The curvature produced by these forces can be minimised by suitable choice of the positions of the abutments and is actually quite negligible. The flexible connection itself cannot set up any appreciable stresses in the plates, and, moreover, it allows the remainder of the "box" to be made of a material having a coefficient of expansion different from that of the glass of the plates. These parts of the prism now to be described are of brass.

It was intended to make two prisms embodying this principle, one a transmitting prism of 63° angle and the other a reflecting prism of $31\frac{1}{2}°$ angle. Owing to a succession of mishaps only the reflecting prism has been completed. It is being used for the present in series with the original rigidly cemented prism, which will be discarded when the new transmitting prism is ready.

Fig. 1 is a vertical cross-section of the prism showing how the flexible connection is arranged. It is a sheet *a* of goldbeaters' skin cut to form flaps *b* stuck to the inner surface of the brass cell *c*, and having its margins

* *M.N.*, 98, 326, 1938.

stuck to the edges of the glass plate *d*. At the corners reinforcing strips *e* are stuck on so as to bridge the gaps between the edges of the flaps *b*. The adhesive used is an alcoholic solution of a substance known as "lac resin," which is extracted from shellac. This substance adheres firmly to any

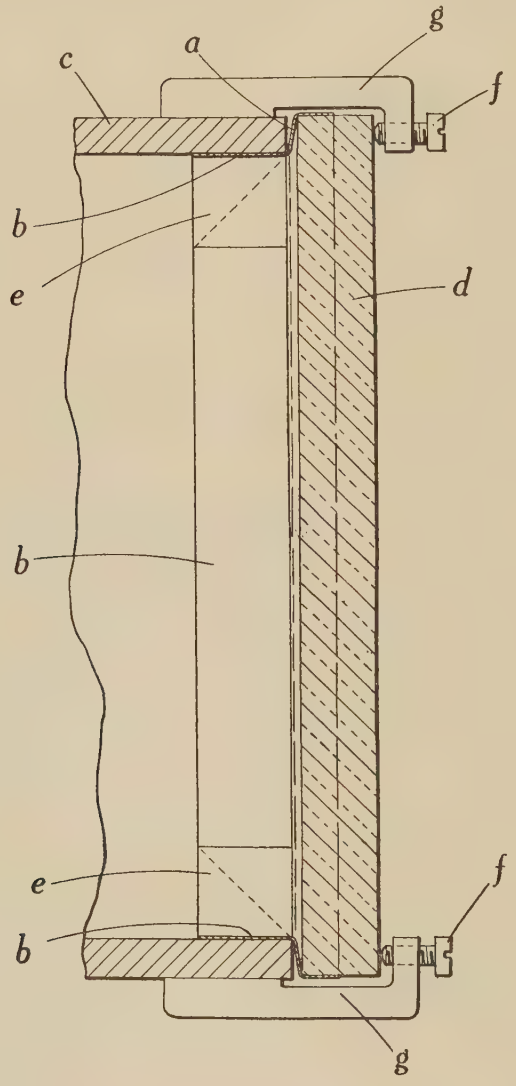

Fig. 1.

solid surface, even a polished glass surface, and is inert to both the liquids which may be used in the prism.

This form of flexible connection was adopted after the failure of an attempt to use bellows of paper impregnated with lac resin. The failure was due to causes peculiar to this particular prism. Paper bellows could be used successfully in the second prism now under construction, but the

A

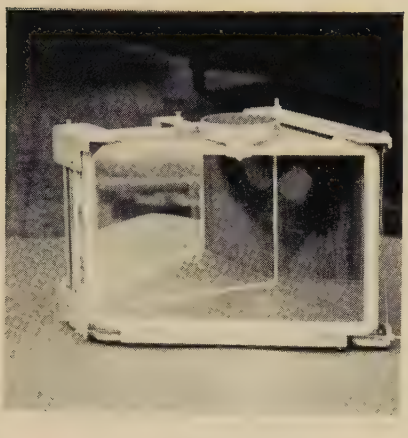

D

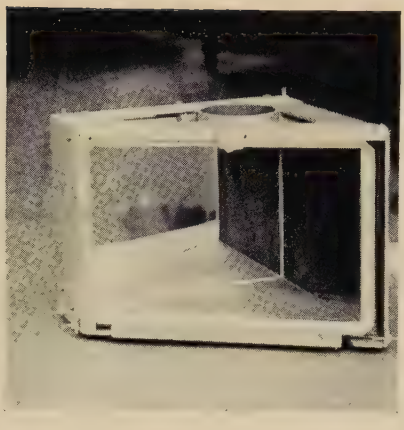

B

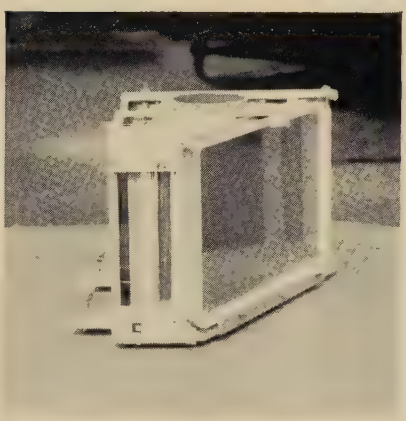

E

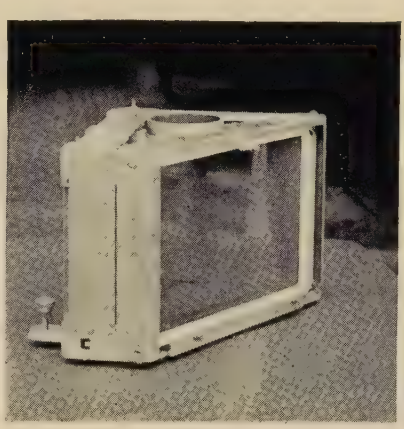

C

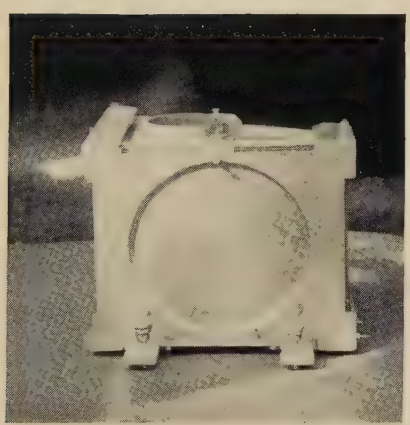

F

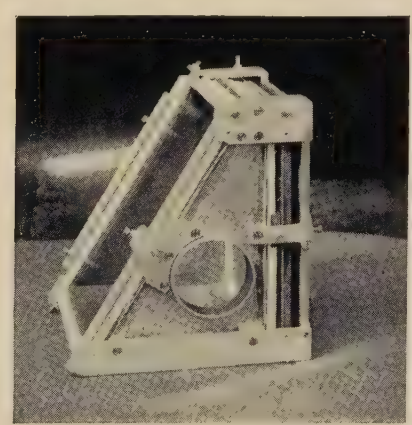

F. J. Hargreaves, An Improved Liquid-filled Prism.

goldbeaters' skin, which has proved to be quite satisfactory, will be used because it is very much easier to manipulate and fit.

The abutments for the plates consist of screws *f* held in brass brackets *g* fixed to the top and bottom of the cell *c*. Fig. 2 is a front view of one face of the prism showing the positions of the three abutments. The two lower abutments are not at the corners of the plate, but at a distance inwards from the corners of about one-fifth the length of the plate. Thus a horizontal strip of the plate at the bottom, considered as a beam uniformly

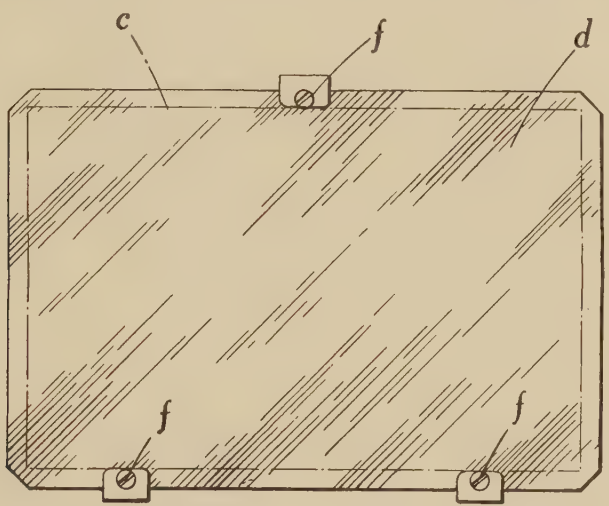

Fig. 2.

loaded by the pressure of the liquid, is supported approximately at the "Airy points," with the result that its curvature is only a small fraction of what it would be if supported at its ends. This device obviously cannot be used to minimise the flexure in the vertical direction of the transmitting plate, but it can be so used for the reflecting plate of the $31\frac{1}{2}^\circ$ prism, and as shown in photograph C (Plate 1) the two lower screws are displaced upwards from the bottom as well as inwards from the sides.

This reflecting plate is aluminised on its inner surface, so that the light does not pass through the glass.

The photographs were taken before the paper bellows referred to above were discarded, but they represent the present appearance well enough. D and E show the cover-plates in position which protect the flexible connection from accidental damage, and A, B, C and F were taken with these cover-plates removed.

The supporting of the weight of the glass plates presented a rather difficult problem, particularly as provision had to be made for inverting the prism to empty it. The goldbeaters' skin is of course not strong enough to support the weight, and even if it were, it would not do to put it on tension permanently because of the possibility of unequal distribution of stress which might distort the surfaces. This problem was solved by using

slings made of phosphor-bronze wire. These are shown in fig. 3 separately for the sake of clearness. One of these supports the plate in the normal position, the second supports it when inverted, and the third, which completely encircles the plate, gives support in the horizontal direction.

In the next prism now being made this arrangement will be modified.

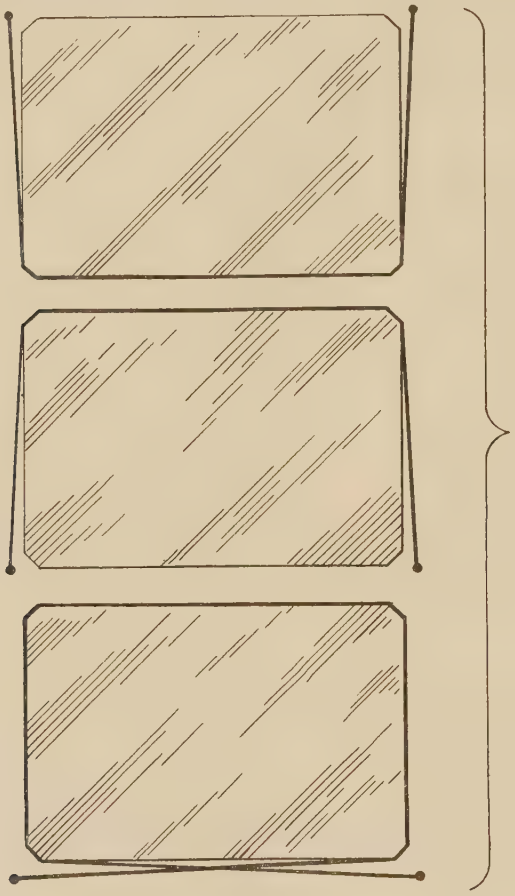

Fig. 3.

As shown in fig. 4, each plate will have in its lower edge a conical recess and a V groove. These will be seated upon two small spherical supports which will not only support the weight in the normal position, but also prevent horizontal movement, as well as serving as the two lower abutments which support the plate against the pressure of the liquid. Only the second of the three wire slings will therefore be needed, to support the plate when the prism is inverted.

The brass plate at the back of the reflecting plate is primarily for the purpose of bracing the cell against distortion, which might tear the gold-beaters' skin. In the transmitting prism this form of bracing cannot be used, but instead a stiff web or rib encircling the cell in its median plane will be provided.

The prism is housed in a recess in the end of Mr. Evershed's underground observatory, twelve feet below the surface, and the mouth of the recess is closed by a thick wooden partition. The temperature within this recess therefore remains constant for long periods. A prism of this kind used in less favourable situations would need to have its temperature controlled within very close limits if it is to perform perfectly.

The aperture of the transmitting side of this prism is $7\frac{5}{8}$ in. long and $5\frac{1}{8}$ in. high, the effective aperture at about 60° incidence therefore being

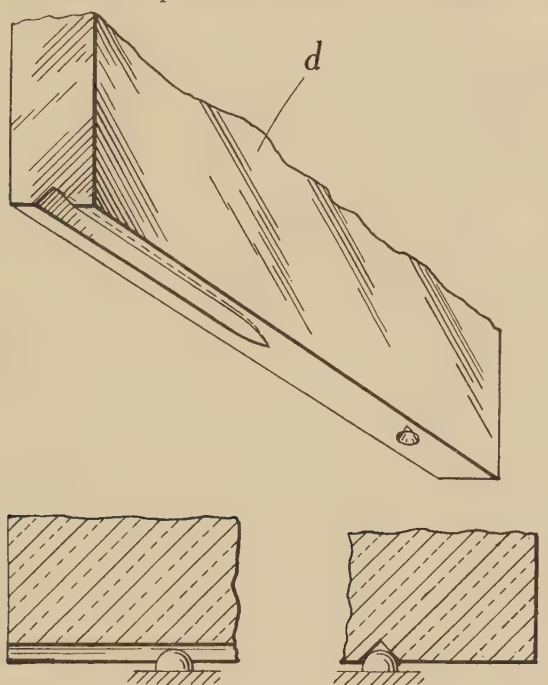

FIG. 4.

$3\frac{3}{4}$ in. The thickness of the glass is $\frac{1}{2}$ in. The transmitting prism will have a slightly greater aperture.

There seems to be no reason why much larger prisms should not be made on this principle, the only limit being set by the size of moderately thin discs that can be made homogeneous. As to this, it is to be remembered that the glass can have any refractive index and dispersive power whatever, the only requirements being transparency, freedom from colour and homogeneity. It should not, therefore, be a difficult matter to produce suitable discs much larger than those of the present prism.

Summary

The paper describes a hollow liquid-filled prism of about $3\frac{3}{4}$ in. effective aperture consisting of a brass cell and two glass plates joined at their edges to the cell by flexible connections incapable of setting up stresses in the plates, which are held against rigid stops or abutments by the hydrostatic pressure of the dispersing liquid in the prism.

REPORT OF THE NEW ZEALAND TOTAL SOLAR ECLIPSE EXPEDITION TO CANTON ISLAND, 1937 JUNE 8.

C. B. Michie.

Every student of solar eclipse work knows of the evident discrepancies between photographs and drawings of the solar corona made at the same eclipse. The writer examined the corona visually at the 1930 eclipse on Niua-fo'ou Island, noting features which had not been revealed in pictures examined and some to which no reference had been made: these features were also absent from the finished photographs made by the expedition, which were of the usual type. The plans for the eclipse of 1937 June 8 had a bearing upon this problem. The party consisted of Major G. W. Buddle, D.S.O., Messrs. I. L. Thomsen, official member, M. Geddes, W. Ross, W. F. Berry, E. P. Alton, F. Gawith and the writer. On arrival at Suva on May 21 the party with their equipment were transferred to H.M.S. *Wellington*, which had been authorised by the Admiralty to convey the party to and from Canton Island. The work of disembarking commenced at dawn on the 27th: the passage into the lagoon from the ocean is narrow and very dangerous owing to the fast tidal current which at times attains a speed of six or seven miles an hour, but through skilful handling of the boats the loads were all safely landed. We were greeted on arrival by Prof. S. A. Mitchell, the scientific leader of the United States party, who offered assistance and such facilities as his party possessed.

By nightfall on the 27th the camp had been pitched, and the work on the erection of concrete and timber structures for the mounting and protection of the instruments and for a dark room followed. By June 1 the cœlostat and 19-ft. coronagraph were erected and ready for adjustment. A 78-in. camera was mounted equatorially on two concrete piers: this was fitted up with a rotating sector to enable photographs to be taken giving detail over a wide range of light intensity. The gramophone driving-motor intended for driving this sector failed and a hand-drive had to be improvised instead.

At 4.30 on June 8 the sky was completely overcast; at daybreak slight rifts in the clouds could be seen and the Sun rose in a small clear space over the eastern reef. The clear space became larger and, although an occasional cloud floated in, the condition appeared much kinder. At first contact the Sun was perfectly clear and it remained so until after totality. The eclipse duties were distributed as follows: The theodolite observations of contacts, time-recording and counting, Lieut. Butler-Bowden, R.N., assisted by Signaller Reed; the 19-ft. coronagraph and cœlostat, Thomsen and Geddes; the 78-in. camera and rotating sector, Michie and Gawith; a 3-ft. sighting tube for visual measurement of the coronal streamers,

Berry ; Alton was observing temperature, wind force, cloud, etc., and was securing a succession of photographs to determine progressive light

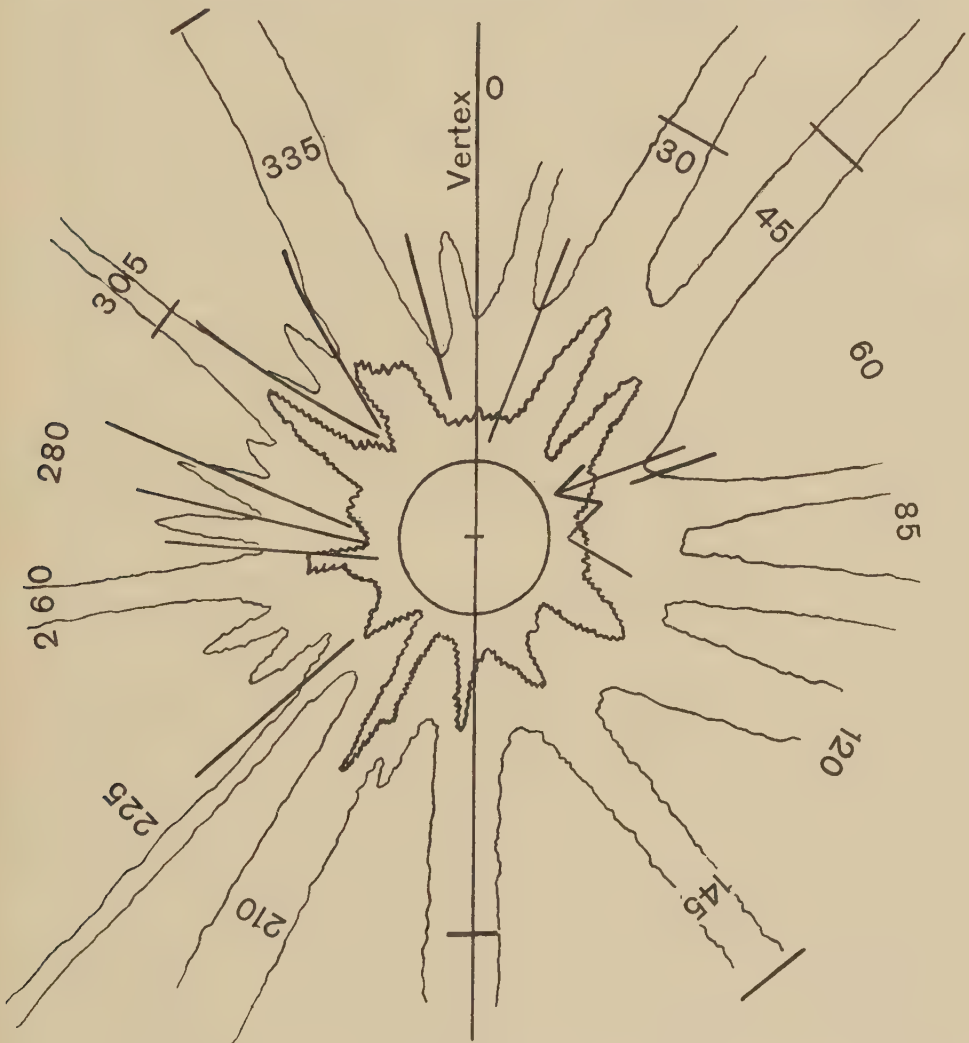

FIG. 1.—*The heavy irregular line shows the sketch by G. W. Buddle of the inner corona. The faint outer lines show outline of streamers on 78-inch camera plates. Heavy lines across the streamers at positions* 30, 45, 145, 180, 305 *and* 335 *indicate visual streamer measurements by W. F. Berry. At* 60 *appears the South Polar rift. In two plates of the 78-inch with rotating sector this is duplicated. Positions are indicated by broad arrows. At* 0, 20, 60, 225, 270–280 *and* 348 *heavy lines show the positions of dark shafts referred to on p.* 135. *At position* 305–335 *two heavy lines indicate boundary of another dark rift.*

diminution during the eclipse ; Buddle was drawing the corona (see fig. 1) and Rose was to note the planets and stars visible ; in addition Geddes searched in vain for traces of the zodiacal light, while Alton and Berry also observed shadow bands.

At 5 seconds before second contact the inner corona was very distinctly visible to me and rapidly extending, especially in the region of the brighter streamers. The corona was of the usual spot maximum type, rather symmetrical in shape, though two exceptionally extensive streamers could be traced visually to a distance of four solar diameters from the eastern and western limbs respectively ; fine brush-like emanations were particularly abundant and bright. Both inner and outer portions of the corona appeared to the writer to be brighter and more extensive and the darkness more intense than at the eclipse in 1930.

Nine photographs 10×8 in. were taken with the 19-ft. coronagraph ; the exposures were of 2, 5, 10, 20, 45, 25, 20, 10 and 2 seconds duration ; the lens was 4 in. working at $f/56$. We were indebted to Professor Mitchell and Dr. Gardner for the loan of five double plate-holders enabling an increased number of exposures to be made. Six photographs $8\frac{1}{2} \times 6\frac{1}{2}$ in. were taken with the 78-in. camera working at $f/14$: three were taken in conjunction with the rotating sector and were of 5, 3, 10 seconds duration ; the sector was then removed and three more were taken of 10, 28, 20 seconds duration. All the plates were successfully developed at Apia in the early morning of June 13 in the developing rooms of Mr. Tattersal, which he had kindly put at our disposal.

There is a great difference between the results obtained with the two instruments. The coronagraph reveals a wealth of detail throughout the inner corona and the prominences are well defined, but even with an exposure of 45 seconds it does not reveal the corona beyond 1·5 diameters from the Sun's limb. With the 78-in. the streamers can be followed, in some instances to distances of 3·5 diameters and more ; the visual observations agreed well with the exposure of 28 seconds.

The principal streamers are given below, their position being measured clockwise from the vertex ; the measurements of extension were taken from the transparency, the bracketed figures are Berry's visual measures—the unit is a solar diameter. At 30° and 45° are two streamers, the first brush-like and diffuse extending to 3·0 (2·5), the second bright and sword-shaped, 4·0 (3·0) : between 80° and 120° a group of moderate streamers are seen, and at 145° a streamer fading out in a diffused area at 2·2. In this streamer is a striking coronal object, much brighter than the enveloping material and quite sharply defined, like a long slender curved bill terminating at 1·2 ; it is shown by both cameras. At 180° and 210° are two streamers extending to 2·4 (2·5) and 3·2 (3·5), accompanied by a bright narrow ray at 228″ coinciding with the position of a prominence : this fades out at 2·5 and then reappears and continues to 3·5. At 305° is shown a narrow and sharply defined streamer extending to 2·7 (2·0), while at 338° there is a group of which the most prominent coincides with a prominence and reaches 3·3 (3·5). The coronagrams portray a wonderful variety of fine bright brush-like rays extending to nearly one solar diameter from the limb and frequently accompanied by overlying leaf-like structures. A dark shaft can be plainly discerned at about 60°.

The dark regions in the corona were one of the objectives in the rotating

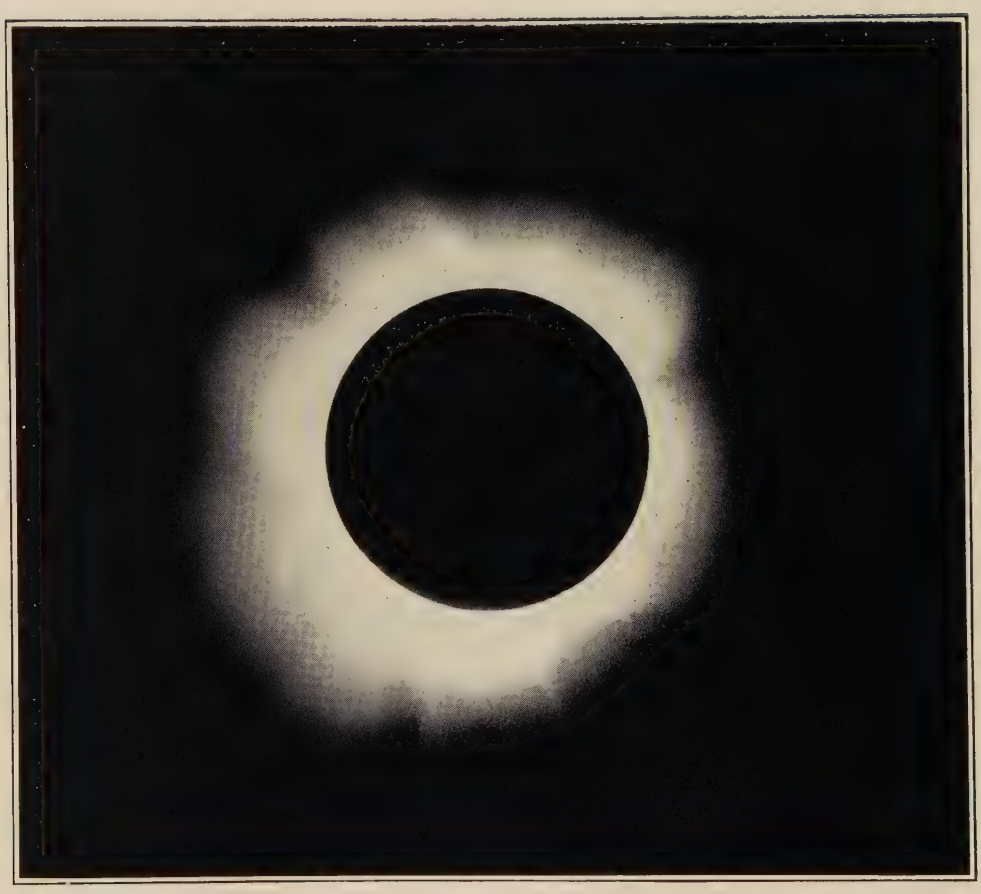

C. B. Michie, Report of the New Zealand Total Solar Eclipse Expedition to Canton Island, 1937 June 8.

C. B. Michie, Report of the New Zealand Total Solar Eclipse Expedition to Canton Island, 1937 June 8.

sector experiments, which were designed to equalise the amount of light reaching the plate so that details in the bright inner corona should be retained in long exposures which would show the faint outer extensions. The sector was made in a shape resembling two bulbous spokes in a wheel, while within the hub a slit, reducing towards the centre, was made to admit a small amount of light to form the image of the inner corona and the prominences. The halation from the inner corona on to the Moon's disc seen on the plates without the sector was much diminished, the limb of the Moon being seen quite sharply : in the exposure of 10 seconds the glare of the inner corona is reduced to 0·16 diameter, while the streamers can be traced out to nearly 3 solar diameters.

The photographs taken with the rotating sector and the short exposure plates taken with the coronagraph reveal several dark regions in the corona extending inwards to the rim of the eclipsed Sun. In the centre of one of these there is a narrow dark shaft actually joining the dark limb and radiating from a point slightly displaced from the centre of the disc. This is accompanied by another dark shaft 8° away which extends parallel to it, but not reaching down to the limb of the Sun. Another system of these dark rays can be seen near the vertex ; three of these though not followed up to the limb would meet, if continued at a point 0·14 diameter within the edge of the disc. They suggest the action of electro-magnetic fields.

The visual tube used by Berry for streamer measurements was a 3-inch tube made from ordinary plain sheet iron. There were no lenses. At the eye end a $\frac{1}{4}$-inch sighting hole was bored : at the objective end a metal strip was fitted with a slot into which one-half of the solar disc just fitted. A series of V-shaped slots corresponded to solar diameters and served as a scale for measuring the lengths of the coronal streamers. The strip could be rotated and its angular position for each streamer noted.

Thanks are due from the expedition to the Royal Irish Academy and the Royal Observatory, Greenwich, for the loan of the 19-ft. coronagraph ; to the Joint Permanent Eclipse Committee and to Dr. Comrie for assistance ; to Sir Arthur Richards, High Commissioner for the Western Pacific, for authority to visit Canton Island ; to Rear Admiral the Hon. E. R. Drummond and the Admiralty for permission to voyage on H.M.S. *Wellington* ; to Commander G. N. Loriston-Clark and his officers and men for their help to our expedition ; to the Rt. Hon. M. J. Savage, Minister for External Affairs, the Hon. D. G. Sullivan, Minister for Scientific and Industrial Research, Mr. Falla, Manager U.S.S. Company, and others for granting concessions ; Dr. E. Marsden for the loan of instruments and for energetic support ; the Defence Department for the loan of tents and camping equipment ; Dr. A. G. Frankau for free storage and transport of instruments ; Professor Burbidge and Mr. A. Harris for aluminising the cœlostat, and to a number of other helpers who made the expedition possible.

Kaitaia, N.Z. :
1937 *November.*

OBSERVATIONS OF OCCULTATIONS MADE AT TEDDINGTON DURING 1937.

John L. Haughton, D.Sc., F.Inst.P.

The occultations were timed with a stop-watch, as in previous years, up to No. 115, after which a chronograph was used. Seconds were marked on the chronograph record by a pendulum without any maintaining mechanism, which continued to swing through a reasonable arc for about 30 minutes. Half-minute signals from the Synchronome clock were superimposed on the record. It was, therefore, only necessary that the error of the rate of the pendulum be less than could be detected (about 1/20 second) during a period of 30 seconds. Actually it was very much better than this.

The difficulty of observing occultations when the Moon was nearly full was considerably reduced by the use of a neutral filter in the eyepiece, so arranged that it covered half the field. The illuminated part of the Moon was placed behind this filter, and thus the glare was greatly cut down. It is probable that some of the observations, made when the sky was hazy, would have been impossible but for this device. Weather conditions were, however, so bad that only nine occultations were observed. The results are given in Table I, a correction for estimated lag having been applied to column 6. The amounts subtracted are: 0·2 second for Nos. 107, 108, 115 and 122; 0·5 second for Nos. 106, 110 and 123; and 1·0 second for Nos. 113 and 119.

The author is indebted to Messrs. Scientific Computing Service Ltd. for the reduction of the occultations, the results of which are given in Table II.

TABLE I

1	2	3	4	5	6	7	8
No.	Date	Star	Mag.	Ph.	U.T.	P.E.	Remarks
					h m s	s	
106	Jan. 2	237 B Leo	6·3	R	01 39 58·3	0·4	
107	Feb. 16	27 Ari	6·4	D	20 35 21·7	0·3	
108	Feb. 17	B.D. +20° 573	7·2	D	19 56 10·2	0·4	
110	May 19	13 B Vir	5·8	D	21 20 09·6	0·3	Haze
113	Aug. 15	B.D. −22° 4205	6·9	D	21 13 22·9	0·6	Difficult
115	Sept. 14	36 Sgr	5·1	D	18 50 10·4	0·4	
119	Nov. 9	B.D. −17° 5832	7·4	D	17 58 21·3	0·8	Difficult
122	Nov. 14	κ Pis	4·9	D	00 07 14·0	0·4	
123	Nov. 21	ν Gem	4·1	R	00 07 31·9	0·3	

TABLE II

No.	p	q	p^2	pq	q^2	$\Delta\sigma$	$p\Delta\sigma$	$q\Delta\sigma$
106	−100	− 9	99	+ 9	1	+3·4	−3·4	−0·3
107	+ 95	+30	91	+29	9	−1·9	−1·8	−0·6
108	+ 51	−86	26	−44	74	+1·7	+0·9	−1·5
110	+ 91	+42	82	+38	18	−1·7	−1·5	−0·7
113	+ 97	+25	94	+24	6	−1·9	−1·8	−0·5
115	+ 19	+98	4	+19	96	−0·9	−0·2	−0·9
119	+ 71	−70	51	−50	49	+2·0	+1·4	−1·4
122	+ 82	−58	67	−47	33	+0·4	+0·3	−0·2
123	− 94	+34	88	−32	12	+3·6	−3·4	+1·2